2mic4

SEL-73-043

Amplitude Variations of Whistler-Mode Signals Caused by their Interaction with Energetic Electrons of the Magnetosphere

by

L. C. Bernard

December 1973

Technical Report No. 3465-2

Prepared under

Air Force Office of Scientific Research
Contract F44620-72-C-0058 and
National Aeronautics and Space Administration
Grant NGL 05-020-008

RADIOSCIENCE LABORATORY

STANFORD ELECTRONICS LABORATORIES

STANFORD UNIVERSITY · STANFORD, CALIFORNIA

SEL 73-043

AMPLITUDE VARIATIONS OF WHISTLER-MODE SIGNALS CAUSED BY THEIR INTERACTION WITH ENERGETIC ELECTRONS OF THE MAGNETOSPHERE

by

L. C. Bernard

December 1973

Technical Report No. 3465-2

Prepared under
Air Force Office of Scientific Research
Contract F44620-72-C-0058
and
National Aeronautics and Space Administration
Grant NGL 05-020-008

Radioscience Laboratory
Stanford Electronics Laboratories
Stanford University Stanford, California

ABSTRACT

Whistler mode waves that propagate through the magnetosphere exchange energy with energetic electrons by wave-particle interaction mechanisms. Using linear theory, a detailed investigation is presented of the resulting amplitude variations of the wave as it propagates. Arbitrary wave frequency and direction of propagation are considered. A general class of electron distributions that are nonseparable in particle energy and pitch-angle is proposed. Comparison with data is obtained by computing the total amplitude variation between two locations along the wave ray path. It is found that the proposed distribution model is consistent with available whistler and particle observations. In particular, this model yields insignificant amplitude variation over a large frequency band, a feature commonly observed in whistler data. This feature of the data implies a certain equilibrium between waves and particles in the magnetosphere over a wide spread of particle energy, at least during certain (magnetically quiet) times, and is relevant to plasma injection experiments. Application of our analysis for monitoring the distribution of energetic electrons in the magnetosphere is discussed.

ACKNOWLEDGMENTS

I wish to express my sincere appreciation to my research supervisors, Professor R. A. Helliwell and Dr. T. F. Bell, for their advice and encouragement during the course of this work.

I benefited at various stages of my research from fruitful discussions with members of the VLF Group of the Radioscience Laboratory and in particular with Dr. D. L. Carpenter and Dr. C. G. Park. Mr. N. Dunckel initiated me into the intricacies of ray tracing calculations. Many thanks also to Mr. T. L. Crystal, with whom I not only had many constructive discussions but who also shared an office with me for almost three years. This could have been a traumatic experience for Mr. Crystal, were it not for his happy and even disposition.

This research was supported in part by the Air Force Office of Scientific Research under Contract F44620-72-C-0058 and in part by the National Aeronautics and Space Administration under Grant NGL-05-020-008.

CONTENTS

CONTENTS (cont.)

LIST OF TABLES

ILLUSTRATIONS

ILLUSTRATIONS (cont.)

LIST OF PRINCIPAL NOTATIONS

B = Magnetic (induction) field

B_0 = Earth's static magnetic field

B_1 = Wave magnetic field

c = Velocity of light in free space $\sim 3\times10^{8}$ m/s

D = Electric induction field or whistler dispersion

e = Elementary charge (positive) = 1.602×10^{-19}C; in subscript refers to electrons

E = Electric field; in subscript, refers to equatorial values

f = Particle distribution function or wave frequency (Hz)

g = Particle distribution function normalized to unity or acceleration of gravity

G_u = Whistler gain per 1000 km

G = Integrated whistler gain over a ray path

i = $\sqrt{-1}$; in subscript, refers to ions

J = Current density

k = Wave number

K = Boltzmann's constant = 1.38×10^{-23}J $(^{o}K)^{-1}$

L = McIlwain geomagnetic dipole coordinate

m = Order of cyclotron harmonic

M = Particle mass

M_0 = Rest particle mass

M_{0e} = 0.911×10^{-30} kg

M_{0H} = Proton rest mass = 0.167×10^{-26} kg

n = Particle density

N = Refractive index

p = Particle momentum

q = Particle charge (algebraic)

LIST OF PRINCIPAL NOTATIONS (cont.)

r = Geocentric distance

R, In subscript, refers to resonance

R_0 = Earth radius = 6370 km

R_E = Equatorial geocentric distance to dipole magnetic field lines

s, In subscript, refers to particle species

T = Temperature

v_p = Phase velocity

v_g = Group velocity

W = Energy

α = Particle pitch angle

α_g = $\langle) (\underline{k}, \underline{v}_g)$

β = ω_p/ω_c

θ = $\langle) (\underline{k}, \underline{B}_0)$

θ_G = Gendrin angle

θ_R = Resonance cone angle

$\mathcal{K}$ = Dielectric tensor

λ = Latitude

Λ = ω/ω_c

φ = $\langle) (\underline{p}_\perp, \underline{O}x)$

ψ = $\langle) (\underline{p}_\perp, \underline{B}_1)$

ω = Wave frequency (rd/s)

ω_c = Gyrofrequency

ω_p = Plasma frequency

γ = $(\omega_p/\omega)^2$

DEFINITIONS OF IMPORTANT TERMS USED THROUGHOUT THE TEXT

1. "parallel" and "perpendicular" refer to the direction of the wave normal $\underline{k}$ with respect to the static magnetic field $\underline{B}_0$

2. "longitudinal" and "transverse" refer to the direction of $\underline{k}$ with respect to electric field of the wave $\underline{E}_1$

3. the subscripts $\parallel$ and $\perp$ at the right of letters refer to vector components along and across $\underline{B}_0$ respectively. Subscript $\parallel$ at the left of letters refer to the special case of parallel propagation.

4. the particle energy is referred to as:

   "cold" or "thermal" in the approximate range: $0 - 10^{-1}$ eV

   "very low" in the range: 10^{-1}eV to 100 eV

   "low" in the range: 100 eV to 40 keV

   "high" in the range: 40 keV and above

5. "gain" will be used for "wave amplitude variation," often with a quantitative connotation. Positive (negative) gain means wave growth (damping).

6. Because of inhomogeneity, a wave starting at one location may not be able to propagate to a second location in space. The second location is described as being "accessible" if, according to the laws of geometrical optics, it can be reached by the wave.

7. The term "instability" will refer to wave amplitude variation due to wave particle interaction.

8. The waves vary in proportion to $\exp[\zeta i(\underline{k}\cdot\underline{r}-\omega t)]$, $\zeta = \pm 1$.

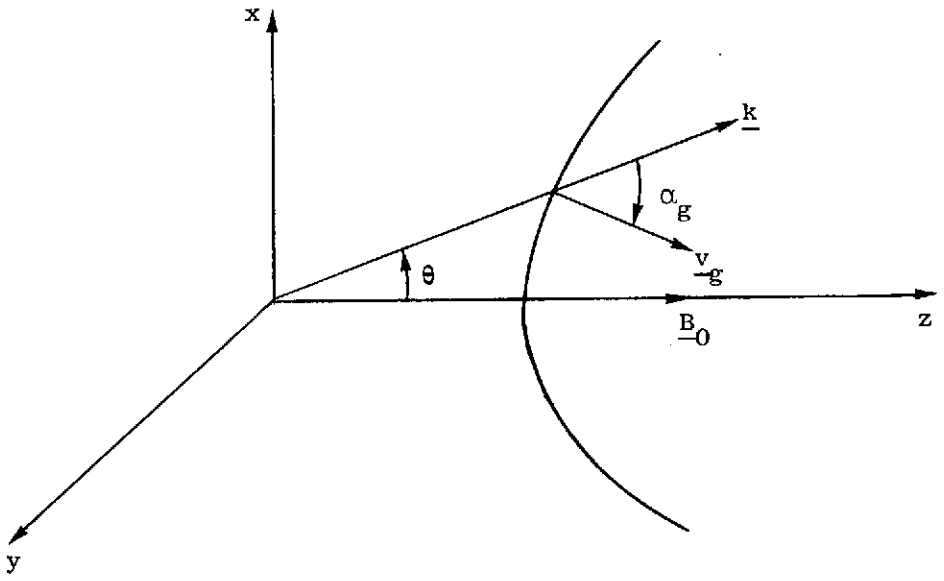

WAVE COORDINATE SYSTEM

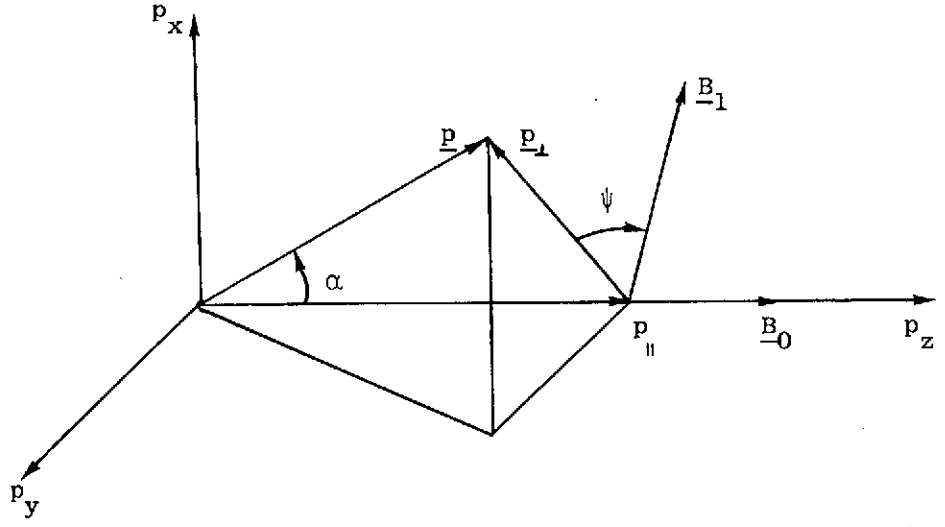

PARTICLE COORDINATE SYSTEM

I. INTRODUCTION

The magnetosphere extends many earth radii above the ionosphere. It is the region in space where the earth's magnetic field has dominant control over the motions of charged particles.

The presence of these charged particles in turn determines the characteristics of the different electromagnetic wave modes which can propagate in the magnetosphere. Our interest will be focused on the "whistler" mode. The frequency range of the whistler mode extends approximately between the proton and electron gyrofrequencies. Its sense of polarization corresponds to the sense of gyration of electrons compelled to gyrate and drift along the earth's magnetic field lines.

The charged particles can be divided into two classes according to their energy: the 'cold' or 'thermal' particles and the 'hot' or 'energetic' particles. The cold particles have a distribution approximately Maxwellian with an average energy of the order of 10^{-1} eV [Angerami, 1966] and determine the ray path of a wave between two locations in the magnetosphere. The hot particles can generate waves [Kennel and Petscheck, 1966; Helliwell, 1967] or cause amplitude variations of a preexisting wave along its ray path. Such an interaction involves a possible exchange of energy between waves and particles. This transfer of energy into the wave can be either positive or negative, depending upon the precise values of wave, cold, and hot plasma parameters.

Since Storey's [1953] investigation, the study of whistler wave propagation characteristics has provided an invaluable diagnostic tool to determine the distribution of thermal particles in the magnetosphere. In contrast, the study of whistler-electron interaction characteristics has not led to the development of a successful diagnostic tool for the

determination of the energetic particle population. The importance of this interaction study is considerable though. Such a study may provide a better knowledge of the energetic particle population. It may provide also a better understanding of the magnetospheric medium. The interaction mechanism in itself may furnish an explanation of features of the magnetosphere or the generation of electromagnetic waves.

Knowledge and understanding of particle distribution characteristics are of fundamental importance in the whole field of plasma physics, from laboratory plasma experiments to astrophysics. In the laboratory, for example, knowledge of particle distributions is primordial in the field of plasma ion sources [Bernard, 1967; Benoit-Cattin and Bernard, 1968]. Understanding of wave-particle interaction mechanisms is most important in fusion research. These mechanisms certainly play a role in astrophysical phenomena, like pulsars.

The purpose of our work is to compute the whistler amplitude growth/damping rates due to whistler-electron interaction, to discuss its variations with regard to all parameters of concern, and, using a number of whistler observations, to infer possible models of the energetic electrons of the magnetosphere.

Wave amplitude variations are due both to "instability"[1] and "accessibility"[2] and it is often difficult to separate the two effects. When there is a frequency cutoff of a broadband signal, the question arises whether the frequencies above (or below) the frequency cutoff were damped by

---

[1] "Instability, as defined here, means wave amplitude variations due to wave-particle interaction.

[2] A location in space is "accessible" if, according to geometrical optics, it can be reached by a wave starting from another point.

wave-particle interaction, or whether these frequencies could not propagate from the location of generation to the location of reception. This frequency cutoff phenomenon is illustrated in Figure 1.1 which represents an example of a "nose whistler" spectrogram recorded at a ground station. Typically, such a signal presents an upper cutoff at some frequency f_u. The spectral shape of the signal is explained schematically in Figure 1.2. A broadband wave signal is generated by a lightning discharge close to the earth's surface. The generated frequencies are transmitted in part in the earth-ionosphere waveguide to the receiver in the other hemisphere where they appear on the spectrogram practically without dispersion as a frequency impulse or "atmospheric." The generated frequencies travel also in the magnetosphere and are guided or "ducted" along a magnetic field line. The magnetosphere is highly dispersive, that is, different frequencies travel with different velocities. As a result, the whistler has the characteristic shape shown on Figure 1.1. Notice from the figure that there is a characteristic frequency, namely the frequency of minimum time delay t_n or "nose" frequency f_n. Measurements of t_n and f_n have provided an invaluable technique for magnetospheric diagnostics [Smith, 1960; Carpenter, 1962, 1963, 1966, 1970; Carpenter and Smith, 1964; Carpenter et al., 1972; Helliwell, 1965; Angerami, 1966; Angerami and Carpenter, 1966; Park, 1970, 1973; Park and Carpenter, 1970; Bernard, 1973; Ho and Bernard, 1973].

Smith [1961], proposed an elegant explanation of the upper frequency cutoff f_u. As the magnetosphere is practically a collision free medium, density irregularities can exist for a long time. He showed that small field-aligned enhancements of ionization or "ducts" can trap low frequencies below f_u (path 2 on Figure 1.2), whereas high frequencies above f_u are

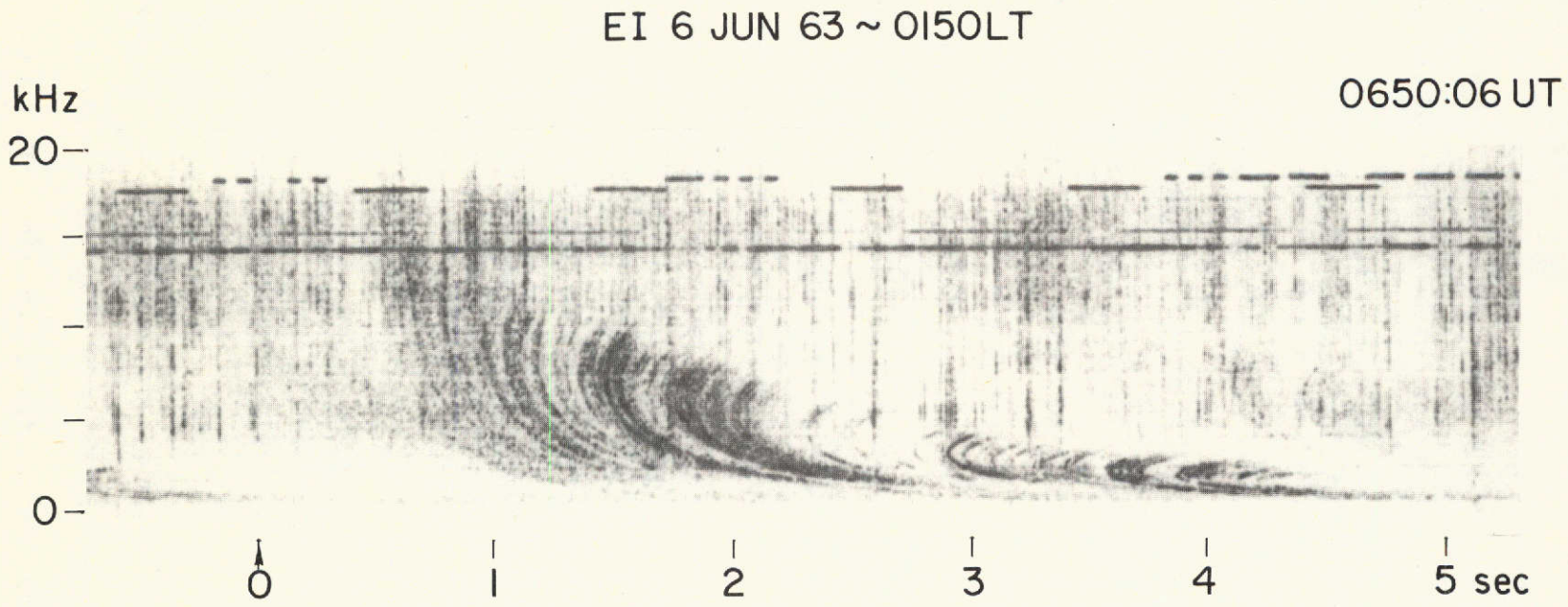

FIGURE 1.1. TYPICAL NOSE WHISTLER SPECTROGRAM SHOWING AN UPPER FREQUENCY CUTOFF.

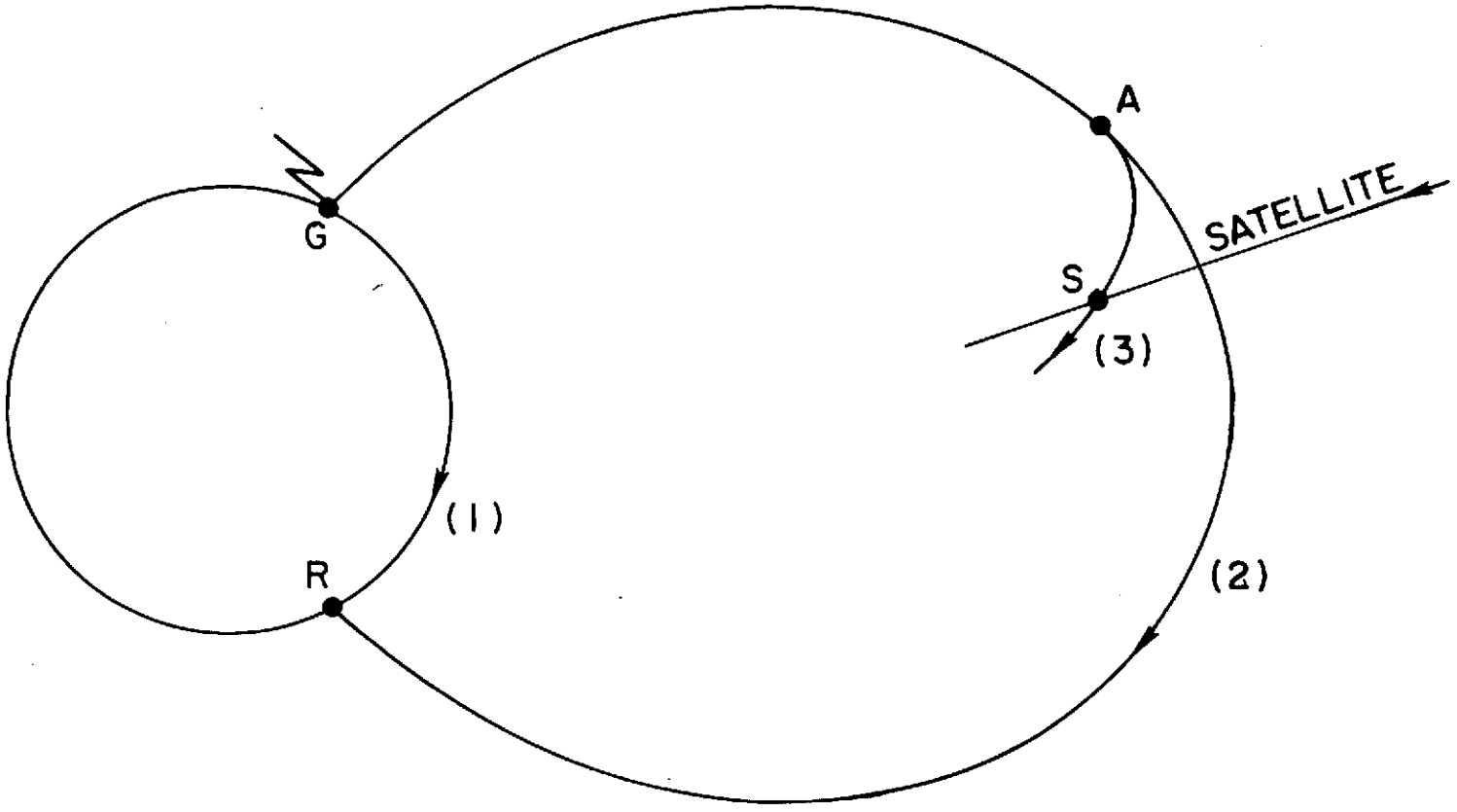

FIGURE 1.2. RAY PATHS INVOLVED IN PRODUCTION OF A TYPICAL NOSE WHISTLER. Frequencies generated at point G by a lightning discharge travel in part close to the earth along path 1 and in part along a magnetic field line along path 2 up to an upper frequency f_u above which they propagate along path 3. Wave components of frequency below f_u can be recorded on the ground to point R. Frequencies above f_u can only be recorded on satellites.

untrapped at some point A (path 3) and cannot reach the receiver location R.

Scarf [1962] proposed an alternative explanation for the upper cutoff f_u based on hot plasma effects. Taking an isotropic Maxwellian distribution for the hot electrons he found that whistlers could be attenuated due to wave-particle interaction, the attenuation increasing rapidly with frequency. Postulating that the high frequency cutoff was indeed caused by such a mechanism, he determined in turn what should be the temperature. He found an order of 10^5 ^oK. This analysis was subsequently refined by Liemohn and Scarf [1964].

Guthart [1964, 1965] then showed that a temperature $\approx 10^5$ ^oK would produce a slight, but a measurable change in the dispersion curve f(t) of Figure 1.1. Because he could not observe this change, he proposed another type of distribution which would produce the observed cutoff but no change in the curve f(t). Liemohn [1967] made a quantitative analysis where he integrated the variation of amplitude along the field line path (2). He chose a particle distribution function $f(W,\alpha)$ which was a product of a function of W alone and a function of α alone where W and α are respectively the particle energy and pitch-angle:

$$f(W,\alpha) \propto W^{-\nu} \sin^q \alpha \qquad (1.1)$$

and found that a value of the parameter $q = 2$ would produce the right value of frequency cutoff. He found also an increasing in amplitude just below f_u, compatible with observation. The question of whether this cutoff is caused by accessibility or wave-particle instability was reopened when Carpenter [1968] made a statistical study of over 500 nose whistlers propagating along a wide variety of locations. He showed that the ratio

f_u/f_{cE} (where f_{cE} is the equatorial gyrofrequency of the path) was statistically very constant: $f_u/f_{cE} = 0.51 \pm 0.03$. This value is almost exactly the value predicted by Smith's [1961] theory of trapping ($f_u/f_{cE} = 0.50$). These facts favored the accessibility explanation rather than the instability explanation because the predicted value of the accessibility ratio f_u/f_{cE} is practically independent of any parameter whereas the instability ratio depends upon many parameters and should vary with different propagation paths. This is contrary to observation.

Evidence of the accessibility explanation was put forth by Angerami [1970], who observed some unducted frequency components of whistlers on a satellite. Briefly, referring to Figure 1.2, high frequency components are trapped up to a certain point A on the field line and become untrapped after, that is, no longer follow a field line but follow a path such as (3). A satellite intersecting the ray path (3) can record these components (see Figure 4.1).

Since the validity of the accessibility cutoff appears to be clearly established, the distribution proposed by Liemohn [1967] seems somewhat doubtful. One of our aims has been to find more realistic distributions.

Furthermore, Liemohn's [1967] computations include only propagation parallel to the magnetic field. Now that a body of very interesting satellite data, such as Angerami's [1970], has been obtained showing evidence of nonparallel propagation, these computations should include nonparallel propagation as well. A qualitative study of wave instability for nonparallel propagation limited to low frequency ($f \ll f_c$), has been done by Kennel [1966], and Kennel and Thorne [1967]. Brinca [1972] extended this study to waves of frequency $\sim f_c/2$. Thorne [1968] made a quantitative

instability study for "MR whistlers" (see Section 4E) which are again low frequency whistlers. The observations of whistler signals at high normalized frequencies [Angerami, 1970; Dunckel and Helliwell, 1972], show the necessity to make a quantitative study of the high frequency oblique whistler instability. This study has been our second goal.

The contributions of the present work can be briefly stated as follows:

1. We propose a new model for the energetic particle distribution function. This model has some important characteristics and among them, it yields very small amplitude variations over a large band of wave frequencies, and we believe it represents the energetic electron distribution more realistically than previous models.

2. We derive a new general expression for the variation of wave amplitude caused by wave-particle interactions for an arbitrary angle of propagation. This expression is algebraically simpler than previously derived expressions and permits easier numerical computations. A Fortran program has been developed to compute gain rates of a whistler integrated along its ray path for a certain class of hot plasma distributions.

3. We have integrated gain rates along whistler ray paths deduced from some whistler observations. We have determined some bounds on the values of the parameters of our proposed distribution. We make some suggestions concerning the explanation of certain features of the observed particle spectrum.

4. We discuss the application of our analysis to the development of a diagnostic tool for monitoring the distribution of hot electrons, and to plasma injection experiments.

In Chapter 2, the theory of whistler-mode wave particle interactions is presented. First, we describe briefly the physics of the interaction, followed by the formulation of solving the coupled system of Maxwell equations and linearized Vlasov equation. Then we derive a general expression for the rate of variation of wave amplitude for an arbitrary angle between the wave normal and the earth's magnetic field and for an arbitrary frequency below the gyrofrequency.

In Chapter 3, we study in detail the variation of the wave gain for parallel propagation and for both a distribution separable and nonseparable in energy and pitch angle. We present a detailed study of the influence of the angle between wave normal and earth's magnetic field.

In Chapter 4, we compute gain rates along ray paths deduced from some whistler observations.

Finally, in Chapter 5, conclusions are drawn and recommendations are made for future work. The details of numerical computations of gain rates, and various derivations and auxiliary material are presented in the appendices.

II. THEORY

A. INTRODUCTION

This work is concerned with the amplitude variations of an electromagnetic wave caused by the presence of energetic electrons.

The physics of such a mechanism can already be understood from the interaction of a single particle with an electromagnetic wave. We describe the interaction from this point of view in Section B. We define there such notions as "resonance" and "trapping." It is then possible to establish a qualitative relation between the interaction of one particle to the interaction of a distribution of particles.

More rigorously, the interaction between wave and particle is a solution of a wave-plasma system. As such, it involves the solution of Maxwell's equations coupled with a kinematics equation. Since the magnetospheric medium can generally be treated as collision-free, the evolution in time of the particle distribution function can be described by the Vlasov equation.

Section C describes the formulation for solving the coupled system of equations after linearization of Vlasov's equation.

In Section D, a general expression is derived for wave amplitude variation, including relativistic effects, arbitrary wave frequency, and arbitrary direction of propagation.

B. PHYSICS OF THE INTERACTION DESCRIBED FROM A TEST PARTICLE MOTION

1. Interaction of One Particle with an Electromagnetic Wave

The motion of a particle interacting with an electromagnetic wave has been described in great detail by a number of authors (e.g., Roberts and Buchsbaum [1964]; Laird and Knox [1965]; Bell [1965]; Lutomirski and

Sudan [1966]; Laird [1968]; Dungey [1969]; Roux and Solomon [1970]; Palmadesso and Schmidt [1971]; Dysthe [1971]; Palmadesso [1972]). In this section we will give a brief description of the interaction.

Because of its motion a particle can experience the electric field of an electromagnetic wave, which is time-varying in the laboratory frame, as a constant electric field. In general this condition is realized only when the momentum or a component of the momentum of the particle takes a particular set of values. This condition is referred to as the resonance condition. Because the particle sees a constant electric field at resonance, it can experience a strong acceleration (deceleration) which means there is an energy exchange between the particle and the wave as the particle gains (loses) energy at the expense (benefit) of the wave energy. This mechanism is responsible for damping (growth) of the wave.

Off resonance, the particle sees a time-varying field and therefore it alternatively experiences both acceleration and deceleration; the exchange of energy between the wave and the particle averages to zero as time elapses. A particle initially at resonance will not stay in this state for a very long time, its momentum changing its value due to its acceleration (deceleration). It is shown that, provided the value of the particle momentum is close enough to one of the resonance values, a stable situation called trapping can develop: a particle initially in phase with the wave field will be accelerated, will eventually see a phase reversal of the field, be decelerated and will again be in phase with the wave field, the process repeating itself in a stable way.

Not too close to resonance, the particle will not be trapped, that is it will drift along successive peaks and valleys of the wave.

In any case, the interaction is most important at resonance and its vicinity because the further from resonance the less the particle is perturbed by the wave.

For this reason, we rederive the resonance condition [Bell, 1964] which is deduced in the linear treatment. We also rederive the expression for the minimum energy of resonance.

Linear behavior: The electric field of the wave is taken of the form $\underline{E} = \underline{E}_0 \, e^{i(\underline{k}\cdot\underline{r}-\omega t)}$. Within the linear approximation, we evaluate the phase of the field at the unperturbed ($\underline{E} = 0$) location of the particle at the time t [Quemada, 1968]. According to what we have said previously, the resonance condition will be obtained when the phase of the field becomes constant. The unperturbed motion of the particle is defined by:

$$\frac{d\underline{p}}{dt} = q_e \frac{\underline{p}}{M} \times \underline{B}_0 = \underline{\omega}_c \times \underline{p} \tag{2.1}$$

where the relativistic mass

$$M = M_0 \sqrt{1 + \frac{p^2}{M_0^2 c^2}} \tag{2.2}$$

and

$$\omega_c = \frac{|q_e| B_0}{M} \, . \tag{2.3}$$

The motion of the particle (neglecting radiation) is a helix whose axis is parallel to $\underline{B}_0$; therefore:

$$\begin{cases} p_z(t) = p_{z0} \\ p_x(t) = p_\perp \cos\omega_c t \\ p_y(t) = p_\perp \sin\omega_c t \end{cases} \qquad \begin{cases} z = p_{z0} t/M \\ x(t) = \dfrac{p_\perp}{M\omega_c} \sin\omega_c t + x_0 \\ y(t) = -\dfrac{p_\perp}{M\omega_c} \cos\omega_c t + y_0 \end{cases} \tag{2.4}$$

with $\underline{k} = (k_x, 0, k_z)$, the wave phase becomes:

$$\underline{k}\cdot\underline{r} - \omega t = \underline{k}\cdot\underline{r}_0 + \frac{k_x p_\perp}{M\omega_c}\sin\omega_c t + \left(k_z \frac{p_{0z}}{M} - \omega\right)t \qquad (2.5)$$

where $\underline{r}_0 = \underline{r}(t = 0)$.

Using the identity:

$$e^{ix\sin\varphi} = \sum_{m=-\infty}^{\infty} J_m(x) e^{im\varphi} \qquad (2.6)$$

$$e^{i(\underline{k}\cdot\underline{r}-\omega t)} = e^{i\underline{k}\cdot\underline{r}_0} \sum_{m=-\infty}^{\infty} J_m\left(\frac{k_\perp p_\perp}{M\omega_c}\right) \exp\left(i\left(k_z \frac{p_{0z}}{M} + m\omega_c - \omega\right)t\right) \qquad (2.7)$$

This last expression shows that the particle sees a superposition of waves propagating in the $\underline{0z}$ direction and sees a constant field when

$$k_z \frac{p_{0z}}{M} + m\omega_c - \omega = 0 \qquad (2.8)$$

Now, $\omega' = \omega - k_z \frac{p_{0z}}{M}$ is the Doppler shifted frequency of the wave seen by the particle and the resonance condition is rewritten as:

$$\omega' = m\omega_c, \quad m=0,\pm1,\pm2,\ldots \qquad (2.9)$$

The resonance $m = 0$ is excited by both the parallel and the perpendicular components of the electric field (referenced to the static magnetic field) and includes the well known Landau resonance. (For convenience we will refer to the $m = 0$ resonance as the Landau resonance.) All other resonances $m \neq 0$ are excited by the perpendicular component of the electric field and are called the cyclotron resonances. The infinity of harmonics is due to the spatial variation of the electric field in planes perpendicular to the static magnetic field.

In the general case, there are two roots of Eq. (2.8) ($m \neq 0$;

m = 0 → only one positive root):

$$p_{Rm1,2} = \frac{-\frac{m}{\Lambda} \pm \sqrt{\frac{m^2}{\Lambda^2 N_{\parallel}^2} + \left(1 - \frac{1}{N_{\parallel}^2}\right)\left(1 + \frac{p_{\perp}^2}{p_0^2}\right)}}{1 - 1/N_{\parallel}^2} \frac{p_0}{N_{\parallel}} . \qquad (2.10)$$

The minimum energy of resonance $W_R(p_{\perp} = 0)$ is given by:

$$W_{Rm} = W_0 \left[\sqrt{1 + \frac{p_{Rm}^2(p_{\perp} = 0)}{p_0^2}} - 1 \right]; \quad W_0 = M_0 c^2 . \qquad (2.11)$$

$p_0 = M_0 c$

$\theta = \langle) (\underline{k}, \underline{B}_0)$

$\Lambda = \omega/\omega_{c0}$ where here ω_{c0} is the rest mass gyrofrequency

N = refractive index

$N_{\parallel} = N\cos\theta$

In the non-relativistic limit the resonance condition is satisfied for one value of p_R for each m:

$$p_{Rm0} = \frac{\Lambda - m}{\Lambda} \frac{p_0}{N_{\parallel}} . \qquad (2.12)$$

In Figure 2.1 we have plotted W_R versus $N_{\parallel}$ with Λ as a parameter for the Landau (m = 0) and the fundamental cyclotron (m = 1) resonances. Note in Figure 2.1 that departure from a straight line represents departure from the non-relativistic limit and that in the non-relativistic range W_{R0} is lower (higher) than W_{R1} when Λ is smaller (larger) than 0.5.

Nonlinear behavior: To see what happens after the initial (linear)

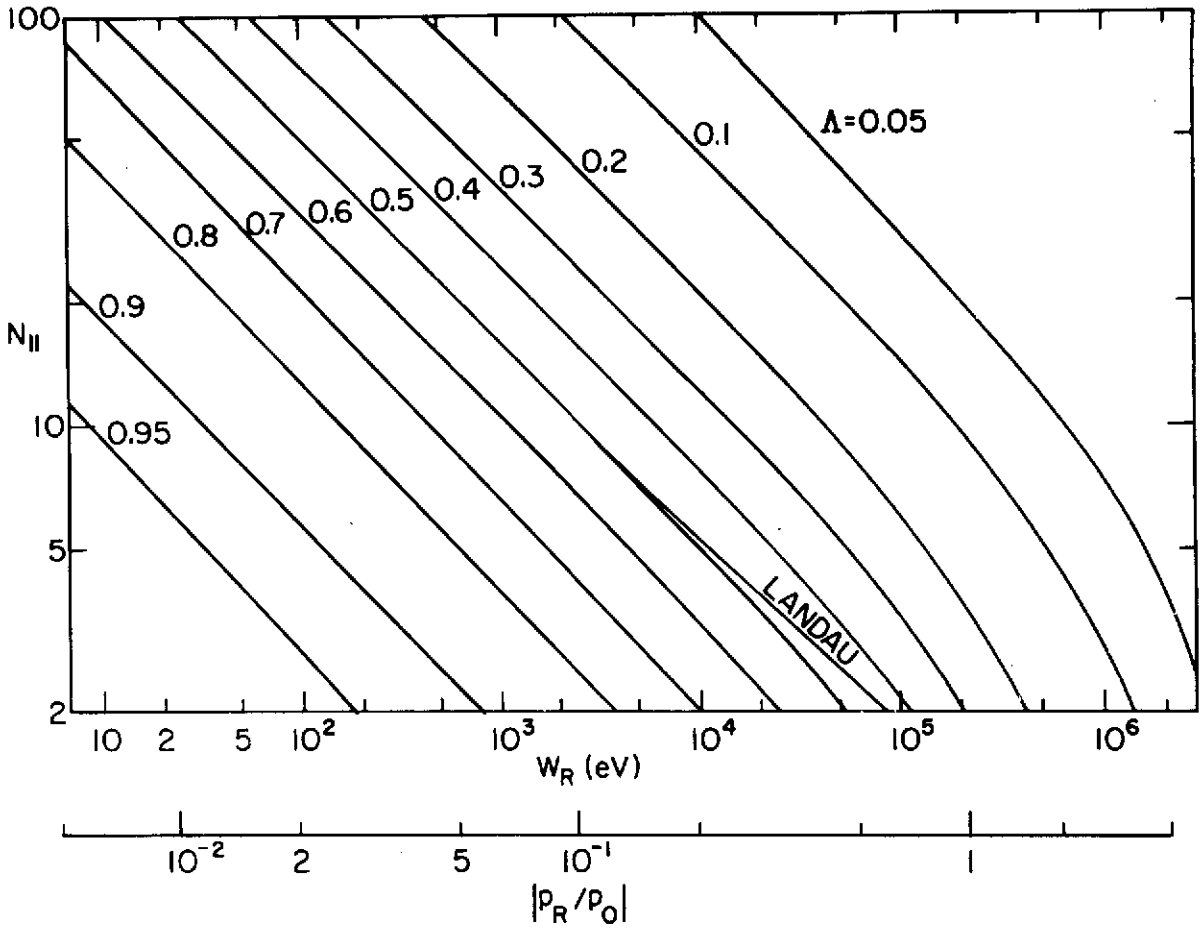

FIGURE 2.1. A PLOT OF THE MINIMUM ENERGY OF INTERACTION OF AN ELECTRON WITH A WHISTLER VERSUS THE COMPONENT OF THE WHISTLER REFRACTIVE INDEX ALONG THE STATIC MAGNETIC FIELD ($N_{||}$). Landau and fundamental cyclotron resonances are shown for different values of Λ.

development of the interaction, we have to integrate the equations of motion. Though the general case ($\theta \neq 0$) is fairly involved and has only been tackled recently [Palmadesso, 1972], it is basically the superposition of Landau and cyclotron cases and it suffices to look at these two cases separately.

In the Landau interaction (E field alone), the equation of motion is simply:

$$\frac{d^2x}{dt^2} = \frac{q}{M_0} E \sin(kx-\omega t) \tag{2.13}$$

which becomes by change of variable $\xi = kx-\omega t$:

$$\frac{d^2\xi}{dt^2} = \frac{qEk}{M_0} \sin\xi \ . \tag{2.14}$$

This equation is analogous to a pendulum equation. Note that ξ is merely the deviation from the resonance position $x_R = \frac{\omega}{k} \cdot t$.

Now the solution of Eq. (2.14) can be of two types depending upon initial conditions. The particle can oscillate back and forth around the resonance position or can "rotate" completely. In the first case the particle is said to be trapped. Trapping is an important phenomenon because the motion of the particle is significantly altered by the presence of the field and energy exchanges with the wave can be quite important.

In the case of trapping, the solution is periodic.

The case of small oscillations gives an order of magnitude of the period (called trapping time T_L):

$$T_L = \frac{2\pi}{\omega_{TL}} = 2\pi \left(\frac{M}{|q|kE}\right)^{1/2} \ . \tag{2.15}$$

Note that particles close to resonance are most likely to be trapped (small oscillations case). Note also that Landau trapping means bunching of particles in space.

The situation will be found to be similar for cyclotron interaction. Consider a particle in the field of a circularly-polarized electromagnetic wave propagating along $\underline{B}_0$:

Let $\underline{B}_1 = [B_{10}\cos\zeta_s(kz-\omega t), B_{10}\sin\zeta_s(kz-\omega t), 0]$ be the magnetic field vector of the wave. ($\zeta_{i,e} = \pm 1$, which defines polarization for normal interaction with either an electron or an ion.)

The equations of motion of the particle are [Dysthe, 1971]:

$$\begin{aligned} \dot{v}_{\parallel} &= -\zeta_s v_{\perp}\omega_{c1}\sin\psi \ , \\ \dot{v}_{\perp} &= \zeta_s (v_{\parallel} - v_p)\omega_{c1}\sin\psi \ , \\ \dot{\varphi} &= -\zeta_s\omega_{c0} - \zeta_s\omega_{c1}\frac{(v_{\parallel}-v_p)}{v_{\perp}}\cos\psi \end{aligned} \qquad (2.16)$$

where the particle velocity is $\underline{v} = [v_{\perp}\cos\varphi, v_{\perp}\sin\varphi, v_{\parallel}]$ and where $\psi = \sphericalangle\,(\underline{v}_{\perp}, \underline{B}_1)$, $v_p = \frac{\omega}{k}$, $\omega_{c0} = \frac{eB_0}{M}$, and $\omega_{c1} = \frac{eB_1}{M}$. By definition the angle ψ can be written as $\psi = -\varphi + \zeta_s(kz-\omega t)$ and two differentiations with respect to time produces the expression

$$\ddot{\psi} = -\ddot{\varphi} + \zeta_s k\dot{v}_{\parallel} \ . \qquad (2.17)$$

Since $\omega_{c1} \ll \omega_{c0}$ in the magnetosphere, the last equation in (2.16) shows that (provided $v_{\perp}$ is not too small) $\dot{\varphi} \sim$ constant and therefore Eq. (2.17) becomes $\ddot{\psi} \sim \zeta_s k\dot{v}_{\parallel}$. Thus the first equation in (2.16) can be rewritten

$$\ddot{\psi} = -\omega_{Tc}^2 \sin\psi \qquad (2.18)$$

where

$$\omega_{Tc} \equiv \frac{2\pi}{T_c} = (\omega_{c1} k v_{\perp})^{1/2} \ .$$

We find again a pendulum type equation, this time with respect to the variable ψ, that is, in velocity space. The same conclusions apply as in the Landau case. There will be trapped particles and the period of trapping will be of the order of $T_c \sim \omega_{Tc}^{-1}$.

From the first two equations of (2.16) a constant of motion is immediately found [Dysthe, 1971]:

$$v^2 - 2v_{\parallel} v_p = \text{constant} \quad . \tag{2.19a}$$

2. Relation of Particle Motion to Wave Growth

Now we would like to know what happens when we include an ensemble of particles. It is possible to get a qualitative answer without going to the full Maxwell Vlasov treatment described in some detail in the next section.

In the Landau interaction case, particles initially having energy slightly above the energy of resonance will tend to be trapped and on the average oscillate at the resonance energy while it is the opposite for particles initially having energy slightly below resonance. Therefore, the former particles will tend to lose energy while the latter will tend to gain energy. If more particles tend to lose energy than to gain energy, there will be wave growth and vice versa.

In terms of the distribution function:

$$\left.\frac{\partial f}{\partial v_{\parallel}}\right|_{v_R} > 0 \rightarrow \text{GROWTH}$$

$$\left.\frac{\partial f}{\partial v_{\parallel}}\right|_{v_R} < 0 \rightarrow \text{DAMPING}$$

For the cyclotron interaction case, it is useful to recall Eq. (2.19a). It is written also as:

$$\frac{1}{2} Mv_{\perp}^2 + \frac{1}{2} M(v_{\parallel}-v_p)^2 = \text{constant} = W' \qquad (2.19b)$$

Equation (2.19b) is very easily interpreted. In the wave frame (where we shall denote quantitites by prime superscript), by Lorentz transformations [Feynman, 1964]:

$$\underline{E}'_{\parallel} = \underline{E}_{\parallel}$$

$$\underline{E}'_{\perp} = \frac{(\underline{E} + \underline{v}_p \times \underline{B})_{\perp}}{\sqrt{1-v_p^2/c^2}}$$

Now from Maxwell's equations:

$$\underline{E}_{\perp} = - \underline{v}_p \times \underline{B}_{\perp} \qquad \text{or,} \qquad \underline{E}'_{\perp} = 0 \ .$$

Also since $\underline{E}_{\parallel} = 0$, $\underline{E}'_{\parallel} = 0$.

Therefore Eq. (2.19b) simply means that the particle energy W' in the wave frame stays constant. Following Gendrin [1968], Eq. (2.19b) is graphically interpreted in Figure 2.2.

In the $(v_{\parallel}, v_{\perp})$ plane, particles of constant energy follow a circle centered at the origin. From Eq. (2.19b) particles interacting with the wave follow a circle centered on v_p (taking v_p as > 0; remember that $v_R < 0$). From Figure 2.2, it is obvious that particles with parallel velocity initially slightly above $|v_R|$ and resonating with the wave will gain energy. At the same time their pitch angle increases. The situation is reversed for particles with $|v_{\parallel}|$ slightly below $|v_R|$. In the cyclotron interaction, the 'slow' particles cause wave growth in contrast to the Landau interaction, a condition already drawn by Bell [1964]. This reflects merely the fact that for (normal) cyclotron interaction, wave and resonating particles are moving in opposite directions. For anomalous

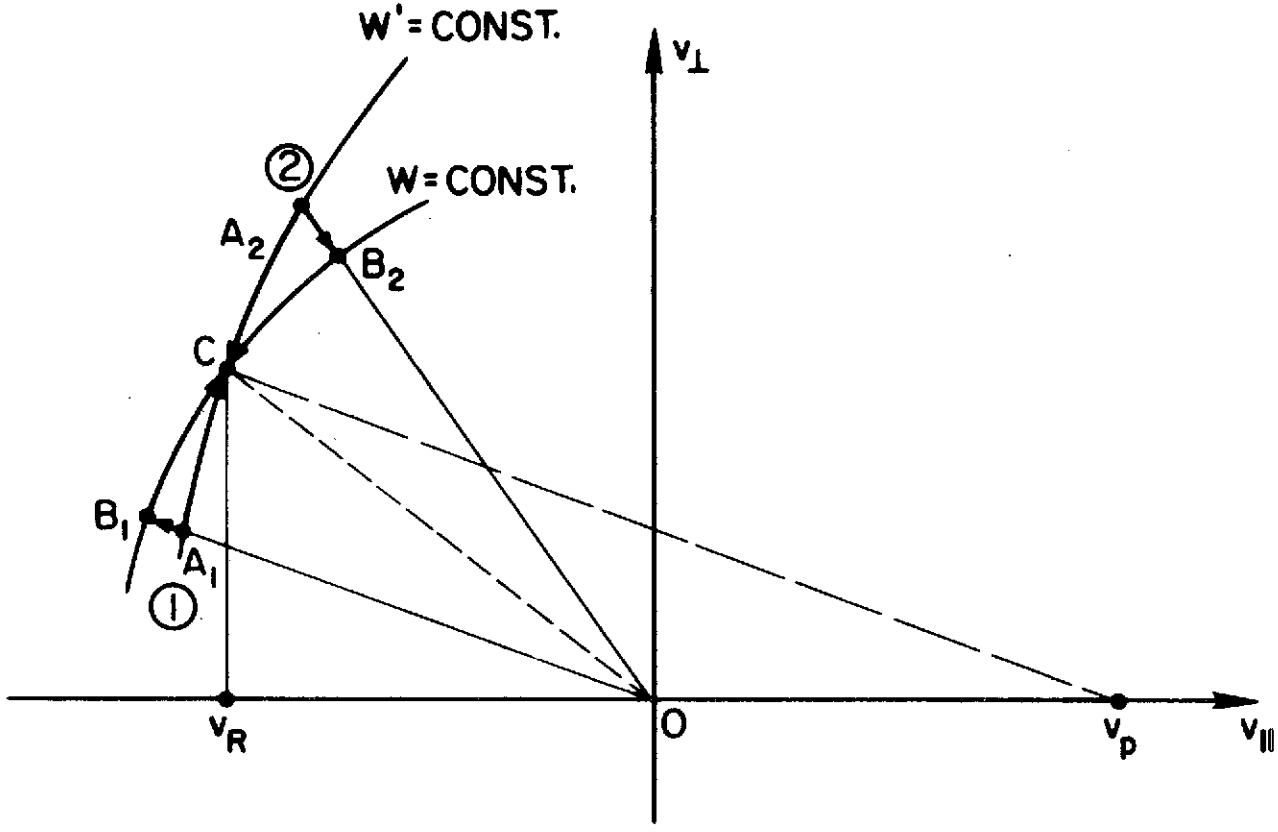

FIGURE 2.2. GRAPHICAL INTERPRETATION OF THE FIRST CONSTANT OF MOTION OF AN ELECTRON INTERACTING WITH A WHISTLER WAVE PROPAGATING ALONG THE STATIC MAGNETIC FIELD.

cyclotron interaction (e-L or p-R interaction) v_R and v_p are of the same sign and 'fast' particles cause wave growth. In this case particle energy increase is associated with pitch angle decrease, which was algebraically demonstrated by Brice [1964].

From Figure 2.2, it is also seen that resonant particles with high energy ($|v_R| \gg v_p$) interact with the wave with practically no change of energy because the circles of $W' =$ constant are practically coincident with the circles $W =$ constant. There is 'pure pitch angle' diffusion [Kennel and Petschek, 1966]. For particles with $|v_R|$ comparable or less than v_p, the curves of constant W and W' differ significantly. There can be energy diffusion at a rate comparable to pitch angle diffusion. This is confirmed quantitatively by the quasi-linear theory [Kennel and Engelmann, 1966].

Now

$$v_R = \frac{\omega_c - \omega}{k} , \quad v_p = \frac{\omega}{k} . \tag{2.20}$$

Therefore high-energy resonant particles interact with low frequency ($\omega \ll \omega_c$) waves and vice versa.

We have seen that in the Landau case, gain rates are related to the derivative of the distribution function measured at the resonant velocity. We expect a similar situation in the cyclotron interaction but in contrast to the Landau case which was clearly a one-dimensional problem, several derivatives should be involved. The azimuthal variable plays a fundamental role in trapping but in the linear case this variable is not of primary importance (we shall find more rigorously in the next section that a necessary condition for the time invariance of the unperturbed system is that f must be φ-independent). So two variables remain to be considered,

$v_{\parallel}$ and $v_{\perp}$ for example. However, since in experimental measurements of particle fluxes, the energy W and the pitch angle α of the particle are most readily measurable, we shall use rather those two variables.

From Figure 2.2 we can qualitatively see how the signs of the derivatives $\frac{\partial f}{\partial W}$ and $\frac{\partial f}{\partial \alpha}$ influence the wave gain. On Figure 2.2, particles (1) and (2) refer respectively to particles with $|v_{\parallel}|$ slightly faster and slower than $|v_R|$. Either particle resonating with the wave follows a curve of constant W'. The trajectories can be decomposed as paths at constant pitch-angle, A_1B_1 and A_2B_2, and paths at constant energy B_1C and B_2C.

At constant pitch angle: particle (1) causes damping while particle (2) tends to cause growth. Now particle (1) has a lower level of energy than particle (2). Therefore, at constant pitch angle, if f is such that there are more particles of type (1) than of type (2), there will be damping, in other words:

$$\frac{\partial f}{\partial W}\Big|_{v_R} < 0 \rightarrow \text{DAMPING}$$

At constant energy: particle (1) causes damping while particle (2) causes growth. More particles of type (2) than of type (1) will cause growth:

$$\frac{\partial f}{\partial \alpha}\Big|_{v_R} > 0 \rightarrow \text{GROWTH}$$

This gives a qualitative picture of wave gain by wave-particle interaction, a result found more rigorously in the next section. The correct expressions for gain rates involve such derivatives of the particle distribution function evaluated at the resonant velocities. The gain expression depends upon the number of resonant particles as anticipated,

but because it depends also upon derivatives of f not only the amplitude of the distribution function is important but also the fine details of the distribution function. For this reason there is possibly a great range of wave gain rates while still considering realistic models of particle distributions in the magnetosphere.

3. Whistler Mode Refractive Index Characteristics and the Standard Approximation

To know the energies of resonance of particles, we need the refractive index values. In a cold collisionless plasma immersed in a static magnetic field B_0, electromagnetic waves of frequency below the electron gyrofrequency can propagate in either of two modes. These modes are elliptically polarized and the mode whose sense of polarization corresponds to the sense of gyration of electrons is defined as the "whistler mode." The other mode corresponds to a polarization in the opposite sense to the sense of gyration of the electrons. As we will be concerned essentially with electron interaction and wave of frequency $\omega \gg \omega_{ci}$, we will be concerned uniquely with the whistler mode. It can be shown that in fact throughout most of the inner magnetosphere the other mode does not propagate.

The full expression of the refractive index is given in Stix [1962]. A first approximation is to neglect the ions. It is valid when $\omega \gg \omega_{LHR}$, where ω_{LHR} is the lower hybrid resonance frequency. For a high density, two species plasma consisting of electrons of mass M_e and ions of mass M_i,

$$\omega_{LHR} \sim \omega_c \sqrt{\frac{M_e}{M_i}} \, . \tag{2.21}$$

Neglecting ions, N^2 can then be written in the form

$$N^2 = 1 + \frac{\beta^2}{\sqrt{\Lambda^2\cos^2\theta + C^2\sin^4\theta} + C\sin^2\theta - \Lambda^2} , \qquad (2.22)$$

where

$$C = \frac{\Lambda^2}{2(\Lambda^2-\beta^2)} .$$

Equation (2.22) shows that the whistler mode is a propagating mode over the angular range from $\theta = 0$ to the resonance cone angle

$$\theta_R = \cos^{-1}\left[\frac{\Lambda}{\beta}\sqrt{\beta^2 + 1 - \Lambda^2}\right] \qquad (2.23)$$

High-plasma frequency approximation: Equation (2.22) can be simplified when $\beta^2 \gg 1$ or $\omega_p^2 \gg \omega^2$. With this approximation $\cos\theta_R \sim \Lambda$ and C can be neglected in Eq. (2.22) as well as the factor 1 in front of the fraction term:

$$N^2 \sim \frac{\beta^2}{\Lambda(\cos\theta - \Lambda)} \qquad (2.24)$$

Quasi-parallel approximation: This approximation holds when $C\sin^2\theta$ can be neglected in Eq. (2.22), i.e., $|C|\sin^2\theta \ll \Lambda^2$. It is related to the "quasi-longitudinal" approximation of Stix [1962] and Helliwell [1965] or "quasi-circular" approximation of Allis et al [1963]. It holds for small θ or for $|C| \ll \Lambda^2$, that is, $2(\beta^2-\Lambda^2) \gg 1$ or $\beta^2 \gg 1$. This shows that the quasi-parallel approximation can be considered as a particular case of the high plasma-frequency approximation.

Non-relativistic approximation and standard approximation: When $\beta^2 \gg 1$, relativistic corrections can be neglected for Landau resonance energy and, except in the case of extremely low frequencies, for fundamental cyclotron resonance energy. For that reason, the non-relativistic and the high plasma frequency (and a fortiori the quasi-parallel)

approximations overlap almost completely. From now on, we will use the term "standard approximation" to mean explicitly that the three approximations are satisfied.

Ion correction for very low frequencies: For ω comparable to ω_{LHR}, the ions cannot be neglected but a simple approximation can be used [Edgar, 1972] within the standard approximation:

$$N^2 \sim \frac{\beta^2}{\Lambda(\cos\theta - \varepsilon\Lambda)} \tag{2.25}$$

where:

$$\varepsilon = 1 - \frac{\omega_{LHR}^2}{\omega^2} .$$

For $\omega \gg \omega_{LHR}$, we find expression (2.24). Equation (2.25) shows that propagation is possible for all angles when $\omega < \omega_{LHR}$. $N(\theta)$ is sketched in polar coordinates on Figure 2.3 to point out the different topologies of the refractive index surface according to frequency. Precise values of $N_{\parallel} = N\cos\theta$ are plotted versus θ for different values of Λ, in Figure 2.4.

Knowledge of the polarization of the whistler mode will be important also.

$$\frac{E_z}{E_x} = \frac{N^2 \sin\theta\cos\theta}{N^2\sin^2\theta - P} , \quad \frac{E_y}{E_x} = i\,\frac{D_S}{N^2 - S} \tag{2.26}$$

where P, D_S, and S are defined later in Eq. (2.58). The square of these ratios is represented in Figure 2.5, using the standard approximation. They increase monotonically from $\theta = 0$ to θ_R. As $\theta \to \theta_R$, $\frac{E_z}{E_x} \to \cot\theta_R$, $\frac{E_y}{E_x} \to 0$, and the wave becomes longitudinal ($\underline{E} // \underline{k}$) and linearly polarized. For $\Lambda \ll 1$, $\left|\frac{E_z}{E_x}\right| \to \Lambda$ at resonance, that is the parallel component of the electric field stays small compared to the perpendicular component.

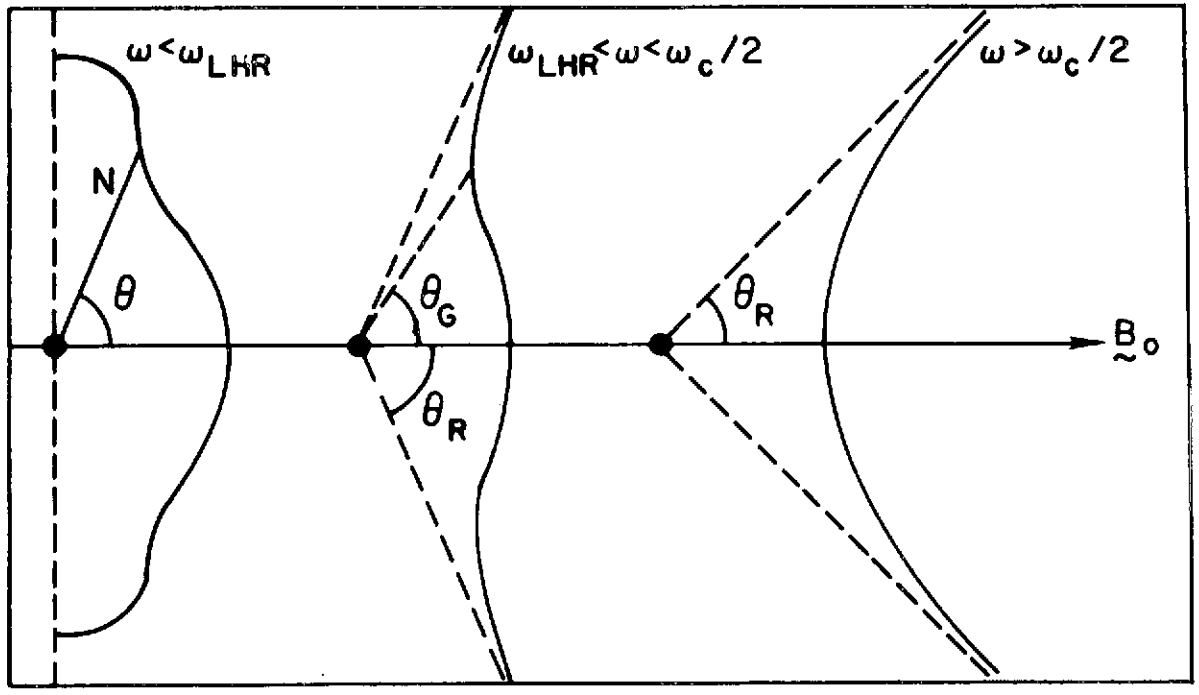

FIGURE 2.3. POLAR DIAGRAMS OF WHISTLER REFRACTIVE INDEX FOR THREE RANGES OF FREQUENCY.

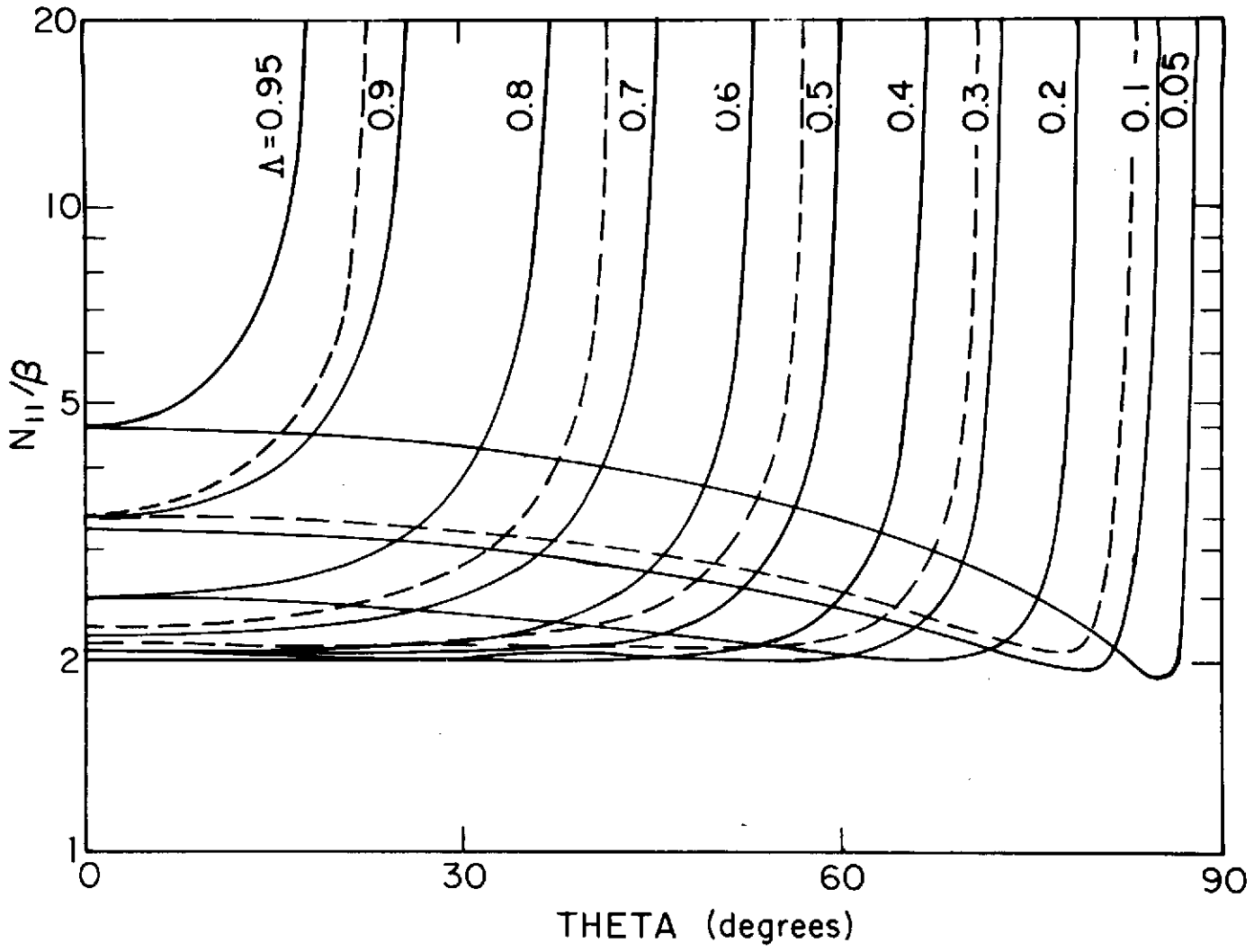

FIGURE 2.4. VARIATIONS OF $N_{\parallel}$ VERSUS THE ANGLE θ BETWEEN THE WAVE NORMAL AND THE STATIC MAGNETIC FIELD FOR DIFFERENT VALUES OF THE PARAMETERS Λ AND β. Solid lines: $\beta \gg 1$; dashed lines: $\beta = 2$.

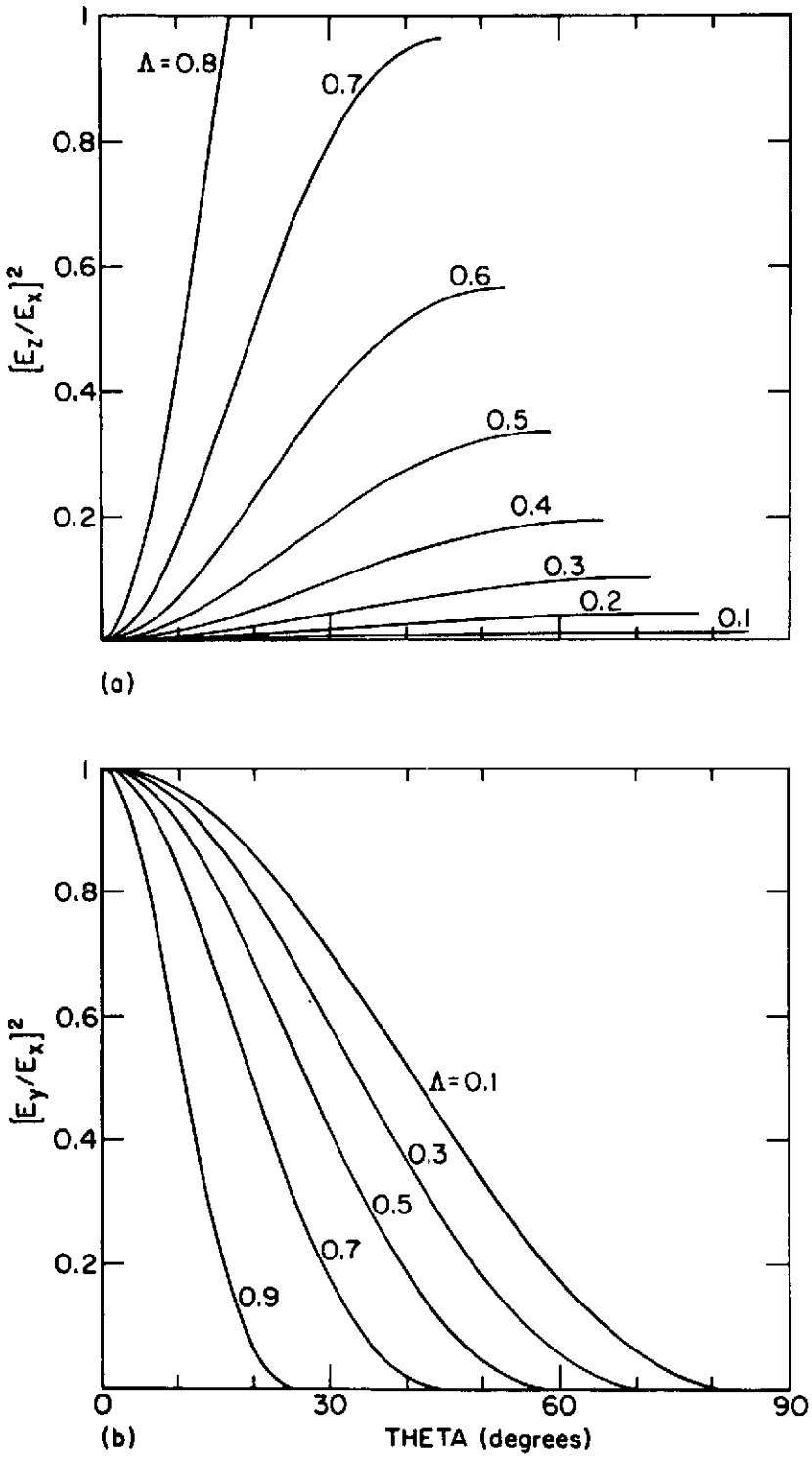

FIGURE 2.5. POLARIZATION RATIOS OF A WHISTLER MODE WAVE VERSUS ANGLE OF PROPAGATION.

C. MAXWELL-VLASOV DESCRIPTION OF THE INTERACTION

To deal with an ensemble of particles we introduce the particle distribution functions $f_s(\underline{r},\underline{p},t)$ where subscript s refers to the type of particle. We chose a momentum variable $\underline{p}$ in order to include relativistic effects. Assuming no collisions between particles, Liouville's theorem implies that each distribution function is conserved as time elapses:

$$\frac{d}{dt} f_s(\underline{r},\underline{p},t) = 0 \qquad (2.27a)$$

Equation (2.27a) when expressed in terms of partial derivatives yields the Vlasov equation:

$$\frac{\partial f_s}{\partial t} + \frac{\underline{p}}{M_s} \cdot \frac{\partial f_s}{\partial \underline{r}} + q_s \left(\underline{E} + \frac{\underline{p} \times \underline{B}}{M_s} \right) \cdot \frac{\partial f_s}{\partial \underline{p}} = 0 \qquad (2.27b)$$

In the last equation, the force term is written explicitly (Lorentz force law; we assume only electromagnetic forces are important).

The solution of the self-consistent system of Maxwell and Vlasov equations is the solution of the wave-plasma system. The precise form of the Maxwell set depends upon whether the plasma is regarded as a collection of particles in free space, or as a dielectric with an equivalent permittivity.

The Maxwell equations written below show the relationship between one description and the other one:

Description as particles in free space:

$$\nabla \times \underline{E} = -\frac{\partial}{\partial t}\underline{B}$$

$$\nabla \times \underline{H} = \frac{\partial}{\partial t}\underline{D} + \underline{J} + \underline{J}_{ext}$$

$$\nabla \cdot \underline{B} = 0$$

$$\nabla \cdot \underline{D} = \rho + \rho_{ext}$$

$$\underline{D} = \epsilon_0 \underline{E}$$

$$\underline{B} = \mu_0 \underline{H} \qquad (2.28a)$$

Dielectric description:

$$\nabla \times \underline{E} = -\frac{\partial}{\partial t}\underline{B}$$

$$\nabla \times \underline{H} = \frac{\partial}{\partial t}\underline{D} + \underline{J}_{ext}$$

$$\nabla \cdot \underline{B} = 0$$

$$\nabla \cdot \underline{D} = \rho_{ext}$$

$$\underline{D} = \epsilon_0 \underline{\kappa} \cdot \underline{E}^{3}$$

$$\underline{B} = \mu_0 \underline{H} \qquad (2.28b)$$

In the preceding sets of equations, ρ_{ext} and $\underline{J}_{ext}$ represent external particle and current densities. We need also the charge relations:

$$\rho = \sum_s q_s \int f_s d^3p \qquad (2.29)$$

$$\underline{J} = \sum_s q_s \int \frac{\underline{p}}{M_s} f_s d^3p \qquad (2.30)$$

In the context of the linear theory we assume that the wave is a small perturbation which causes a perturbation of the particle distribution function which is small with respect to the equilibrium distribution function which exists in the absence of the wave:

$$\underline{E} = 0 + \underline{E}_1(\underline{r},t)$$

$$\underline{B} = \underline{B}_0 + \underline{B}_1(\underline{r},t)$$

$$f_s = f_{0s}(p) + f_{1s}(\underline{r},\underline{p},t) \qquad (2.31)$$

---

[3] Strictly speaking, this expression is valid only for plane waves. If the medium is homogeneous and stationary, the most general linear relationship between $\underline{D}$ and $\underline{E}$ is a convolution whose Fourier-Laplace transform yields this expression (cf. Quemada [1968]).

Assuming the medium as infinite, we can Fourier transform fields and distribution functions in space. Laplace transform is used to transform the time variable. Use of the Laplace transform introduces the physical principle of casuality (the perturbation is considered as beginning at a given time). This condition, initiated by Landau [1946], enables one to give a sense to some integrals otherwise indefinite. After transformation the kinetic equation reads:

$$f_{1s}[\underline{k},\underline{p},\omega] = \underline{Q}_s[\underline{k},\underline{p},\omega]\cdot\underline{E}_1[\underline{k},\omega] + \text{i.t.} \qquad (2.32)$$

(i.t. stands here and hereafter for initial terms involving the spatial Fourier transform of quantities at $t = 0$).

Square brackets are used to distinguish spectral functions from functions in the space-time domain. A transform pair is defined by:

$$f[\underline{k},\underline{p},\omega] = \int_{-\infty}^{\infty} e^{-i\underline{k}\cdot\underline{r}}\, d^3r \int_0^{\infty} dt\, e^{\zeta i\omega t} f(\underline{r},\underline{p},t) \qquad (2.33a)$$

$$f(\underline{r},\underline{p},t) = \frac{1}{(2\pi)^4} \int_{-\infty}^{\infty} d^3k e^{\zeta i\underline{k}\cdot\underline{r}} \int_W d\omega e^{-\zeta i\omega t} f[\underline{k},\underline{p},\omega] \qquad (2.33b)$$

(similar transform pairs are defined for the electromagnetic field). The quantity $\zeta = \pm 1$ is introduced to take care of the two most common conventions in the literature. The contour W is a straight line parallel to the axis $\mathrm{Re}\omega$ and lying above (for $\zeta = +1$) or below (for $\zeta = -1$) the poles of the integrand in order to conserve casuality in the system.

$\underline{Q}_s$ is an operator whose expression is determined by solving the coupled Maxwell and Vlasov equations after linearization.

The current relation is

$$\underline{J}_1 = \sum_s q_s \int_{-\infty}^{\infty} \frac{\underline{p}}{M_s} f_{1s} d^3p = \underline{\sigma}[\underline{k},\omega]\cdot\underline{E}_1[\underline{k},\omega] + \text{i.t.} \qquad (2.34)$$

where the components of the conductivity tensor are given by

$$\sigma_{ab} = \sum_s q_s \int_C \frac{p_a Q_b}{M_s} d^3p \qquad (2.35)$$

where C is a mapping of the contour W. It has been introduced by Landau [1946] in order to facilitate the integration of Eq. (2.35) (see Stix [1962] for example).

In both descriptions (particles in free space and dielectric description) the first Maxwell equation reads:

$$\underline{k}\times\underline{E}_1 = \omega\underline{B}_1 + \text{i.t.} \qquad (2.36)$$

while the second equation, written differently in each description, defines the equivalent dielectric tensors $\underline{\underline{\mathcal{K}}}$:

$$-\underline{k}\times\underline{B}_1 = \frac{\omega}{c^2}\underline{E}_1 + \zeta i\mu_0\underline{J}_1 + \text{i.t.} = \frac{\omega}{c^2}\underline{\underline{\mathcal{K}}}\cdot\underline{E}_1 + \text{i.t.} \qquad (2.37)$$

From this equation we deduce the equivalent dielectric tensor

$$\underline{\underline{\mathcal{K}}}[\underline{k},\omega] = \underline{\underline{I}} - \frac{\underline{\underline{\sigma}}[\underline{k},\omega]}{\zeta i\omega\varepsilon_0} \qquad (2.38)$$

The elimination of vector $\underline{B}_1$ in both Eqs. (2.36) and (2.37) yields the wave equation:

$$\underline{\underline{\Lambda}}[\underline{k},\omega]\cdot\underline{E}_1[\underline{k},\omega] = \underline{S}[\underline{k},\omega] \qquad (2.39)$$

where S takes into account all the initial terms, and

$$\Lambda_{ab} = N_a N_b - N^2\delta_{ab} + \mathcal{K}_{ab} \qquad (2.40)$$

where the refractive index

$$\underline{N} = \frac{c}{\omega}\underline{k} \ . \qquad (2.41)$$

The electric field solution is obtained from Eq. (2.39):

$$\underline{E}_1[\underline{k},\omega] = \underline{\underline{\Lambda}}^{-1}[\underline{k},\omega]\cdot\underline{S}[\underline{k},\omega] = \frac{\underline{\underline{\Lambda}}^{T}[\underline{k},\omega]\cdot\underline{S}[\underline{k},\omega]}{D[\underline{k},\omega]} ,$$

where

$$D[\underline{k},\omega] = \mathrm{Det}(\underline{\underline{\Lambda}}) . \tag{2.42}$$

By inverse Fourier-Laplace transform of Eq. (2.42), we arrive at the solution for $\underline{E}_1$ in the space-time coordinate system. By the residue theorem (assuming the components of $\underline{S}$ to be entire), the only contribution to the integral of the inverse transform comes from the poles of the integrand, that is, the zeros of the denominator.

The equation which gives the zeros of the denominator in Eq. (2.42), i.e.,

$$D[\underline{k},\omega] = 0 \tag{2.43}$$

is called the dispersion equation. Its solutions define the wave modes of the wave-plasma system. Equation (2.43) can be satisfied for complex values of $\underline{k}$ or ω (in fact to be consistent with previous convention ω has to be considered in general as complex). For instance a complex value of ω for real $\underline{k}$ means either wave growth or damping according to signs of $\omega_i = \mathrm{Im}\omega$. If $\zeta\omega_i > 0$, the perturbation will grow without limit with time and the distribution is unstable. However, the fact that the perturbation can grow with time is not enough to determine the spatial characteristics of the growth. The perturbations are not single monochromatic plane waves but a superposition of them given by the Fourier-Laplace integrals (2.33a,b). A single frequency may grow exponentially with time but the amplitude of the wave packet as a whole may remain finite at a fixed point in space. This leads to the distinction of two kinds of instabilities, "convective" and "absolute" (or nonconvective) instabilities. In convective growth, the wave packet is amplified as it moves along (that is, at each point in space it first grows and then

decays), whereas in the second case it grows without limit in each point of space as $t \to \infty$. For further discussion, see for instance Akhiezer et al [1967]. This distinction has been discussed by Sturrock [1958]. Rather involved criteria have been developed to distinguish between the two kinds of instability [Briggs, 1964; Derfler, 1967, 1970]. For the first kind of instability, the medium acts like an amplifier, whereas for the second case, it works like an oscillator.

The work of Lee [1969], and Lee and Crawford [1970], though restricted to strictly parallel propagation, showed that in the magnetosphere absolute instabilities appear to occur only under extreme conditions. Therefore, we shall assume hereafter that we deal only with convective instabilities. For convective instabilities it is immaterial whether we consider ω real and $\underline{k}$ complex or vice versa. Provided $|\underline{k}_i| \ll |\underline{k}|$ and $|\omega_i| \ll \omega$, it can be shown that $\underline{k}_i$ and ω_i are related by the relationship

$$\omega_i = - \underline{k}_i \cdot \underline{v}_g \tag{2.44}$$

where $\underline{v}_g$ is the group velocity of the wave packet. The physical content of Eq. (2.44) is that ω_i describes the wave packet amplitude variation in the wave group velocity frame. Convenience will dictate the choice of the complex variable. For present purposes it will be more convenient to discuss gain rates per unit distance whereas in ray tracings parameterized in the time variable, it will be more convenient to work with gain rates per unit time.

We derive in the next section the expression giving the growth rates of small amplitude waves propagating in a magnetoplasma composed of a cold plasma permeated by a tenuous energetic particle population.

D. GROWTH RATE EXPRESSIONS

In order to derive the dispersion relation for our system it is first necessary to determine the tensor $\underline{\underline{K}}$. The derivation of the expression of $\underline{\underline{K}}$ is somewhat lengthy but does not present any particular difficulty. It has been given in a number of textbooks [Montgomery and Tidman, 1964; Bekefi, 1966] and we do not repeat it here. In general $\underline{\underline{K}}$ can be expressed in the form (where we have explicitly derived the relativistic form):

$$\underline{\underline{K}} = \underline{\underline{I}} - \sum_s \gamma_s \sum_{m=-\infty}^{\infty} \int_0^{\infty} \int_{-\infty}^{\infty} 2\pi \, dp_\perp \frac{dp_\parallel}{|k_\parallel|} \frac{\underline{\underline{\pi}}(p_\parallel, p_\perp)}{p_\parallel - p_{Rm}} , \qquad (2.45)$$

where:

$$\frac{1}{p_\parallel - p_{Rm}} = V(p_\parallel, p_\perp) \left(\frac{1}{p_\parallel - p_{Rm1}} - \frac{1}{p_\parallel - p_{Rm2}} \right) ,$$

$$V(p_\parallel, p_\perp) = \frac{N_\parallel p_\parallel + \frac{m}{\Lambda} p_0 + \sqrt{p_0^2 + p_\perp^2 + p_\parallel^2}}{2\sqrt{\frac{m^2}{\Lambda^2 N_\parallel^2} p_0^2 + (1 - \frac{1}{N_\parallel^2})(p_0^2 + p_\perp^2)}}$$

In Eq. (2.45) the expressions for $p_{Rm1,2}$ are as given by Eq. (2.10), provided in the expression of $N_\parallel = kc/\omega$, ω is considered now as complex. In the non-relativistic limit $V(p_{Rm1}, p_\perp) \to 1$, $V(p_{Rm2}, p_\perp) \to 0$, and $p_{Rm1} \to p_{Rm0}$, with p_{Rm0} given by Eq. (2.12) (where again ω must be considered as complex).

In Eq. (2.45)

$$\underline{\underline{\pi}} = \underline{\underline{J}}_s \cdot \underline{\underline{U}}_s ,$$

and

$$\underline{\underline{J}}_s = \begin{pmatrix} \left(\frac{mJ_m}{a_s}\right)^2 p_\perp^2 & \zeta\zeta_s i \frac{mJ_m J'_m}{a_s} p_\perp^2 & \frac{mJ_m^2}{a_s} p_\parallel p_\perp \\ -\zeta\zeta_s i \frac{mJ_m J'_m}{a_s} p_\perp^2 & (J'_m)^2 p_\perp^2 & -\zeta\zeta_s i J_m J'_m p_\parallel p_\perp \\ \frac{mJ_m^2}{a_s} p_\parallel p_\perp & \zeta\zeta_s i J_m J'_m p_\parallel p_\perp & J_m^2 p_\parallel^2 \end{pmatrix} \quad (2.46)$$

where $\zeta_{i,e} = \pm 1$ and J_m and J'_m are the Bessel functions of order m and their derivatives of argument:

$$a_s = \frac{k_\perp p_\perp}{M_s \omega_{cs}} \quad (2.47)$$

The quantity $\underline{\underline{U}}_s$ has the definition:

$$\underline{\underline{U}}_s = \begin{pmatrix} U_s & 0 & 0 \\ 0 & U_s & 0 \\ 0 & 0 & U_{ls} \end{pmatrix},$$

$$U_s = (M_s\omega - k_\parallel p_\parallel) \frac{\partial g_{0s}}{\partial p_\perp} + k_\parallel p_\perp \frac{\partial g_{0s}}{\partial p_\parallel} ,$$

$$U_{ls} = M_s\omega \frac{\partial g_{0s}}{\partial p_\parallel} - M_s \frac{m\omega_{cs}}{p_\perp} \left(\frac{\partial g_{0s}}{\partial p_\parallel} p_\perp - \frac{\partial g_{0s}}{\partial p_\perp} p_\parallel \right). \quad (2.48)$$

where g_{0s} is the equilibrium distribution function of particles of species s normalized to unity:

$$\int g_{0s} \, d^3p = 1 \quad (2.49)$$

When g_0 can be represented as a relatively high density cold plasma background permeated by a relatively low density energetic particle distribution (as is the case in the inner magnetosphere), then we can write

$$\begin{cases} g_0 = g_{0c} + g_{0H} \\ \int g_{0H}\, d^3p \ll g_{0c}\, d^3p \end{cases} \tag{2.50}$$

and use the approximation:

$$\begin{cases} \int \frac{u(p_\parallel)}{p_\parallel - p_{Rm}}\, dp_\parallel \sim P \int_{-\infty}^{\infty} \frac{u(p_\parallel)}{p_\parallel - p_{Rm}}\, dp_\parallel + \zeta i\pi \cdot u(p_{Rm}) \\ \zeta \ \mathrm{Im}\ p_{Rm} > 0 \end{cases} \tag{2.51}$$

and its analytical continuation in the other half-plane in the Landau sense. P means that the principal part of the integral, in the Cauchy sense, has to be taken and u stands for an arbitrary function of $p_\parallel$. Inserting the expression of p_{Rm} given by Eq. (2.8) into Eq. (2.48) we find:

$$U_{1s}\Big|_{p_{Rm}} = \frac{p_\parallel}{p_\perp} \cdot U_s\Big|_{p_{Rm}} \tag{2.52}$$

and in this case the Onsager relations hold ($\mathcal{K}_{xz} = \mathcal{K}_{xz}, \mathcal{K}_{yz} = \mathcal{K}_{zy}$; the relation $\mathcal{K}_{xy} = \mathcal{K}_{yz}$ was already fulfilled).

Condition (2.50) enables one to develop Eq. (2.43) in the form [Kennel, 1966]:

$$D[\underline{k},\omega] \sim D_0[\underline{k},\omega] + D_1[\underline{k},\omega] = 0 \tag{2.53a}$$

where D_0 is the cold plasma dispersion relation (given later by Eq. (2.57)) and $|D_1| \ll |D_0|$. Since the energetic population is dilute, the real part of the refractive index is determined by $D_0[\underline{k}_r,\omega] = 0$ (see Appendix C). Assuming real ω and complex $\underline{k}$, Eq. (2.53a) is rewritten as

$$D[\underline{k}_r + i\underline{k}_i,\omega] \sim D_0[\underline{k}_r,\omega] + i\underline{k}_i \cdot \frac{\partial D_0}{\partial \underline{k}} + \mathrm{Re}\left\{D_1[\underline{k}_r,\omega]\right\} + i\ \mathrm{Im}\left\{D_1[\underline{k}_r,\omega]\right\} = 0 \tag{2.53b}$$

which shows that:

$$\underline{k}_i \cdot \frac{\partial D_0}{\partial \underline{k}} = - \text{Im } D_{1r} \tag{2.54}$$

where $\text{Im } D_1[\underline{k}_r, \omega]$ is rewritten as $\text{Im } D_{1r}$ for short.

Now,

$$\underline{v}_g = - \frac{\partial D_0}{\partial \underline{k}} \Big/ \frac{\partial D_0}{\partial \omega} \tag{2.55}$$

that is $\frac{\partial D_0}{\partial \underline{k}}$ is colinear with $\underline{v}_g$ and Eq. (2.54) enables one to evaluate k_{ig} (component of $\underline{k}_i$ along $\underline{v}_g$), which is the physically meaningful quantity since wave amplitude gain has to be evaluated along the ray path. It can be shown that $\frac{\partial D_0}{\partial \omega} > 0$, so that, according to Eq. (2.55)

$$k_{ig} = \frac{-\underline{k}_i \cdot \frac{\partial D_0}{\partial \underline{k}}}{\left| \frac{\partial D_0}{\partial \underline{k}} \right|} = \frac{\text{Im } D_{1r}}{\left[\left(\frac{\partial D_0}{\partial k} \right)^2 + \left(\frac{\partial D_0}{\partial k_\perp} \right)^2 \right]^{1/2}} \tag{2.56}$$

where:

$$D_0 = A_S N^4 - B_S N^2 + C_S \tag{2.57}$$

where A_S, B_S and C_S are the parameters introduced by Stix [1962]:

$$A_S = \sin^2\theta + P \cos^2\theta ,$$

$$B_S = RL \sin^2\theta + PS (1 + \cos^2\theta) ,$$

$$C_S = PRL ,$$

$$S = \frac{1}{2} (R + L) , \quad D_S = \frac{1}{2} (R - L) ,$$

$$R = 1 - \sum_s \gamma_s \frac{\omega}{\omega + \zeta_s \omega_{cs}} , \quad L = 1 - \sum_s \gamma_s \frac{\omega}{\omega - \zeta_s \omega_{cs}} ,$$

$$P = 1 - \sum_s \gamma_s ; \tag{2.58}$$

so that:

$$k_{ig} = \frac{\text{Im } D_{lr}}{2\left|2A_S N^2 - B_S\right|\frac{Nc}{\omega}} \cos\alpha_g \quad . \tag{2.59}$$

If time gain is more appropriate, it is immediately given by Eq. (2.44), i.e.,

$$\omega_i = - k_{ig} \left|\underline{v}_g\right| \tag{2.60}$$

where

$$\underline{v}_g = \frac{c}{\frac{\partial(\omega N)}{\partial\omega}} \left[\underline{e}_k - \frac{1}{2}\frac{\partial}{\partial\theta} \ell n(N)^2 \underline{e}_\theta\right] \tag{2.61}$$

and $\underline{e}_k$ and $\underline{e}_\theta$ are the unit vectors along and across $\underline{k}$ respectively. With condition (2.50) we have:

$$\underline{\underline{\kappa}} = \underline{\underline{\kappa}}^h + i\underline{\underline{\kappa}}^a \quad \text{with} \quad \left|\kappa^a_{ab}\right| \ll \left|\kappa^h_{ab}\right| \tag{2.62}$$

where $\underline{\underline{\kappa}}^h$ and $\underline{\underline{\kappa}}^a$ are respectively the Hermitian and antiHermitian part of the dielectric tensor:

$$2\underline{\underline{\kappa}}^h = \underline{\underline{\kappa}} + \underline{\underline{\kappa}}^\dagger \quad , \quad 2i\underline{\underline{\kappa}}^a = \underline{\underline{\kappa}} - \underline{\underline{\kappa}}^\dagger \tag{2.63}$$

where $\dagger$ denotes the Hermitian conjugate (complex conjugate of the transpose). With Eq. (2.63):

$$\begin{aligned} \text{Im } D_{lr} &= \kappa^a_{xx} (S-N^2)(P-N^2\sin^2\theta) \\ &+ \kappa^a_{yy} [(S-N^2\cos^2\theta)(P-N^2\sin^2\theta) - N^4\cos^2\theta\sin^2\theta] \\ &+ \kappa^a_{zz} [2D_S(P-N^2\sin^2\theta)] - \kappa^a_{xz}[2(S-N^2)N^2\cos\theta\sin\theta] \\ &- 2\zeta D_S [\kappa^a_{xy}(P-N^2\sin^2\theta) + \kappa^a_{xz}(N^2\cos\theta\sin\theta)] \end{aligned} \tag{2.64}$$

and with approximation (2.51):

$$\underline{\underline{\kappa}}^a = -\zeta \sum_s \frac{2\pi^2\gamma_s}{k_\parallel} \sum_{m=-\infty}^{m=\infty} \int_0^\infty \sum_{i=1}^{2} \underline{\underline{J}}_s(p_{Rmi}, p_\perp) U_s(p_{Rmi}, p_\perp) V(p_{Rmi}, p_\perp) dp_\perp \tag{2.65}$$

so that:

$$\text{Im } D_{lr} = -\zeta \sum_s \frac{2\pi^2 \gamma_s}{k_\parallel} \sum_{m=-\infty}^{\infty} \int_0^\infty \sum_{i=1}^{2} U_s(p_{Rmi}, p_\perp) V(p_{Rmi}, p_\perp)$$

$$\left\{ p_\perp^2 \left[(S-N^2)(P-N^2\sin^2\theta) \left(\frac{mJ_m}{a_s}\right)^2 + 2\zeta_s D_S (P-N^2\sin^2\theta) \frac{mJ_m J'_m}{a_s} \right] \right.$$

$$+ p_\perp^2 \left[(S-N^2\cos^2\theta)(P-N^2\sin^2\theta) - N^4\cos^2\theta \right] (J'_m)^2$$

$$- 2p_{Rmi} p_\perp N^2 \cos\theta\sin\theta \left[\frac{m^2 J_m^2}{a_s} (S-N^2) + \zeta_s D_S J_m J'_m \right]$$

$$\left. + p_{Rmi}^2 \left[(S-N^2\cos^2\theta)(S-N^2) - D_S^2 \right] J_m^2 \right\} dp_\perp \qquad (2.66)$$

Apart from the relativistic correction and the simplification (2.52) this expression has been derived by Kennel [1966]. Equation (2.66) has been further simplified by Brinca [1972] by making use of the cold plasma dispersion relation rewritten as:

$$[(S-N^2\cos^2\theta)(S-N^2)-D_S^2](P-N^2\sin^2\theta) = (S-N^2)N^4\sin^2\cos^2\theta \ . \qquad (2.67)$$

Using Eq. (2.52) brings still further simplification compared to Brinca's expression (enabling one to use once more Eq. (2.67)) and Eq. (2.66) can be cast into the compact and relatively simple form:

$$\text{Im } D_{lr} = \Gamma \sum_{m=-\infty}^{\infty} \int_0^\infty \sum_{i=1}^{2} V(p_{Rmi}, p_\perp) \Theta_{ms}(p_{Rmi}, p_\perp) U_s(p_{Rmi}, p_\perp) p_\perp^2 \, dp_\perp$$

where:

$$\Gamma = -\zeta \sum_s \frac{\pi^2}{2} \frac{\gamma_s}{\omega^2 |k_\parallel| H}, \qquad H = \frac{N_\perp^2 - P}{N^2 - S},$$

$$\Theta_{ms} = (C_{m1} J_{m-1} + C_{m2} J_{m+1})^2, \quad m \neq 0,$$

$$\Theta_{0s} = 4[M_s c N_\perp J_0 + \zeta_s D_s H p_\perp J_1]^2 \frac{1}{p_\perp^2},$$

$$C_{m1} = H(N^2 - L_s) + N_\perp^2 \left(\frac{\Lambda_s}{m} - 1 \right), \quad C_{m2} = H(N^2 - R_s) + N_\perp^2 \left(\frac{\Lambda_s}{m} - 1 \right),$$

$$R_{e,i} = R, L, \quad L_{e,i} = L, R .^4 \tag{2.68}$$

The expression of k_{ig} is easily obtained by inserting Eq. (2.68) into Eq. (2.56) or Eq. (2.59):

$$k_{ig} = -\zeta \frac{\pi^2}{4} \frac{\cos\alpha_g}{\cos\theta} \sum_s \frac{\omega_{ps}^2}{\omega^2 N^2 F H} \sum_{m=-\infty}^{\infty} \int_0^\infty \sum_{i=1}^{2} V(p_{Rmi}, p_\perp) \Theta_{ms}(p_{Rmi}, p_\perp) U_s(p_{Rmi}, p_\perp) p_\perp^2 dp_\perp,$$

$$F = \left[(RL - PS)^2 \sin^4\theta + 4P^2 D_S^2 \cos^2\theta \right]^{1/2} \tag{2.69}$$

It can be shown that $V(p_{Rmi}, p_\perp)$, $i=1,2$, are positive-definite quantities, therefore the integral in Eq. (2.69) is positive-definite. Furthermore the quantity H is positive. Therefore Eq. (2.68) facilitates a straightforward discussion of stability. The distribution function g_0, being a solution of the Vlasov equation, can be expressed according to Liouville's theorem in terms of invariants of the particle motion. In the magnetosphere the simplest choice of invariants is p (we assume no dc electric field) and the first adiabatic invariant $\frac{\sin\alpha}{\sqrt{b}}$ (where $b \equiv |\underline{B}_0 / \underline{B}_{0E}|$ is the dc magnetic field normalized to equatorial value).

---

[4] Notice the inversion between R and L according to the sign of the particle charge. We have defined as $m = +1$ the resonance at parallel propagation for either sign. In that case only $C_{11} \neq 0$ as $N^2 - R_s = 0$ either for normal electron interaction ($N^2 = R$) or for normal ion interaction ($N^2 = L$).

Therefore it will be more convenient to express U_s given by Eq. (2.48) in terms of derivatives with respect to p and $\sin\alpha$:

$$U_s = M_s \omega \left[\sin\alpha \frac{\partial g_{0s}}{\partial p} + \frac{1}{p} \frac{\partial g_{0s}}{\partial(\sin\alpha)} (-\sin^2\alpha + \frac{m}{\Lambda_s}) \right] \qquad (2.70)$$

If we now assume that the energetic component of the plasma consists only of electrons whose distribution function decreases monotonically with energy $\left(\frac{\partial g_0}{\partial p} < 0 \right)$ (see Section 3B) and increases monotonically with pitch angle $\left(\frac{\partial g_0}{\partial(\sin\alpha)} > 0 \right)$, we reach the following conclusion concerning stability:

1. Landau interaction: $m = 0$, always damping ($U < 0$ always)
2. Anomalous gyroresonance interaction: $m < 0$, always damping ($U < 0$ always)
3. Normal gyroresonance interaction: $m > 0$, U can be > 0 or < 0 and there will be accordingly growth or damping; because of the positive term m/Λ in Eq. (2.70), small values of Λ will favor growth [Kennel, 1966; Liemohn, 1967]. Isotropic distribution $(\partial g_0)/\partial(\sin\alpha) = 0$ cause only damping.

For parallel propagation ($k_\perp = 0$), $a_s = 0$ and all Bessel functions are null except J_0, that is, only the term $m = 1$ is to be considered. Kennel [1966] found that the gain is maximum for parallel propagation for low frequency waves though a thorough investigation not restricted to only very small frequencies may yield an opposite conclusion [Brinca, 1972].

Within the standard approximation, Eq. (2.69) can be written in a simpler form (neglecting ions):

$$k_{ig} = -\frac{\zeta\pi^2}{2}\frac{\cos\alpha_g}{\cos\theta}\frac{|P|}{N^2}\sum_{m=-\infty}^{\infty}\int_0^{\infty}\frac{\Theta_m}{C_0^2\cos^2\theta}U_m p_\perp^2 dp_\perp,$$

$$C_0 = C_{11}(\theta = 0) = 2|P| ,$$

$$C_{m1,2}\Big/ C_0 = \frac{1}{2}(t_1 + t_2), \quad t_1 = 1\pm\cos\theta, \quad t_2 = \frac{\Lambda^2\sin^2\theta}{(\cos\theta-\Lambda)m} , \; m \neq 0 ,$$

$$\frac{\Theta_0}{C_0^2} = \left(\frac{N_\perp}{|P|}\frac{p_0}{p_\perp}J_0 - \cos\theta\, J_1\right)^2 . \qquad (2.71)$$

Expression (2.71) is valid in the context of the standard approximation and for arbitrary frequency (provided the wave is not in the vicinity of both the LHR and the resonance cone). It is practically as simple as the low frequency approximation ($\Lambda \ll 1$) of Kennel [1966]. There are two differences between Eq. (2.71) and Kennel's expression:

1. For the cyclotron harmonics ($m \neq 0$), the coefficients $C_{m1,2}$ are now the sum of two terms: t_1, given already by Kennel and a new term t_2 which increases with θ.
2. For the Landau interaction ($m = 0$), Θ_0 is now the sum of a term involving J_1, given by Kennel, and a new term involving J_0.

Let us test the validity of Kennel's [1966] approximations. At the Gendrin angle θ_G, for low frequencies:

$$t_2 = \frac{\Lambda(1-4\Lambda^2)}{m} \sim \frac{\Lambda}{m} , \qquad (2.72)$$

and still can be considered as small compared to the first term

$$t_1 = 1 \pm 2\Lambda \sim 1 . \qquad (2.73)$$

But this is no longer true when $\theta \to \theta_R$, where on the contrary t_2 is the dominant term and t_1 can be neglected. Therefore Kennel's

approximation for the cyclotron harmonics is valid for $\theta < \theta_G$ but not for $\theta > \theta_G$.

Neglecting the first term in Θ_0 is more drastic because by expansion of J_1, both terms in Θ_0 are of the same order (in small Λ or small θ). This point requires further investigation with respect to Kennel's [1966] conclusions (see Section 3E).

It is possible to give a physical interpretation of each term in Θ_0. The first term corresponds to the "classical" Landau interaction. It is a result of the action of the parallel component of the electric field upon the motion of the particle. The second term corresponds to "transit time" Landau interaction. It is a result of the presence of a non-zero parallel component of the magnetic field for non-parallel propagation [Stix, 1962]. This component acts on the particle according to the equation

$$M \frac{dv_z}{dt} = - \mu \frac{\partial B_z}{\partial z}$$

where $\mu = Mv_\perp^2/2B_0$ is the magnetic moment of the particle. Note that both effects tend to disappear when $\Lambda \to 0$.

When $\theta \to \theta_R$:

$$C_{m1} \to C_{m2} = C_m = N_\perp^2 \frac{\Lambda}{m} ,$$

$$\Theta_m \to \left(2N_\perp \frac{p_0}{p_\perp} J_m \right)^2 , \quad \text{for all } m . \qquad (2.74)$$

In the next chapter, we will obtain quantitative values of k_{ig} by choosing realistic models of distribution functions in the magnetosphere.

III. VARIATIONS OF GAIN RATES WITH MAGNETOSPHERIC PARAMETERS

A. INTRODUCTION

The variations of whistler wave amplitudes caused by wave-particle interaction depend upon both the cold plasma and hot plasma distributions. Although models of the cold plasma are fairly extensively known, mainly from nose whistler measurements (cf. references of Chapter 1), energetic particle distributions are much less known. Both for lack of information and for computational convenience only simple models of hot plasma will be considered here. Limits on these models will be set by whistler observations.

The purpose of the chapter is to study in detail the variation of wave amplitude gain with respect to various magnetospheric parameters.

In Section B we review models of the cold plasma as deduced from nose whistler measurements, and a few energetic particle measurements. The assumption of parallel propagation has played a considerable role in whistler analysis, in part because the first whistler observations were made on the ground where only ducted whistlers could be recorded, and in part because of substantial simplifications in the analysis. In Section C, we study in detail the variation of wave gain for parallel propagation, assuming that the class of distributions is similar to that chosen by Liemohn [1967]:

$$f(W,\alpha) \propto W^{-\nu} \sin^{q}\alpha \qquad (3.1)$$

This model has several advantages. It is mathematically simple. The energy variation is reasonable, compared to particle data. As of now, no experimental data have confirmed the pitch angle variation, but a general pitch angle distribution can be decomposed as a superposition of such functions.

The model (3.1) is most likely oversimplified. It assumes separability in energy and pitch-angle. This simplification is relaxed in Section D where we study a more general class of distributions that are nonseparable in energy and pitch-angle. This new class of distributions can have radically different characteristics from the previous class.

In Section E, we make a detailed study of the variation of the gain with respect to arbitrary angles of propagation and frequency, and in Section F, we review the important contributions of the chapter.

B. PARTICLE DISTRIBUTIONS IN THE MAGNETOSPHERE

1. Cold Plasma Distribution

Inside the plasmapause, the cold plasma distribution has been very successfully described by the diffusive equilibrium model of Angerami [1966] (see also Park [1973]).

Apart from the vicinity of the top of the ionosphere and beyond $L \gtrsim 6$, the full model with three types of ions and a gravity term does not differ significantly from the following idealized model:

$$n = n_E \exp\left[\frac{R_1}{2H_H}\left(\frac{R_1}{r} - \frac{R_1}{R_E}\right)\right] \tag{3.2}$$

Subscripts E and 1 refer respectively to equator and base level (1000 km altitude),

n = density

r = geocentric distance

R_1 = geocentric distance at 1000 km altitude

R_E = dipole magnetic field equatorial geocentric distance

H_H = hydrogen scale height = $KT/M_H g_1$

K = Boltzmann's constant

T = temperature

g = acceleration of gravity.

To complete the description of the model, we need the equatorial density profile. C. G. Park [private communication] has established an average equatorial profile based on whistler measurements in the month of June, 1965. It is given in Figure 3.1 (solid line). An equatorial density decrease as L^{-2} for $L \lesssim 4$ and as L^{-4} for $L \gtrsim 4$ seems to fit closely the actual variation. Contours of constant $\beta = \omega_p/\omega_c$ are plotted in Figure 3.2, assuming an average variation $n_E(L) \propto L^{-3}$ and $n_E(4) = 250\ cm^{-3}$, to which corresponds $\beta_E(4) \sim 10$. Using values of β given by the figure, one can deduce from Figures 2.1 and 2.4 the minimum energy of resonance for cyclotron and Landau interactions at each point of the plasmasphere. This is a very useful quantity to know, since the number of particles available at a given resonance provides an estimate of the importance of the resonance. Since $W_{Rm} \propto n^{-1}$, it is a simple matter to deduce W_{Rm} from a density profile different from Figure 3.2. It can be seen from Figure 3.2 that the standard approximation is valid practically everywhere inside the plasmasphere. A few values of $W_{R1}(\Lambda = 0.5, \theta = 0)$ are given in the figure.

Outside the plasmapause, a completely satisfactory model is not yet available though the collisionless model of Angerami [1966] seems reasonable. This model is close to an r^{-4} model. With such a model the contours of constant β are plotted on Figure 3.3. assuming $n_E(L) \propto L^{-4}$, and $n_E(4) = 10\ cm^{-3}$ to which corresponds $\beta_E(4) \sim 2$.

2. Hot Plasma Distribution

Most of the early particle observations in the magnetosphere were obtained with instruments (such as Geiger tubes or scintillation

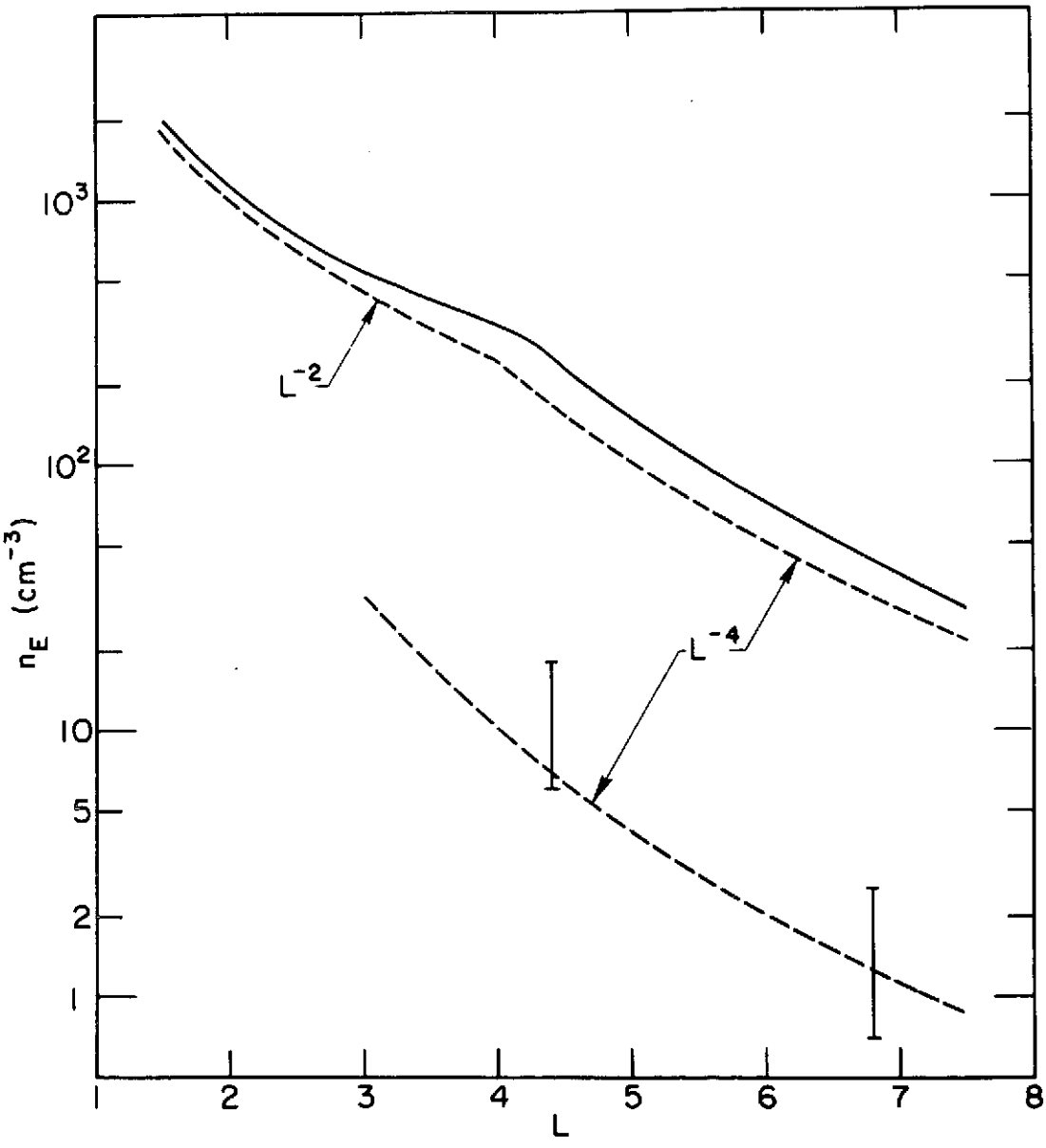

FIGURE 3.1. EQUATORIAL ELECTRON DENSITY PROFILE DEDUCED FROM NOSE WHISTLER DATA ASSUMING A DIFFUSIVE EQUILIBRIUM MODEL (SOLID LINE, C. G. PARK, PRIVATE COMMUNICATION) AND A COLLISIONLESS MODEL (ERROR BARS FROM ANGERAMI [1966]). The dashed curves show comparison with L^{-2} and L^{-4} models for the D.E. model and with an L^{-4} model for the collisionless model.

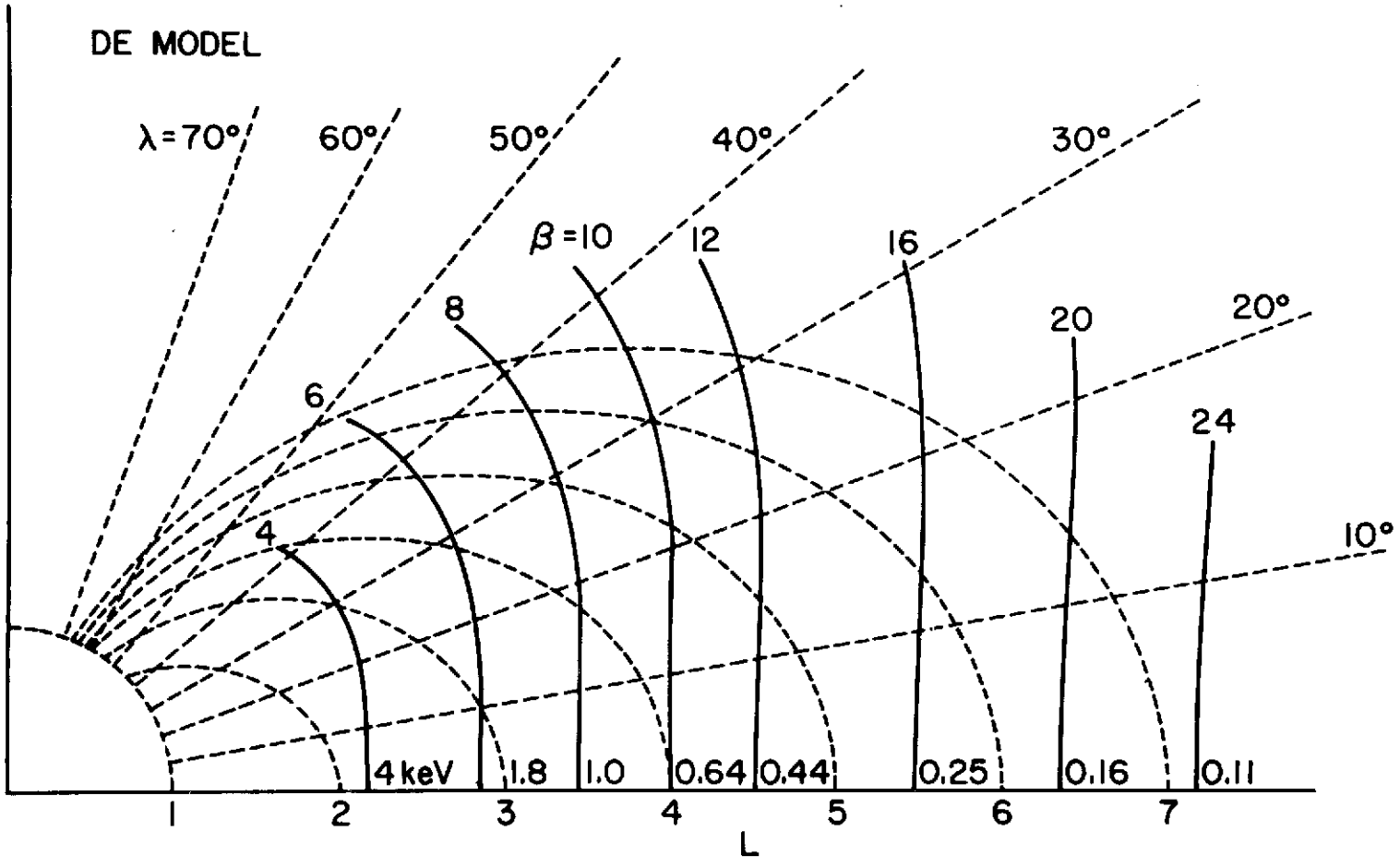

FIGURE 3.2. CONTOURS OF CONSTANT β FOR A SIMPLIFIED D.E. MODEL ASSUMING AN EQUATORIAL ELECTRON DENSITY VARIATION $\propto L^{-3}$. Energy numbers correspond to W_{R1} ($\Lambda = 0.5$; $\theta = 0$).

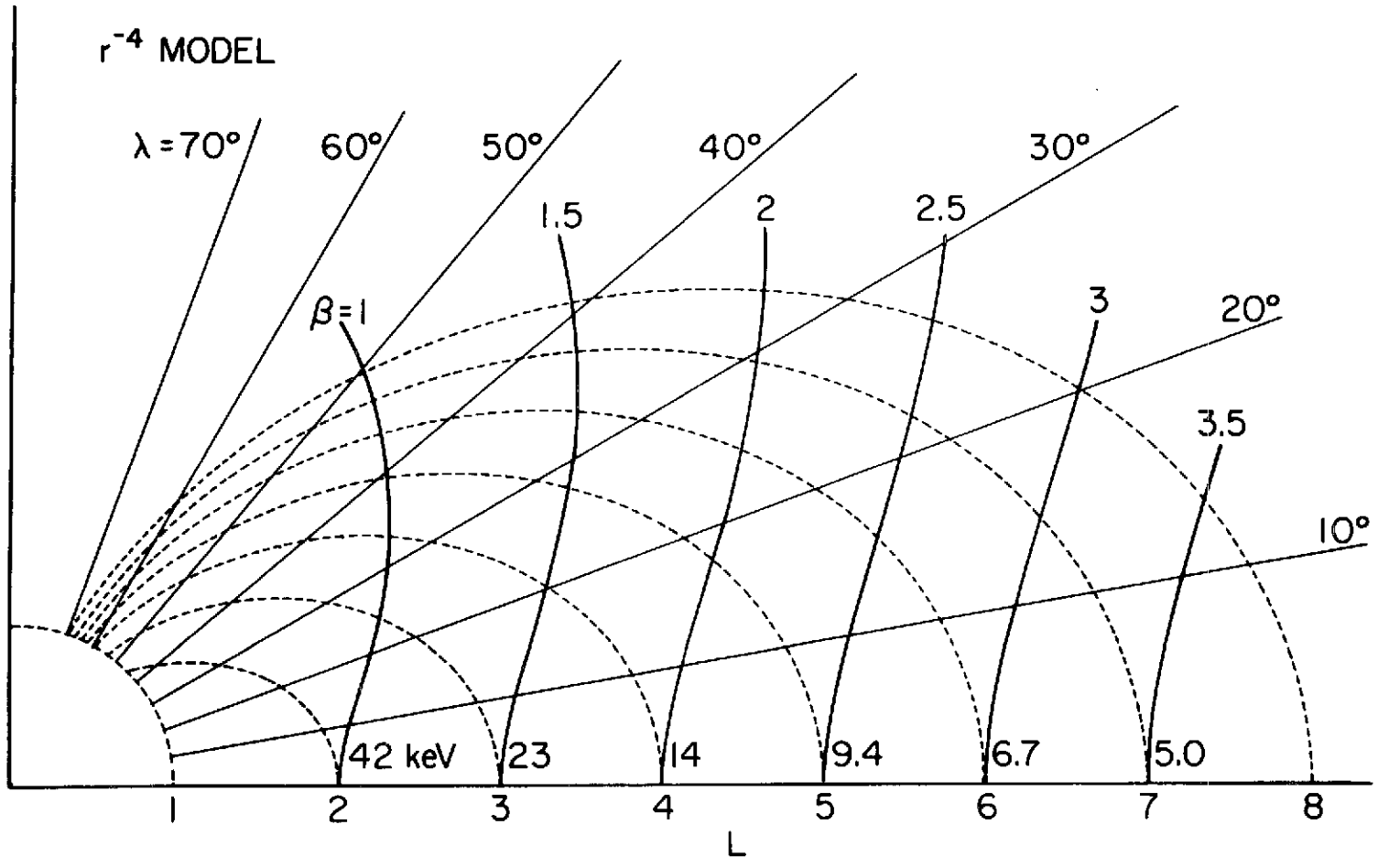

FIGURE 3.3. A PLOT SIMILAR TO FIGURE 3.2 BUT FOR AN r^{-4} MODEL ASSUMING $n_E \propto L^{-4}$.

counters) capable of observing electrons only above an energy of $\sim$ 40 keV (see review in Hess [1968] and also Russell and Thorne [1969] and Vasyliunas [1969]). Now the bulk of whistler-electron resonance interaction occurs within the energy range 100 eV - 40 keV, at least inside the plasmapause and knowledge of particles in that energy range is essential. However, information on the particle distribution in this energy range is still meager.

As of now, to the author's knowledge, the only published data of differential fluxes of 100 eV - 40 keV particles are from Schield and Frank [1970]. We have reprinted on Figure 3.4 two of the figures from this paper which show fluxes observed during times following a long period of low magnetic activity. The features of the distribution functions seem fairly repeatable.

Let us focus our attention on the plasmasphere spectrum. Above $\sim$ 1 keV, the distribution function falls off smoothly like $\sim \frac{1}{v^5}$ (see Figure 3.4). There is a flattening of the distribution in the 500 eV - 1 keV range. In the lower energy range (W < 500 eV), the spectrum[5]

---

[5] Confusion may arise in the term "spectrum." Let us be clear about our definitions. The number of particles in a given velocity range is, by convention:

$$dn = f(v)d^3v$$

where dn is the number density and f(v) is the "particle distribution function." For comparison with data, it is convenient to define the "particle distribution function in energy" F:

$$dn = F(W,\Omega)dWd\Omega$$

where Ω is the solid angle. Experimentally, the current density is measured in terms of the quantity:

$$dJ = evf(v)d^3v$$

from which the differential flux $d\Phi$ is obtained:

$$d\Phi = \frac{dJ}{edWd\Omega} = vF(W,\Omega)$$

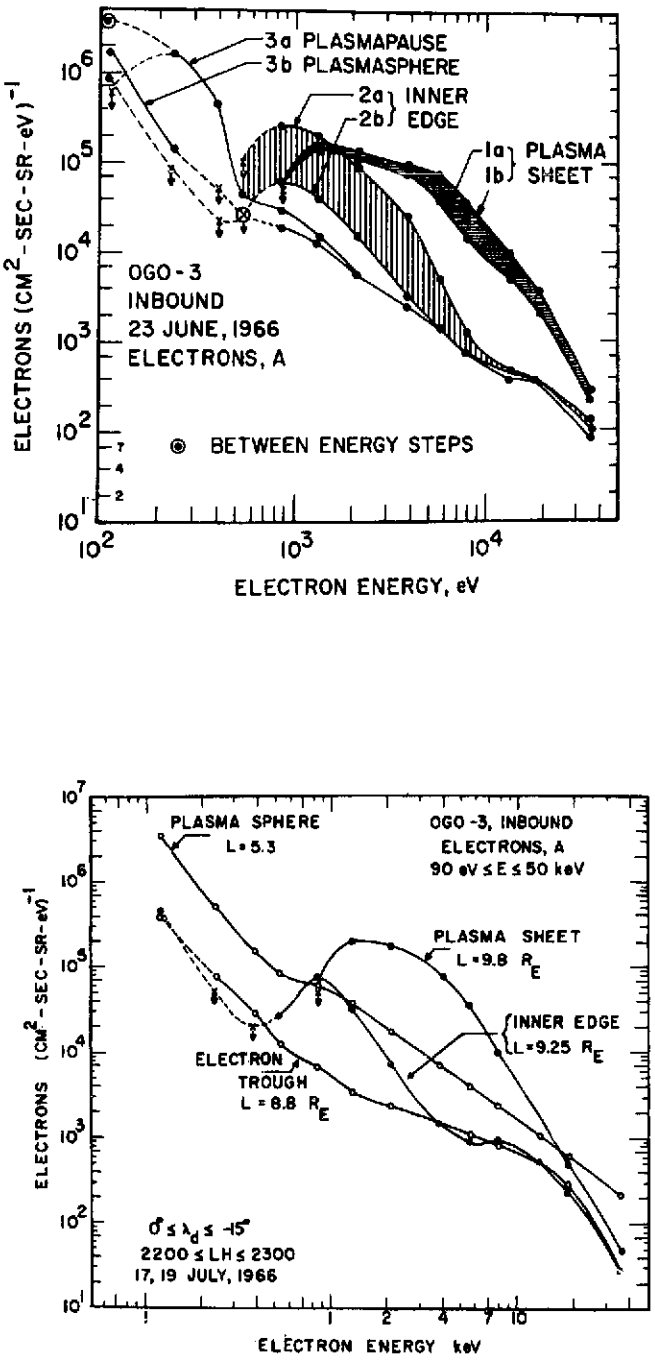

FIGURE 3.4. DIFFERENTIAL ELECTRON FLUXES IN DIFFERENT REGIONS OF THE MAGNETOSPHERE, FROM SCHIELD AND FRANK [1970].

becomes softer with $f(v) \propto \sim \frac{1}{v^7}$. For further details, the reader is referred to Schield and Frank [1970].

C. PARALLEL PROPAGATION FOR A DISTRIBUTION SEPARABLE IN ENERGY AND PITCH ANGLE

1. Introduction

Parallel propagation has played a considerable role in whistler stability analysis (e.g., Scarf [1962]; Tidman and Jaggi [1962]; Liemohn and Scarf [1962a,b, 1964]; Guthart [1964, 1965]; Liemohn [1967, 1969], to limit ourselves to work explicitly related to whistler gain in the magnetosphere). One reason for that choice is that the first observations were made before the satellite era and in that case only ducted signals could be observed. Moreover the abundance of ground data proves that it is a very important case. Therefore the parallel propagation approximation is a valid approximation for all ground whistler data, at least as long as cold plasma propagation is concerned. A second reason is that the gain expression (2.69) which is rather complex simplifies considerably for parallel propagation. It reduces to:

$$_{\parallel}k_{ig} = -\zeta \frac{\pi^2}{2} \sum_s \frac{\omega_{ps}^2}{\omega^2 N^2} \int_0^\infty dp_\perp p_\perp^2 \sum_{1,2} V_{1,2} U_s(p_{Rm}, p_\perp) \qquad (3.3)$$

In the standard approximation and neglecting ions Eq. (3.3) is rewritten following Kennel and Petschek [1966]:

---

and the change of units is the following:

$$d\Phi\,[(cm^2 \times sec \times sr \times eV)^{-1}] = 1.76 \times 10^5 (vF) \quad [C.G.S.]$$

Note that:

$$f \propto vF ,$$
$$d\Phi \propto v^2 f .$$

When we discuss a spectrum $\propto \frac{1}{v^\nu}$, there may arise some confusion about whether we mean f, F or $d\Phi$. Unless otherwise specified, we will always implicitly define ν as the energy parameter of the "spectrum" associated with the distribution function f(v).

$$
{}_{\parallel}k_{ig} = \zeta \frac{\pi^2 \omega_p^2}{\omega^2 N^2} M_0 \omega \left[1 - \left(\frac{1}{\Lambda} - 1\right) A_{KP}\right] \int_0^\infty g_0 p_\perp dp_\perp \Bigg|_R ,
$$

$$
A_{KP} = \frac{\displaystyle\int_0^\infty \sin\alpha \, \frac{\partial g_0}{\partial(\sin\alpha)} \, p_\perp dp_\perp}{2 \displaystyle\int_0^\infty g_0 p_\perp dp_\perp} \Bigg|_R \qquad (3.4)
$$

Equation (3.4) shows that

$$
A_{KP}(\Lambda) > \frac{\Lambda}{1-\Lambda} \Rightarrow \text{ GROWTH} ,
$$

$$
A_{KP}(\Lambda) < \frac{\Lambda}{1-\Lambda} \Rightarrow \text{ DAMPING},
$$

$$
A_{KP}(\Lambda_{st}) = \frac{\Lambda_{st}}{1-\Lambda_{st}} \rightarrow \text{MARGINAL STABILITY } ({}_{\parallel}k_{ig} = 0)
$$

or
$$
\Lambda_{st} = A_{KP}(\Lambda_{st}) / [1 + A_{KP}(\Lambda_{st})] . \qquad (3.5)
$$

Therefore A_{KP} must be at least positive for amplification. A_{KP} is related to the sign of $\frac{\partial g_0}{\partial(\sin\alpha)}$ through Eq. (3.4) which shows that isotropic distributions $\left(\frac{\partial g_0}{\partial(\sin\alpha)} = 0\right)$ always yield damping ($A_{KP} = 0$). The same conclusion is reached a fortiori for distributions with $\frac{\partial g_0}{\partial(\sin\alpha)} < 0$ everywhere ($A_{KP} < 0$). Only distributions with $\frac{\partial g_0}{\partial(\sin\alpha)} > 0$ somewhere may cause amplification. For such distributions and because $\frac{\Lambda}{1-\Lambda}$ is an increasing function of Λ, generally low (high) frequencies will be unstable (stable).

With a simple choice of distribution $g_{0H} \propto p^{-\nu} \sin^q \alpha$, expression (3.4) can be expressed in a simple analytic form. We are then able to discuss relatively easily the variations of the whistler gain rate with various magnetospheric parameters. This discussion is presented in Section 2.

2. The Variation of the Gain with Various Magnetospheric Parameters For a Distribution $\propto p^{-\nu}\sin^q\alpha$

We represent the distribution function by (see Eq. (2.50))

$$g_0 = g_{0c} + g_{0H},$$

$$g_{0H} = \frac{1}{4\pi} H(p-p_H)\delta_{E1} \frac{A_{\nu q}}{b^{q/2}} p_1^{\nu-3} \cdot \frac{\sin^q\alpha}{p^\nu},$$

$$g_{0c} = \frac{1}{4\pi}\left[\left(1 - \frac{\delta_{EH}}{b^{q/2}} - \delta_0\right)\frac{\delta(p)}{p^2} + 3\delta_0 p_H^{-3}\right]. \qquad (3.6)$$

where b = magnetic field normalized to equatorial field value, p_1 corresponds to some convenient normalization energy W_1 (we will use later 100 eV unless otherwise specified); $\delta_{E1} = n_E(W \geq W_1)/n_E(W \geq 0)$. $H(p)$ is the Heaviside (step) function introduced to limit the total number of particles. The quantity p_H is chosen $\gg (M_0KT)^{1/2}$ to insure both that $\delta_{EH} \ll 1$ (where $\delta_{EH} = n_E(W \geq W_H)/n_E(W \geq 0)$), and that the temperature correction need not be included in the cold plasma refractive index [Montgomery and Tidman, 1964]. The condition $\delta_{EH} \ll 1$ is necessary to validate the treatment of Chapter 2 used to find the complex root of the dispersion function. In these conditions it does not matter what is the precise functional form of g_{0c}, which we represent conveniently by a Dirac distribution $\delta(p)$ plus a term $\delta_0 p_H^{-3}$ to represent particles from thermal energies ($\approx$ .1 eV) to $\approx$ 10 eV. This assumes a constant distribution in this last energy range, an assumption which may be far from the true physical representation. However since our results are insensitive to the exact form of g_{0c} in this energy range we feel this representation is as adequate as any.

A general function of pitch angle can be expanded in Fourier series in terms of $\sin(n\alpha)$ and $\cos(n\alpha)$, where n is an integer. It

is reasonable to assume symmetry with respect to the plane $\alpha = \pi/2$ (particle mirroring back and forth along the field line from each side of the equator). Thus the distribution function is expandable in terms of $\sin(2n\alpha-\alpha)$ and $\cos(2n\alpha)$ which can be developed in turn in powers of $\sin\alpha$. Therefore we will consider q as an integer, while ν is arbitrary. (In the following for mathematical convenience, we will derive expressions explicitly when q is even.) The normalizing condition requires:

$$A_{\nu q} p_1^{\nu-3} \int_{p_1}^{\infty} \frac{p^2 dp}{p^{\nu}} \int_0^{\pi/2} \sin^{q+1}\alpha d\alpha = 1$$

or:

$$A_{\nu q} = 2(\nu-3) \prod_{a=0}^{q/2} (a+1/2)/(q/2)! \quad , \; q \text{ even.} \qquad (3.7)$$

The coefficient $A_{\nu q}$ increases with both the energy parameter ν and the pitch-angle parameter q. For a given energy spectrum, the coefficient $A_{\nu q}$ must compensate for the increasing loss of particles at low pitch angle for increasing anisotropy. A similar conclusion is reached for the case in which the anisotropy is given and the spectrum softness parameter ν is increased.

From Eq. (3.4), it is immediately seen that

$$A_{KP} = \frac{q}{2} \qquad (3.8)$$

A_{KP} is in this case independent of Λ and there is correspondingly one single frequency of marginal stability:

$$\Lambda_{st} = \frac{A_{KP}}{1 + A_{KP}} = \frac{q}{2+q} \qquad (3.9)$$

the low frequencies $\Lambda < \Lambda_{st}$ are unstable and the high frequencies

$\Lambda > \Lambda_{st}$ are stable.

Inserting Eq. (3.8) into Eq. (3.4) yields:

$$\left(\frac{k_{ig}}{k}\right)_{\parallel} = \frac{\pi}{4}\, \zeta C_{\nu q} \delta_{El} b^{-q/2} \left[1 - \left(\frac{1}{\Lambda} - 1\right) \frac{q}{2}\right] \left|\frac{p_1}{p_R}\right|_{\parallel}^{\nu-3},$$

$$C_{\nu q} = (\nu-3) \prod_{a=0}^{q/2} [(a + 1/2)/(a-1 + \nu/2)], \quad q \text{ even},$$

$$p_R = \frac{\Lambda-1}{N\Lambda} p_0 \,. \tag{3.10}$$

In Eq. (3.10)

$$C_{\nu q} = A_{\nu q} B_{\nu q} \,, \tag{3.11}$$

$$B_{\nu q} = \left|p_R\right|^{\nu-2} \int_0^{\infty} \frac{\sin^q \alpha}{p^{\nu}} p_{\perp} dp_{\perp} \Big|_R = (q/2)!/\left(2 \prod_{a=0}^{q/2} [a-1 + \nu/2]\right), \quad q \text{ even}.$$

The coefficient $B_{\nu q}$ decreases with parameters ν and q. This expresses the fact that

$$B_{\nu q} \propto \int_0^{\infty} g_0 p_{\perp} dp_{\perp} \Big|_R \tag{3.12}$$

is a measure of the number of particles available at resonance.

Clearly, for increasing anisotropy the average energy of a particle at resonance increases for a given minimum energy of resonance, that is the number of available resonant particles decreases. The same conclusion holds for increasing spectrum softness. Now, as opposite conclusions were reached regarding the coefficients $A_{\nu q}$, there is a cancellation effect between $A_{\nu q}$ and $B_{\nu q}$ and the coefficient $C_{\nu q}$ stays fairly constant for different values of the parameters ν and q.

The expression of $_{\parallel}(k_i/k)$ is somewhat complex with all parameters intricately mixed. There are two geometrical (space) parameters, L and λ, one wave parameter Λ, and three hot plasma parameters δ_{El}, ν and q. The first three parameters influence the cold plasma propagation characteristics. Therefore the gain rate is an intricate combination of wave frequency and both cold and hot plasma parameters.

As our main interest lies in comparing gains with data, it will be more useful to express gains in terms of decibels along a certain distance S_u (1000 km for instance). Let us call this quantity G_u:

$$_{\parallel}G_u = -\zeta\ 8.686\ _{\parallel}k_{ig}S_u \sim -160\zeta\ \frac{\Lambda b}{L^3}\ _{\parallel}\left(\frac{k_{ig}}{k}\right)\ _{\parallel}N \qquad (3.13)$$

From Eqs. (3.13) and (3.10) we can study the variations of $_{\parallel}G_u$ with all the magnetospheric parameters.

First of all, $_{\parallel}G_u$ is directly proportional to the density of hot particles as expressed by the parameter δ_{El}. This is a characteristic of linear theory in contrast to nonlinear theory [Sudan and Ott, 1971; Helliwell and Crystal, 1973]. It is very important to emphasize the normalization of the density of hot electrons we have adopted and we will use throughout. We have chosen to keep δ_{El} constant (ratio of number of hot electrons above 100 eV to number of cold electrons) for a given L shell value. This is in contrast with previous normalizations (e.g., Liemohn [1967]; Kennel and Thorne [1967]; Thorne [1968]) where the choice was to fix a normalization energy of the order of 10 keV or more. The reason for normalizing at such high energies is that at that time only fluxes above a few keV were known. With the more recent measurements of Schield and Frank [1970], fluxes down to 100 eV are known. There is an essential difference between these two types of normalizations which

is as follows: the bulk of resonant cyclotron energy is between 100 eV and 10 keV and therefore for the previous choice of normalization, a softer spectrum means usually more particles at resonance in contrast to our normalization. This difference is clearly shown in Figure 3.5.

For a given value of Λ, the equatorial gain is

$$_{\parallel}G_{uE}(L) \propto \delta_{El}(L)\ L^{-3}\ _{\parallel}N_E^{\nu-2}(L) \propto \delta_{El}(L)\ L^{3\nu-9}\ n_E^{\nu/2-1}(L)\ . \qquad (3.14)$$

With a variation $n_E \propto \sim L^{-3}$,

$$_{\parallel}G_{uE}(L) \propto \delta_{El}(L)\ L^{3\nu/2-6}\ . \qquad (3.15)$$

For a hard spectrum ($\nu = 4$), $_{\parallel}G_{uE}$ varies like $\delta_{El}(L)$ and for softer spectra, $_{\parallel}G_{uE}$ increases with L more rapidly than $\delta_{El}(L)$. There is no detailed information as how $\delta_{El}(L)$ varies but the data of Schield and Frank [1970] suggest that the number of hot particles stays fairly constant across different L shells and it is reasonable to assume that either $\delta_{El}(L)$ increases or at least stays constant with L. For a ducted ray path over a complete field line we have to multiply $_{\parallel}G_{uE}(L)$ by a factor roughly proportional to L. All these factors add up to indicate that the gain rates are increasing with L. This hypothesis appears to be supported by observation. For instance Dunckel and Helliwell [1969] observed that inside the plasmasphere emissions are more frequent close to the plasmapause. Conclusions would be roughly the same for a variation $n_E \propto L^{-2}$, L^{-4}, and therefore outside the plasmapause as well as everywhere inside.

Now we look at the variation of the gain with latitude λ, keeping Λ constant:

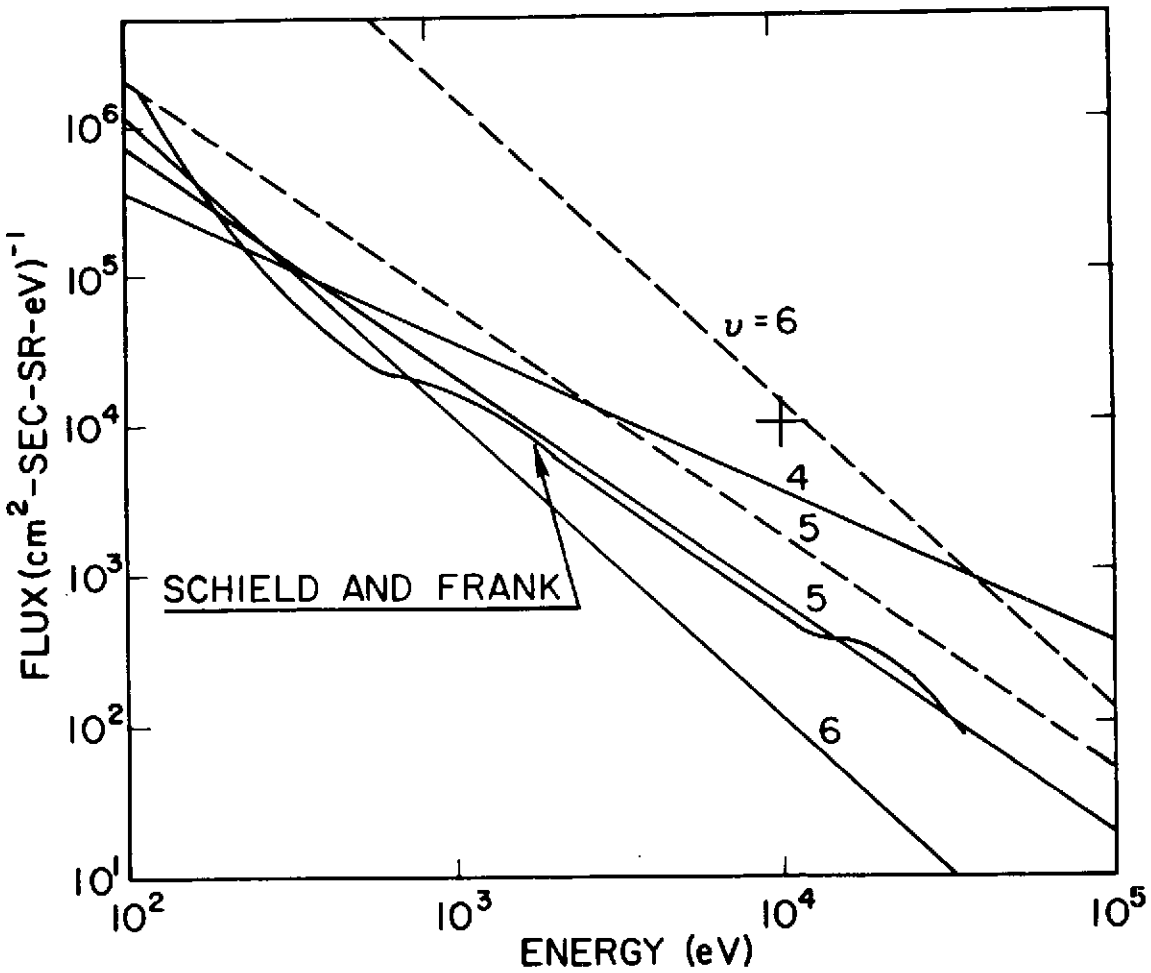

FIGURE 3.5. COMPARISON BETWEEN EXPERIMENTAL AND MODEL FLUXES. The solid curve represents the experimental flux, and is taken from Schield and Frank [1970] (see Figure 3.4a). The solid straight lines represent fluxes for a model of distribution $f(v,\alpha) \sim v^{-\nu}\sin^2\alpha$ and are normalized to $n(W \geq 100\ eV) = 1\ cm^{-3}$. The broken curves show Liemohn's [1967] normalization and the cross shows Thorne's [1968] normalization.

$$\frac{{}_{\parallel}G_u(\lambda)}{{}_{\parallel}G_{uE}} = b^{1-q/2}\left(\frac{{}_{\parallel}N}{{}_{\parallel}N_E}\right)^{\nu-2} = b^{3-q/2-\nu}\left(\frac{n}{n_E}\right)^{\nu-2} \qquad (3.16)$$

${}_{\parallel}G_u(\lambda)$ depends now on q. Away from the equator the gain rate wil decrease because of the factor $b^{-q/2}$ in Eq. (3.16) for an anisotropic distribution. This fact is simply a consequence of the first adiabatic invariant law. The parameter ν affects the gain variation quite differently inside and outside the plasmapause. Inside the plasmapause, $n(\lambda)/n_E \approx$ constant and the gain decreases with increasing λ because the resonant energy is increasing away from the equator. Therefore the number of resonant particles decreases away from the equator. This effect, combined with the particle decrease due to the first adiabatic invariant law, yields a fast decrease in $|{}_{\parallel}G_u|$ with λ as illustrated in Figure 3.6. Therefore the major contribution to gain is concentrated in a relatively narrow latitude range around the equator.

Outside the plasmapause $n(\lambda)/n_E \approx b$ and from Eq. (3.16), ${}_{\parallel}G_u(\lambda)$ is about ν-independent. The decrease of the gain is therefore much slower outside the plasmapause but notice we have not yet taken into account the decreasing of Λ away from the equator and that $|{}_{\parallel}G_u|$ decreases with Λ for reasonably soft spectra ($\nu \geq 5$; see Figure 3.7). Because of this supplementary factor, the gain is still relatively concentrated around the equator.

In order to have a complete picture of the gain variation, it remains to study its variation with ν and q as illustrated in Figure 3.7. The values of the gain are high for a hard spectrum $\nu = 4$ but decrease for softer spectra. Notice it is not too high for $\nu = 5$ and reasonable anisotropy ($q = 2$). As pointed out before the softer the spectrum,

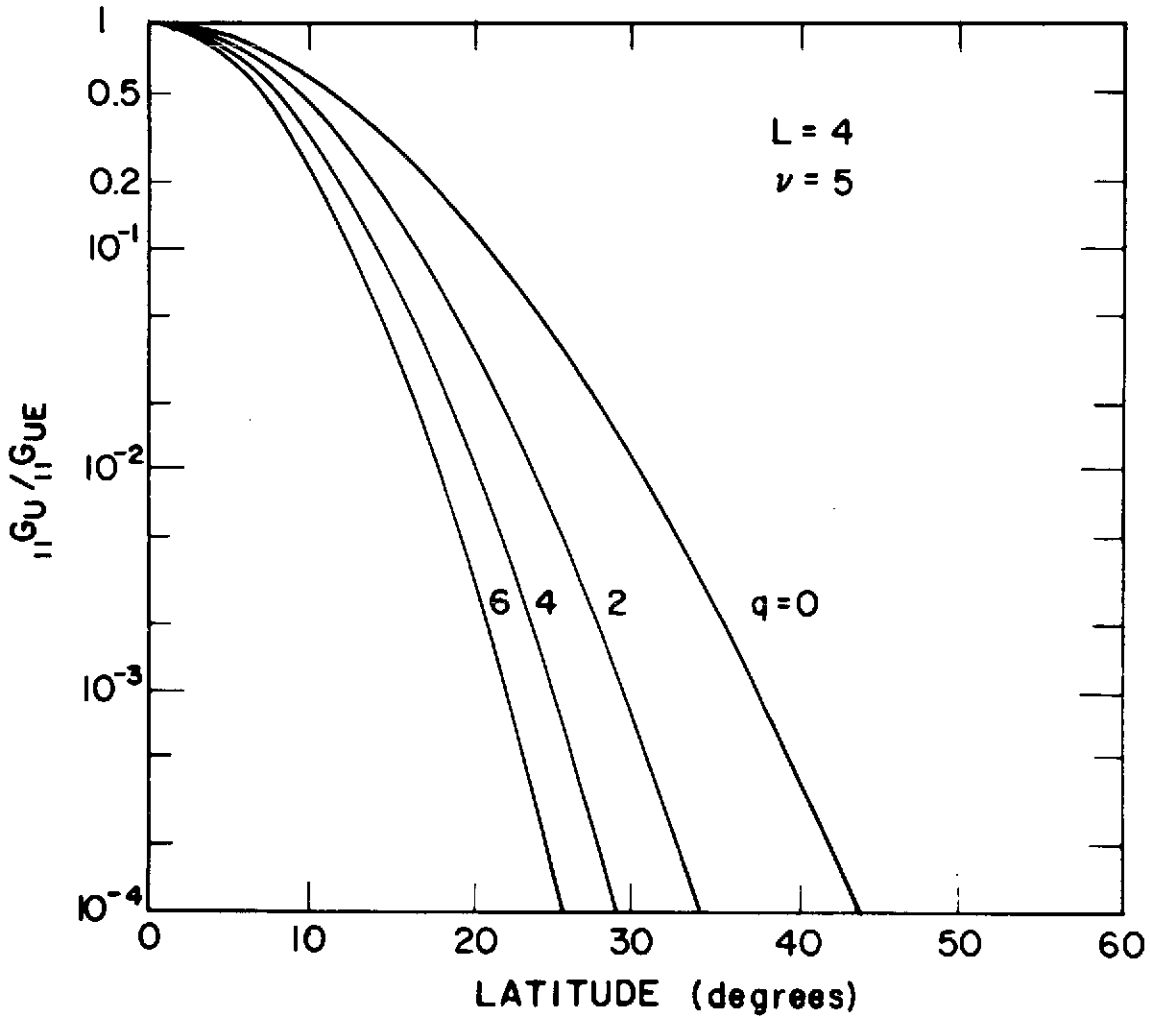

FIGURE 3.6. A PLOT OF PARALLEL WHISTLER GAIN NORMALIZED TO ITS EQUATORIAL VALUE VERSUS LATITUDE ASSUMING DIFFUSIVE EQUILIBRIUM MODEL.

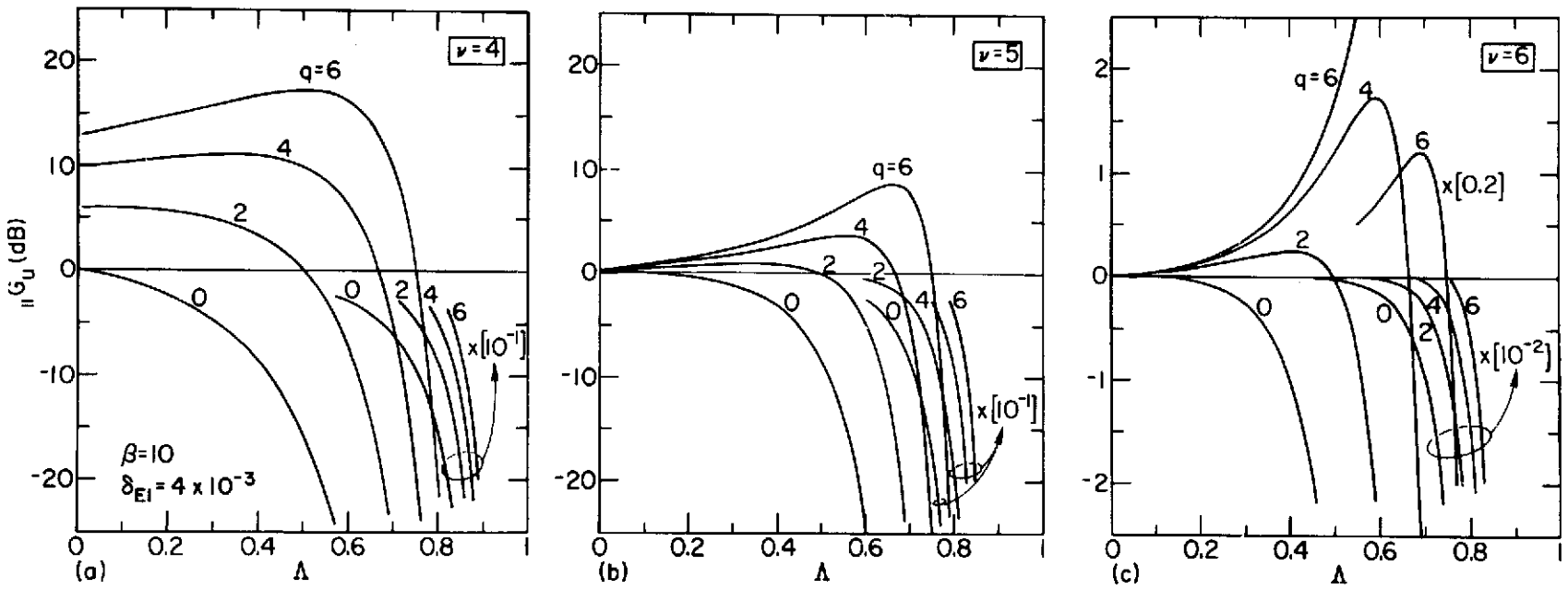

FIGURE 3.7. A PLOT OF PARALLEL WHISTLER GAIN VERSUS NORMALIZED FREQUENCY FOR A FEW VALUES OF ENERGY PARAMETER ν AND PITCH-ANGLE PARAMETER q. δ_{El} is the density of particles of energy > 100 eV normalized to the total density in the magnetic equatorial plane.

the less particles in the mid-frequencies ($\Lambda \sim 0.5$) because of the normalization of the distribution function we have adopted (same number of particles above 100 eV). This effect clearly overtakes the effects of increasing slope. The qualitative behavior of the gain remains the same for a given value of q (same number of marginal stability frequency) and different values of ν because of the factor $[1 - (\frac{1}{\Lambda} - 1)\frac{q}{2}]$ in Eq. (3.10).

D. PARALLEL PROPAGATION FOR A DISTRIBUTION NONSEPARABLE IN ENERGY AND PITCH ANGLE

Up to now, we have assumed a very simple type of distribution. We wish now to discuss the stability with respect to more general types of distributions. One of the characteristics of the previous type of distribution is that it exhibits a single marginal stability frequency Λ_{st}. Moreover for higher frequencies, the gain is a very rapidly decreasing function of frequency. This has led several authors (Liemohn [1967]; Thorne [1968]) to hypothesize that whistler cutoffs in observed data are caused by hot plasma damping effects. Almost invariably, careful investigation has shown that cold plasma accessibility effects are a very plausible alternative explanation [Carpenter, 1968; Edgar, 1972]. Even in the amplification regime ($\Lambda < \Lambda_{st}$), the values of the gain predicted by various workers look very high compared with observations. It is therefore interesting to investigate whether another type of distribution might exhibit not a <u>single frequency</u> marginal stability but a <u>broadband</u> marginal stability.

We know fairly well (see Figure 3.4) the energy law of variation ($\propto p^{-\nu}$), however the pitch-angle law is unknown down to low energies (i.e., $\sim$ 100 eV). Pitch-angle laws different from those considered in the last

section are needed to yield broadband stability. A general distribution still separable and $\propto p^{-\nu}$ can be expanded in a series of the variable $\sin\alpha$. Therefore let us consider a distribution:

$$g_{OH} \propto p^{-\nu} \sum_{q=0}^{\infty} A_q \sin^q\alpha \ . \tag{3.17}$$

For such a distribution:

$$A_{KP} = \sum_{q=0}^{\infty} qB_{\nu q} \Big/ 2 \sum_{q=0}^{\infty} B_{\nu q} \ . \tag{3.18}$$

This shows that A_{KP} is independent of $p_{R_{\parallel}}$, that is of Λ. Such a distribution would have exactly the same characteristics as that of Eq. (3.1) with respect to stability and we can state:

Lemma: a separable distribution in energy and pitch-angle with an energy dependence $\propto W^{-\nu}$ and an arbitrary pitch-angle dependence exhibits a single stability frequency.

Identical conclusions are reached with a function

$$g_{OH} \propto \left(\sum_{\nu} \frac{A_\nu}{p^\nu} \right) \sin^q\alpha \ , \quad q \neq 0 \ . \tag{3.19}$$

Therefore, a fairly general class of distribution functions separable in W and α yields only one stability frequency. In order to look for a function which may yield marginal stability over a broad frequency band (such a function may be thought to have in the limit an infinite number of values Λ_{st} for which $G_u = 0$), we now consider a nonseparable distribution in particle energy and pitch-angle.

This is a natural choice. We have seen that an isotropic distribution yields damping for every frequency. The more the function is anisotropic (the higher the value of parameter q) the higher is the frequency Λ_{st}.

Now high values of Λ correspond to low values of resonance energy, and vice-versa. It is therefore expected that a broadband marginal stability function is one which has a large anisotropy for low particle energy and low anisotropy for high particle energy. Therefore, such a function must have a pitch-angle anisotropy which is energy dependent. This can be seen equally well in a very simple manner from the interaction of a single particle with an electromagnetic wave propagating parallel to the static magnetic field. This interaction is described by the constant of the motion of the particle during the interaction (Eq. (2.19 a or b)) and its graphical interpretation (Figure 2.2). For high resonance energy the interaction results predominantly in pitch-angle scattering (with virtually no energy exchange) whereas for low resonance energy both pitch-angle scattering and energy exchange occur. Therefore if waves and plasma constantly interact in the magnetosphere, as we have every reason to believe, the shape of the particle distribution may eventually be controlled by the process. This change of the particle distribution by the interaction with electromagnetic waves is described (within certain limits of validity) by the quasi-linear theory which shows practically pure pitch-angle diffusion for high particle energies, but for low particle energy, there is energy diffusion as well (e.g., Kennel and Engelmann [1966]). A criterion for making the difference between pitch-angle diffusion only and both pitch angle and energy diffusion can be found in Gendrin [1968], for example. Pure pitch angle diffusion can be considered when:

$$v_p \ll v_R \tag{3.20}$$

In view of the preceding discussion, the hypothesis of separability in energy and pitch-angle may only be considered as valid for low

frequencies of interaction (as given by the criterion Eq. (3.20) and may be an oversimplification for higher frequencies.

The simplest choice of a nonseparable function related to the previous calculations is to choose a superposition of functions $\propto p^{-\nu}\sin^q\alpha$ with different ν and q:

$$g_{0H} \propto \sum_{\nu} \sum_{q} A_{\nu q} \frac{\sin^q\alpha}{p^\nu} . \tag{3.21}$$

For mathematical convenience, we choose:

$$g_{0H} = \frac{1}{4\pi} H(p-p_H)\, \delta_{El} A_1 p_1^{\nu-3} \cdot \frac{\exp[q(p_1/p)^{\nu_q}\sin^2\alpha/b]}{p^\nu} . \tag{3.22}$$

(By expanding the exponential in series, it is immediately seen that this function belongs to the class represented in Eq. (3.21).

The parameters ν, q and ν_q are chosen to match published particle data. The parameters ν and q have the same physical meaning as given previously, i.e., ν expresses the energy variation of the distribution function whereas q is an anisotropy factor. The <u>new parameter</u> ν_q expresses the coupling between energy and pitch-angle of the particle.

The normalizing condition is written with change of variable $y = \frac{p_1}{p}$

$$A_1^{-1} = \int_0^1 dy \int_0^{\pi/2} \exp[qy^{\nu_q}\sin^2\alpha]\, y^{\nu-4}\sin\alpha d\alpha \tag{3.23}$$

and by expansion of the exponential in series:

$$A_1^{-1} = \frac{1}{\nu-3} + \sum_{n=1}^{\infty} \frac{q^n}{\nu-3+n\nu_q} \frac{2^n\, n!}{(2n+1)!} . \tag{3.24}$$

From Eq. (3.24) we obtain:

$$\left(\frac{k_{ig}}{k}\right)_{\parallel} = \zeta \frac{\pi}{4} A_1 \delta_{El} \sum_{n=0}^{\infty} b^{-nq/2} \frac{q^n}{n!} B_{\nu+n\nu_q,\, 2n\left[1-\left(\frac{1}{\Lambda}-1\right)n\right]} \left|\frac{p_1}{p_R}\right|_{\parallel}^{\nu+n\nu_q-3} \tag{3.25}$$

Inserting Eq. (3.24) into Eq. (3.25) we get the gain rates for the distribution Eq. (3.22).

Figure 3.8 represents $_{\|}G_u$ for $\beta = 10$ (corresponding roughly to $L = 4$ at the equator) versus normalized frequency. The values of ν and q are kept constant (4 and 5 respectively) but different values of ν_q are chosen to see the important effect of this newly introduced parameter.

For the case $\nu_q = 0$, which is the particular case of separability, the gain is very similar both qualitatively and quantitatively to that produced by the functions $\propto p^{-\nu}\sin^q\alpha$. However it can be seen that the gain decreases as ν_q increases. For a value $\nu_q = 0.5$, the maximum value of $_{\|}G_u(\Lambda)$ is already less than 1 db. Now a value $\nu = 4$ represents an upper limit in value of $\left|_{\|}G_u\right|$ and the gain is expected to be lower for higher values of ν. In Figure 3.9 the function Eq. (3.22) has been represented for a value $\nu_q = 0.5$ in terms of differential fluxes versus energy and versus pitch angle with an appropriate normalization to closely fit Schield and Frank's data [1970]. The experimental values of α were close to 90^o (the field of view of the electron analyzer was directed earthward while the spacecraft was moving almost parallel to and near the magnetic equatorial plane). The fit is better than a pure power law ($\propto p^{-\nu}$). In particular, the spectrum is softer for lower energies as indicated by the data. This may be a manifestation of increasing energy diffusion at low energies. Bogott and Mozer [1971] measured pitch-angle distributions on ATS-5 satellite at synchronous altitude during quiet time. The data show quite isotropic distributions in the measured energy range (40 keV and above). Our proposed model of distribution also fits this observation.

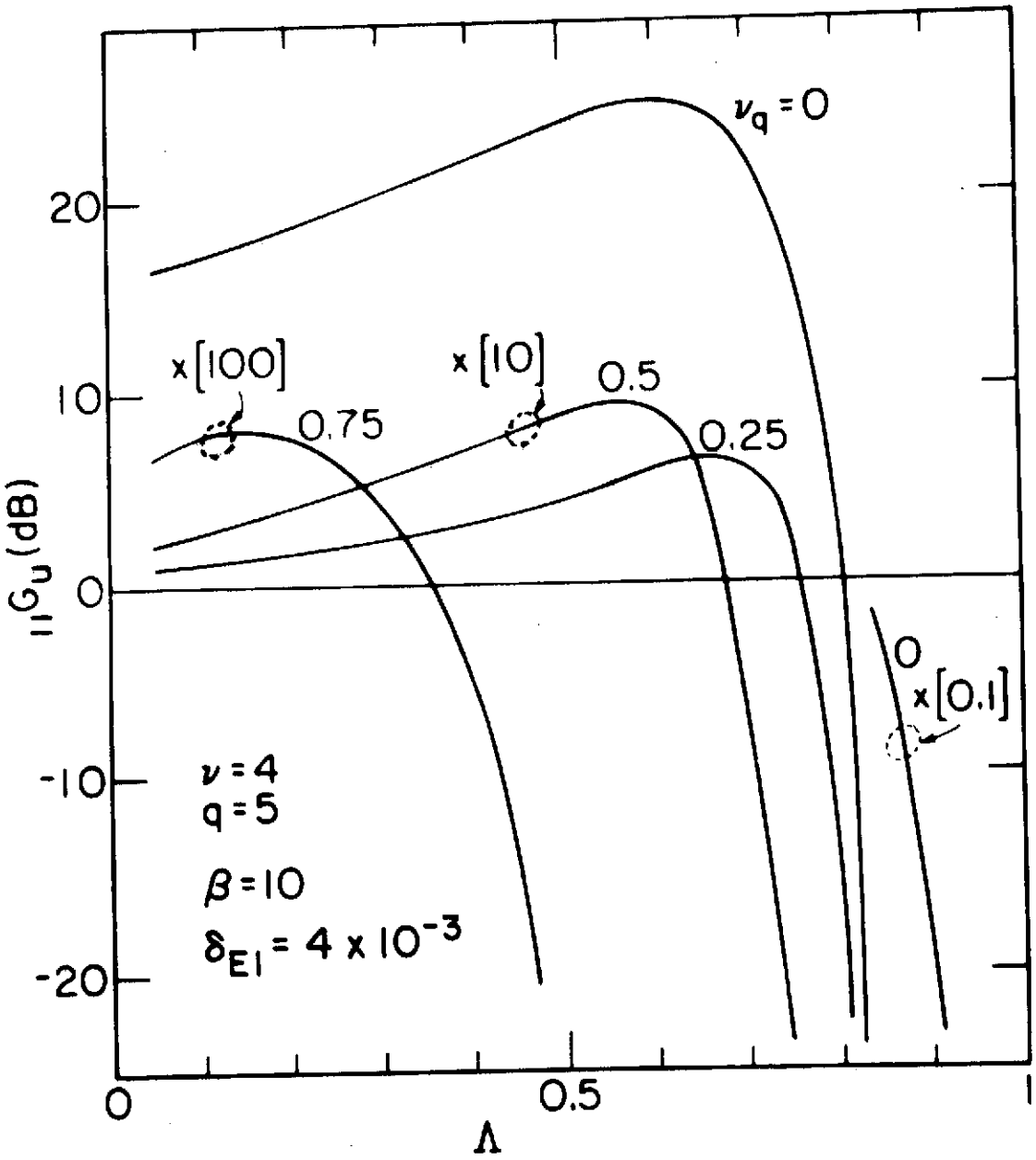

FIGURE 3.8. PARALLEL GAIN FOR A NONSEPARABLE DISTRIBUTION. Notice the important influence of the parameter ν_q of energy and pitch-angle coupling in the amplification regime. δ_{E1} is the same parameter as in Figure 3.7.

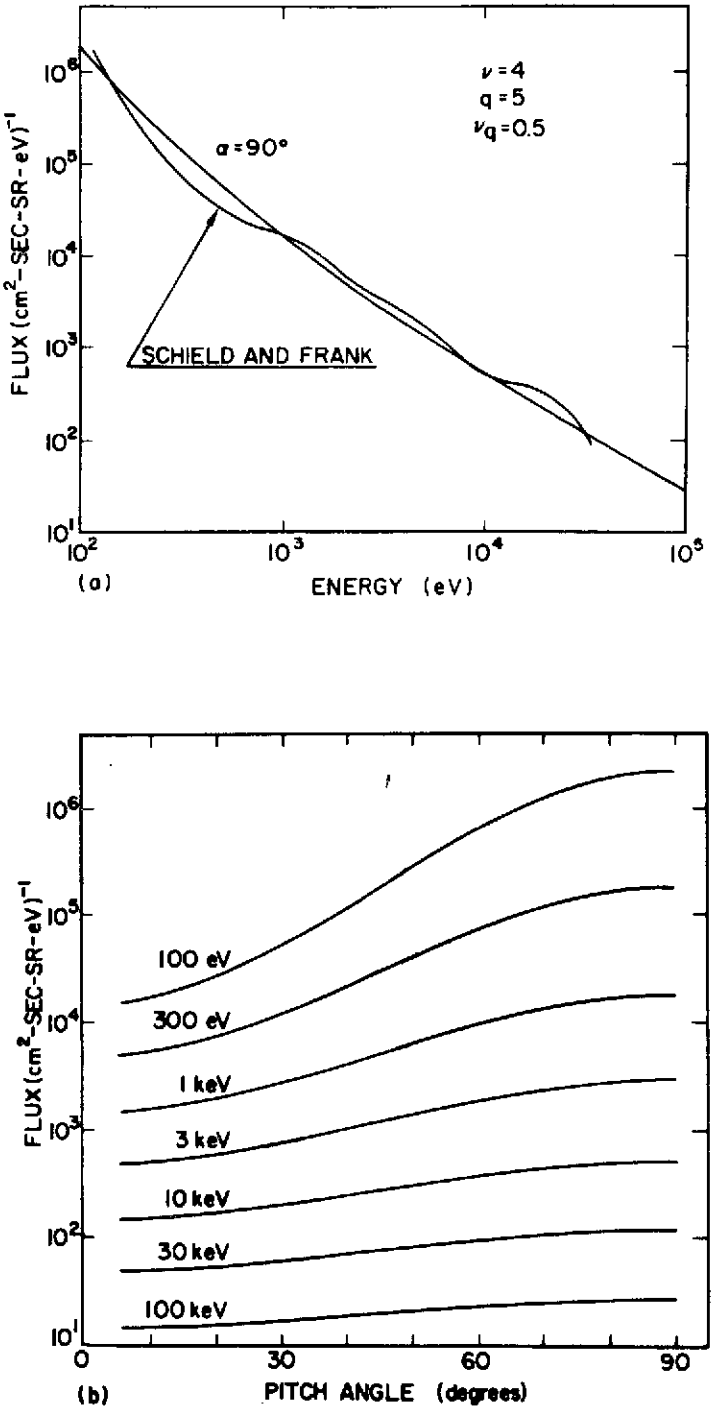

FIGURE 3.9. ELECTRON DIFFERENTIAL FLUX FOR A NONSEPARABLE DISTRIBUTION. Comparison is made with the plasmasphere differential flux of Figure 3.4. The experimental values of pitch-angle α were close to 90^{o}.

There may be some irrelevance in comparing Bogott and Mozer's [1971] measurements which were made outside the plasmapause with measurements made inside the plasmapause. In favor of the comparison, from Schield and Frank [1970], high energy fluxes are fairly similar inside and outside the plasmapause. Secondly, the Kennel and Petschek [1966] mechanism predicts a small anisotropy for 40 keV electrons ($A_{KP} \sim 1/6$, or $q \sim 0.3$). This mechanism has recently been extended by Lyons et al [1972] to include arbitrary angle of propagation and provides a satisfactory explanation to both the "slot" between inner and outer Van Allen radiation belts and the shape of pitch angle distributions of high energy particles [D. Williams, private communication].

E. NONPARALLEL PROPAGATION

The purpose of this section is to compute the variation of the gain with the wave normal angle. The general expression of the gain is much more complex than for the parallel propagation case. For simplicity we study first such simple separable distributions as $p^{-\nu}\sin^{q}\alpha$. Then we study nonseparable distributions for small wave normal angle. In the latter case it is then possible to make an expansion around $\theta = 0$ of the expression (2.69), limiting the mathematical complexity.

1. Separable Distribution

A Fortran program has been developed to compute the nonparallel gain rates for separable distributions with integer values of ν and even integer values of q. The details are given in Appendix A.

The gain rates have been computed for many combinations of the parameters ν and q and Λ varying from 0.1 to 0.9 and θ from 0^{o} to a fraction of a degree from the resonance cone angle θ_R. The values

of the ratio $\frac{G_u(\theta)}{G_u(0)}$ are displayed on Figures 3.10 and 3.11 for a few values of ν and q. The gain decreases with values of θ because of increasing Landau damping. There is a distinction to be made here whether the gain was negative (damping) or positive (growth) for parallel propagation at a given value of Λ. As the absolute value of the gain often decreases for increasing wave-normal angle, it may well be that there is less attenuation, but there is never more amplification at $\theta \neq 0$ than at $\theta = 0$ for $\Lambda < 0.5$. This casts a doubt upon Brinca's [1972] argument that the presence of minimal gain at $\theta = 0$ plays an important role in triggering emissions, at least with this kind of distribution. In fact the cases discussed by Brinca [1972] are cases for which there is only damping at $\theta = 0$. For $\Lambda > 0.5$, maximum growth at $\theta \neq 0$ is possible but this effect is very small ($(G_u(\theta)/G_u(0)$ always stays ~ 1). The frequency $\Lambda = 0.5$ is a transition frequency for several factors whose sense of variation with θ is different for values of Λ above or below 0.5: $N_{\parallel}(\theta)$ and $C_{m1}(\theta)/C_0$ decrease with θ when $\Lambda < 0.5$. At the same time there are more Landau particles than fundamental cyclotron particles for $\Lambda < 0.5$. Therefore, the first cyclotron resonance part of the gain can only decrease (in absolute value) for $\theta \neq 0$ (and $\theta < \theta_G$) and $\Lambda < 0.5$.

We have included in the program harmonics up to order $|m| \leq 3$. The conclusion is close to Brinca's [1972] conclusions: harmonics of order $m \neq 0,1$ (Landau and fundamental cyclotron interaction) are almost always negligible. For $\Lambda \to 1$, $p_{R0} \to p_{R2}$ and if the spectrum is hard enough so that the number of particles at Landau and second harmonics are not too different, the strength of the normal second harmonics interaction and the Landau interaction can be comparable. For $\Lambda \to 0$, $p_{R-m} \to p_{Rm}$, and the

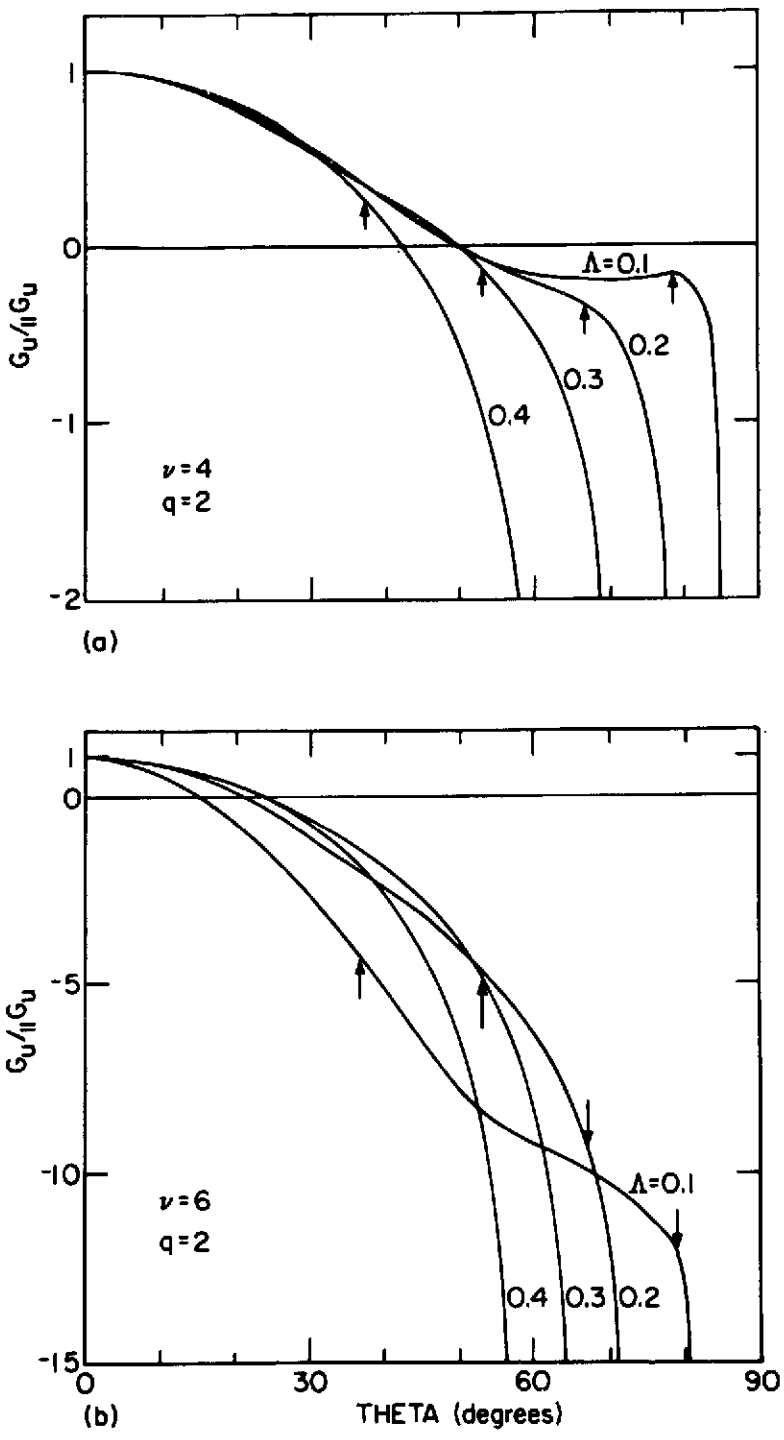

FIGURE 3.10. NONPARALLEL GAIN NORMALIZED TO PARALLEL GAIN VERSUS θ FOR A SEPARABLE DISTRIBUTION AND TWO DIFFERENT VALUES OF ENERGY PARAMETER. The vertical arrows indicate the value of the Gendrin angle corresponding to the value of the parameter Λ.

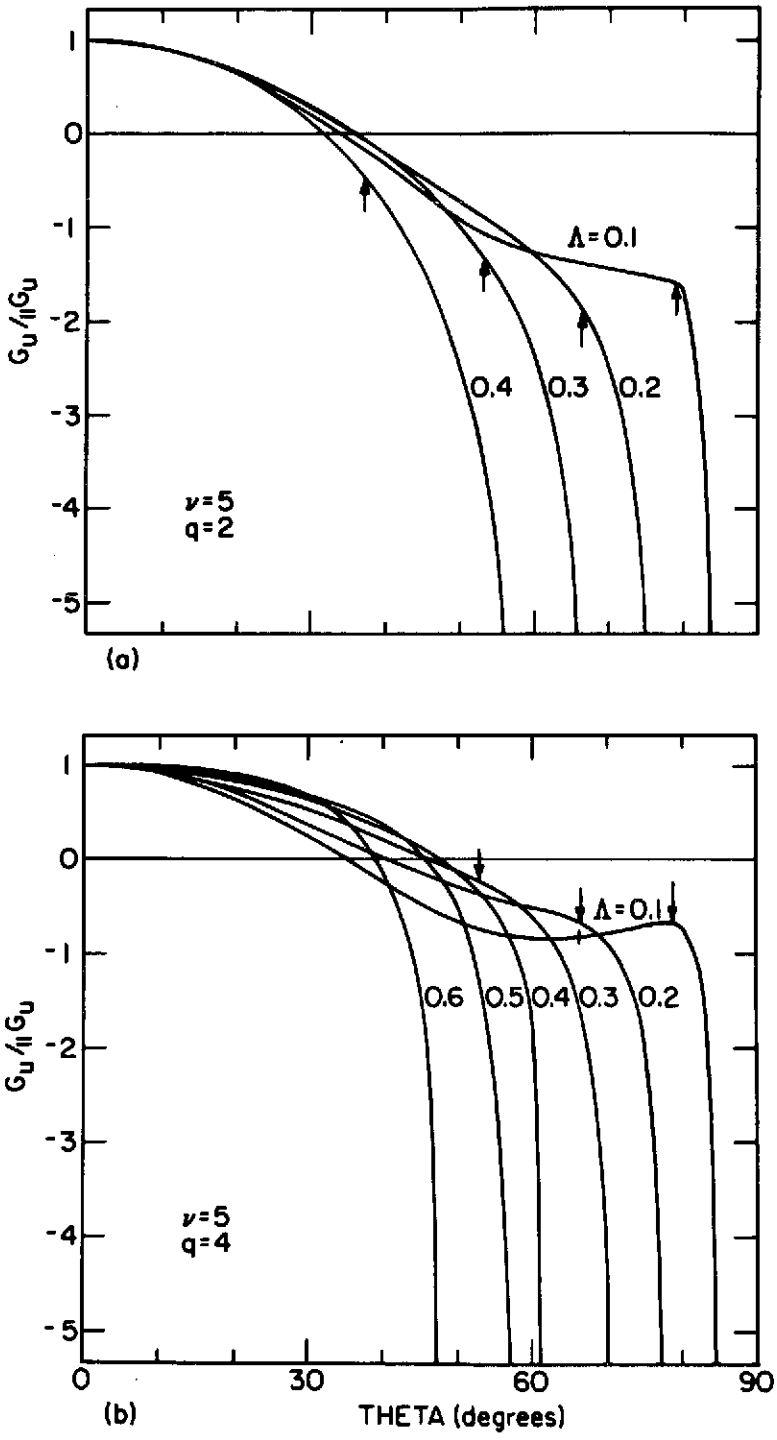

FIGURE 3.11. A PLOT SIMILAR TO FIGURE 3.10 BUT FOR TWO DIFFERENT VALUES OF PITCH-ANGLE PARAMETER.

harmonic $m = -1$ can be non-negligible compared to the harmonic $m = 1$.

It is seen from Figure 3.10 and Figure 3.11 that there is a range of values $\theta < \theta_s (G_u(\theta_s) = 0)$ for which the distribution was unstable. θ_s is decreasing with increasing value of ν, as was already shown by Kennel [1966]. Therefore Kennel's conclusions concerning an unstable case of angle $< \theta_s$ are valid, though his approximation for Landau interaction is incorrect (see Section 2D). For $\Lambda < 0.5$, there are more Landau than cyclotron particles and the number of particles being weighted by the steepness of the energy spectrum, the ratio of available Landau particles to available cyclotron particles is increasing with ν. This ratio is increasing when Λ decreases. It is expected that θ_s is correspondingly decreasing. However, the relative number of particles available at resonance is weighted by the factor Θ_m. As pointed out in Section 2D, Θ_0 decreases when Λ decreases. This has an opposite effect to the increasing number of Landau particles when Λ decreases. For the "classical" part of the Landau interaction, this just expresses the fact that the parallel component of the electric field decreases relatively to the perpendicular component when Λ decreases (see Figure 2.5). For a given value of ν, θ_s is increasing with q. The increasing of anisotropy affects differently cyclotron and Landau interaction. In Eq. (2.70), the derivative $\frac{\partial g_0}{\partial(\sin\alpha)}$ is weighted by a bigger factor $(-\sin^2\alpha + \frac{1}{\Lambda})$ for fundamental cyclotron interaction than for Landau interaction $(-\sin^2\alpha)$.

Close to the resonance cone, there is a rapid change of topology in the refractive index around the Gendrin angle θ_G (see Figure 2.4) which is reflected in the gain of Figures 3.10 and 3.11 where vertical arrows show the location of the Gendrin angle. The gain in absolute value eventually becomes much bigger than for parallel propagation as $\theta \to \theta_R$

because $p_{Rm} \to 0$ and there is an increasing number of particles at resonance. With the values of ν and q chosen on Figures 3.10 and 3.11, there is only damping as $\theta \to \theta_R$.

For $\Lambda \ll 1$, $p_{R(-m)} \to p_{Rm}$, and if g_0 is anisotropic,

$$U_m \to M\omega \frac{1}{p} \frac{m}{\Lambda} \frac{\partial g_0}{\partial(\sin\alpha)} \tag{3.26}$$

Furthermore from Eq. (2.74), $\Theta_{-m} \to \Theta_m$ when $\theta \to \theta_R$. Therefore the cyclotron harmonics tend to cancel each other.

In the general case, using Eq. (2.74) for $\theta \to \theta_R$ and the functions $B^{mm}_{\nu q}(d)$ defined in Appendix A, we find that as $\theta \to \theta_R$:

$$\zeta k_{ig} \to \propto \sum_m \left| p_{Rm}^{-\nu} \right| \left[(q+\nu) B^{mm}_{\nu+2,q} - \frac{mq}{\Lambda} B^{mm}_{\nu+2,q-2} \right] \tag{3.27}$$

where the functions $B^{mm}_{\nu q}$ are evaluated at $d_m = \left|(\Lambda-m)\tan\theta_R\right|$ and the coefficient of proportionality is positive. For high values of Λ, we make a rough analysis treating $d_0 = \Lambda\tan\theta_R$ and $d_1 = (1-\Lambda)\tan\theta_R$ as small quantities and assuming that we can neglect harmonics of order $\neq 0,1$. Growth will occur at the resonance cone if

$$-(q+\nu)\left[B_{\nu+2,q} - \frac{d_0^2}{2} B_{\nu,q+2}\right] + \left[\frac{q}{\Lambda} B_{\nu q} - (q+\nu) B_{\nu,q+2}\right] \frac{d_1^2}{4} \left(\frac{\Lambda}{1-\Lambda}\right)^{\nu} > 0 \tag{3.38}$$

(and damping in the opposite case).

The coefficients $B_{\nu q}$ are given in Eq. (3.11) which shows that:

$$B_{\nu,q+2} = \frac{q+2}{q+\nu} B_{\nu q}; \quad B_{\nu+2,q} = B_{\nu q} \cdot \frac{\nu-2}{q+\nu}, \tag{3.29}$$

and Eq. (3.29) is rewritten as:

$$(q+2) \frac{d_0^2}{2} - (\nu-2) + \left[\frac{q}{\Lambda} - (q+2)\right] \frac{d_1^2}{4} \left(\frac{\Lambda}{1-\Lambda}\right)^{\nu} > 0$$

or

$$q > \frac{2 + \frac{4}{d_1^2}\left(\frac{1-\Lambda}{\Lambda}\right)^{\nu}\left[\nu-2-d_0^2\right]}{\frac{1}{\Lambda} - 1 + \frac{d_0^2}{2}\frac{4}{d_1^2}\left(\frac{1-\Lambda}{\Lambda}\right)^{\nu}} \tag{3.30}$$

For parallel propagation, the corresponding inequality was $q > 2/(\frac{1}{\Lambda} - 1)$ (see Eq. (3.9)). For example for $\nu = 5$ and $\Lambda = 0.6$, Eq. (3.30) requires $q > \sim 6$ for growth at the resonance cone whereas only $q > 3$ was necessary for growth at parallel propagation.

This rough analysis indicates that distributions need to be significantly more anisotropic to yield growth for propagation close to the resonance cone than for parallel propagation.

2. Nonseparable Distribution

By expanding Eq. (2.71) around $\theta = 0$, the variations of the gain for small angle can be found:

$$\begin{aligned} k_{ig} \sim -\frac{\zeta\pi^2}{2}\frac{\cos\alpha_g}{\cos^3\theta}\frac{|p|}{N^2}\int_0^{\infty}\Bigg\{ & \theta^2\left[\frac{\Lambda}{1-\Lambda}\,{}_{\parallel}p_{R0}\frac{1}{p_{\perp}} - \frac{1}{2}\frac{p_{\perp}}{p_0}\,{}_{\parallel}N\Lambda\right]^2 {}_{\parallel}U_0 \\ & + \left[1 + \theta^2\left(\frac{\Lambda^2}{1-\Lambda} - \frac{1}{2}\right)\right]{}_{\parallel}U_1 - \frac{\theta^2}{2}\,{}_{\parallel}N^2\Lambda^2\left(\frac{p_{\perp}}{p_0}\right)^2{}_{\parallel}U_1 \\ & + \frac{{}_{\parallel}p_{R1}}{2}\,\theta^2\left[1 - \frac{1}{2(1-\Lambda)}\right]\frac{\partial U}{\partial p_{\parallel}} \\ & + \left({}_{\parallel}\frac{N\Lambda\theta}{2}\right)^2{}_{\parallel}U_2\Bigg\}\, p_{\perp}^2 dp_{\perp} \end{aligned} \tag{3.31}$$

where ${}_{\parallel}U_m = U({}_{\parallel}p_{Rm}, p_{\perp})$, and the quantity $\frac{\partial U}{\partial p_{\parallel}}$ is to be evaluated at $p_{\parallel} = {}_{\parallel}p_{R1}$.

Inserting Eq. (3.22) into Eq. (3.31), we find the variation of the gain for a nonseparable distribution and small angle. (Numerical

computations are made with a program developed in Appendix A.) This time the θ range of instability is fairly small. The type of nonseparable distribution we have chosen gives only damping for the $m = 0$ resonance whereas it gives an almost marginally stable cyclotron gain over a wide range of frequencies. The cyclotron gain does not change much with θ small (its stays practically marginally stable for small θ) and therefore the Landau interaction overtakes the cyclotron interaction very rapidly when θ increases. This effect is more pronounced when the coefficient of coupling ν_q increases as shown on Figure 3.12 where a value of $\nu_q = 0.25$ still gives growth at $\theta = 10^o$ whereas for $\nu_q = 0.50$ there is already damping at $\theta = 10^o$.

F. CONCLUSION

A new model of distribution function has been proposed. The new characteristic of the distribution is that it is nonseparable in particle energy and pitch angle, or in other terms, particles with different energies have different pitch-angle distributions. It has a very important effect on wave amplitude gains caused by wave-particle interaction, namely, this distribution produces a gain which is almost stable for a wide range of frequencies in contrast to previous separable distributions such as Liemohn's [1967] which yield large positive gains (amplification) for low frequencies and large negative gains (attenuation) for high frequencies. This offers an explanation for the accessibility/instability controversy about the high-frequency cutoff of nose whistlers presented in Chapter 1. As of now, electron energy spectrums have been measured over the range (100 eV - 40 keV) in which the bulk of interactions takes place between whistlers and electrons in the magnetosphere (see Schield and Frank's [1970] data). On the other hand, pitch angle information is not yet

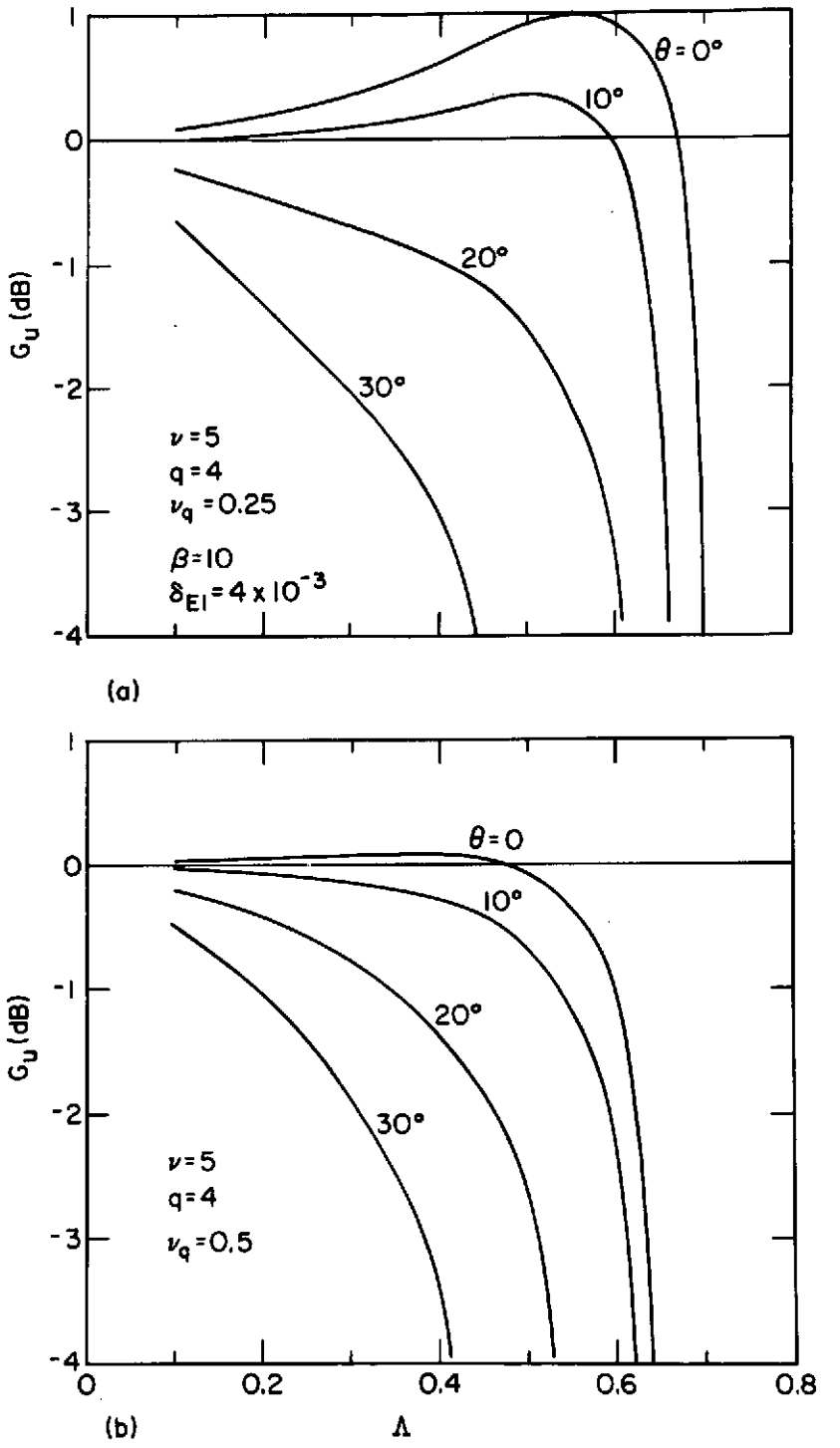

FIGURE 3.12. GAIN FOR A NONSEPARABLE DISTRIBUTION AND DIFFERENT DIRECTIONS OF PROPAGATION.

available in this energy range. Therefore immediate confirmation of our model is not possible. We feel it is reasonable though, because, 1) it predicts an increase in the slope of the energy spectrum in the low particle energy range, in agreement with Schield and Frank's [1970] data; 2) it predicts almost isotropic fluxes in the high particle energy range, in agreement with Bogott and Mozer's [1971] measurements and Kennel and Petschek's [1966] predictions.

A detailed study of the influence of the angle θ between wave vector and static magnetic field upon the gain rates has been presented. For separable distributions, the study has been made for the complete range $0 < \theta < \theta_R$. We have emphasized the importance of the weighting factor of the Landau interaction which weights the number of Landau particles. This factor and the number of resonant Landau particles vary in opposite phase with frequency. We have shown that significantly more anisotropic distributions are required for growth at the resonance cone than for parallel propgation. For nonseparable distributions, the gain is evaluated for small values of θ. It is found that the cyclotron part of the gain stays small and is rapidly overtaken by Landau damping when θ increases. Our new model of distribution may be over simplified in the sense that it was derived by looking for a wave-plasma equilibrium over a large frequency band but only considering cyclotron interaction. A suggestion for a distribution model giving equilibrium also in the presence of the Landau interaction will be given in the next chapter.

This chapter was concerned with the evaluation of gain over a narrow region in space considered as homogeneous. To compare with actual data the gain must be integrated over a ray path. It is the object of the next chapter.

IV. INTEGRATED GAIN RATES AND COMPARISON WITH DATA

A. INTRODUCTION

The variation of the wave amplitude gain per 1000 km has been studied in the previous chapter. The influence of the numerous parameters of concern have been investigated in detail. To compare with actual data, it remains to integrate the gain over a complete whistler wave ray path. To carry out the numerical computations we use the ray tracing program developed by Walter [1969] and refined by Angerami [1970]. Certain parameter values of the ray tracing program are used as input numbers to our computer program. This procedure is explained in more detail in Appendix A.

In Section B we use our program, including arbitrary angle of propagation θ for separable distributions and small values of θ for non-separable distributions, to test the validity of the parallel propagation approximation (which assumes $\theta = 0$) for ducted whistlers.

The observations of Angerami [1970] were very important in determining the nature of nose-whistler upper cutoffs. Taking the same values of ray tracing parameters as Angerami, we are able to test the validity of our model of distribution against models of separable distributions. This investigation is carried out in Section C.

Recently, Dunckel and Helliwell [1973] observed signals with very high normalized frequency (above $\Lambda = 0.9$) and explained by ray tracing the accessibility characteristics of these signals. We investigate the instability characteristics of these signals in Section D.

The magnetospherically reflected (MR) whistlers were first observed and explained in terms of accessibility by Smith and Angerami [1968].

Edgar [1972] made an extensive study of this type of whistler. Using the results of some ray tracings of Edgar [1972], we study the instability characteristics of MR whistlers in Section E and compare our calculations to similar computations made by Thorne [1968].

In Section F, we summarize the most important contributions of the chapter, and discuss their implications. In particular we note the relevance of our results to plasma injection experiments, and to plasma diagnostic techniques.

B. DUCTED WHISTLERS

The gain has been integrated along a realistic model of a whistler duct for a few distributions. The duct is described mathematically by the following expression [Angerami, 1970]:

$$n(L) = n_0 \cdot \left\{ 1 + C \exp \frac{-(L-L_0)^2}{2 \cdot \Delta L^2} \right\} \qquad (4.1)$$

where n_0 is the background density, C is the relative enhancement (depletion) of density at the center of the duct (L_0) and ΔL represents the duct semi-thickness.

We have chosen the following values:

$C = 0.2$

$L_0 = 4$

$\Delta L = 0.02$

$n_0(\lambda=0) = 340 \text{ cm}^{-3}$

$n_0(1000 \text{ km}) = 3130 \text{ cm}^{-3}$ ($T = 1000\ ^{o}K$, 80% O^+ and 20% H^+ at 1000 km altitude).

The results are presented in Table 4.1 for a few separable distributions and a nonseparable one, where we give both exact and approximate

TABLE 4.1. GAIN FOR A DUCTED WHISTLER. GT and GP are respectively the total and parallel approximation gains (in decibels), integrated between conjugate points at 1000 km altitude along ray paths in a duct centered at L = 4 (see text for the other duct parameters). The rays were started at vertical incidence at 1000 km altitude and at center of the duct, with the exception of the 6.65 kHz ray. Λ_E is the normalized frequency at the equator. Three separable distributions are chosen and one non-separable distribution whose parameter values are determined in Section 4C.

f(kHz)	Λ_E	ν = q =	5 0	5 2	5 4	5 4.8 ν_q = 0.4
1.36	0.1	GT = GP =	-2.08 -2.08	+10.3 +10.4	+13.5 +13.6	+0.56 +0.62
2.72	0.2	GT = GP =	-8.94 -8.82	+17.1 +17.2	+24.4 +24.6	+1.32 +1.48
4.08	0.3	GT = GP =	-24.2 -24.0	+22.2 +22.4	+36.6 +36.8	+2.52 +2.76
5.44	0.4	GT = GP =	-54.6 -54.4	+22.8 +23.0	+47.4 +47.8	+3.92 +4.38
6.65	0.483	GT = GP =	-115.4 -114.8	+14.5 +16.4	+57.0 +60.0	+2.48 +6.62

gain values. Our results confirm the validity of the parallel approximation used by Liemohn [1967] in the case of ducted whistlers. In almost all cases the difference between the full treatment and the parallel approximation is negligible. There are two reasons for that. One reason is that the angle θ stays small when a wave propagates in a duct. The second is that we deal with low frequencies ($\Lambda \lesssim 0.5$) and though there are more Landau particles than cyclotron particles, the parallel component

of the E field stays very small. The only big discrepancy is for the nonseparable distribution and the frequency $f = 6.65$ kHz, to which corresponds a normalized frequency $\Lambda = 0.483$. This frequency is very close to the limit frequency of duct trapping. The choice of input parameters is very critical in order to trap this wave and many attempts had to be made to find the correct values necessary for trapping, in contrast to lower frequencies for which a choice of vertical incidence at 1000 km at the middle of the duct was sufficient for trapping. It turned out that the variations of θ for $f = 6.65$ kHz were significantly higher than for lower frequencies.

As expected from the results of Chapter 3, the gain is considerably lower for the nonseparable distributions (only a few db) than for the separable distributions. Therefore, unless pitch angle information is available, it is impossible to conclude that nose-whistler upper cutoffs are caused by hot plasma effects. Therefore the use of nose whistlers as a diagnostic tool for monitoring electrons may be limited. Our nonseparable distribution is constructed to imply a certain equilibrium between waves and plasma (neglecting sources and sinks) and in quiet times, nose whistlers may tell us only that indeed this situation is reached. In quiet times, it may be possible to correlate a noted change in electron distribution with a noted change in nose whistler amplitude characteristics, especially if there is a tendency towards isotropy. The observation on satellites of much higher cutoffs is very important because: 1) it is evidence of the accessibility explanation of nose whistler upper cutoff observed on the ground; 2) it sets up some limits on the values of the parameters of the hot plasma distribution. An investigation of this high cutoff case is given in the next section.

C. DUCT LEAKAGES

The observations of Angerami [1970] provide an almost unique source of information for correlating the whistler amplitude spectrum with the distribution of energetic electrons within the plasmapause since his data and Schield and Frank's [1970] data are from exactly the same period. In particular the spectra of Figure 3.4 were measured on June 23, 1966. During the period between June 15 and June 23, the magnetic activity was quiet; K_p index $\sim$ 1,2; the DST index was low and the plasmapause was located beyond L $\sim$ 5.5. It may be therefore reasonable to assume there was no major change in the distribution function during that period.

Briefly, the data recorded on OGO 3 on June 15, 1966, between L = 4.1 and 4.7, showed whistler frequencies far above the cutoff frequencies observed on ground data. Sometimes these high frequencies were still ducted when they reached the satellite (see Figure 4.1a). More often, they were already unducted (Figure 4.1b). Careful ray tracing explained the propagation of these waves (see Figures 4.2 and 4.3). For further details, the reader is referred to Angerami [1970]. The suggestions of Liemohn [1967] that the high frequency whistler cutoff on ground data at a normalized frequency of $\sim$ 0.5 is caused by hot plasma effects is therefore questionable, particularly because without ducting we expect increased damping with the class of distribution functions previously considered.

To look at that question in detail, we chose the ray tracing parameters that Angerami used to explain the duct leakages. We integrated the gain rates on these ray paths and present the results in Table 4.2 (see Table 4.2 caption for all details). None of the distributions are compatible with the data: either there will be too much damping or there will be too much amplitude difference between two different frequency

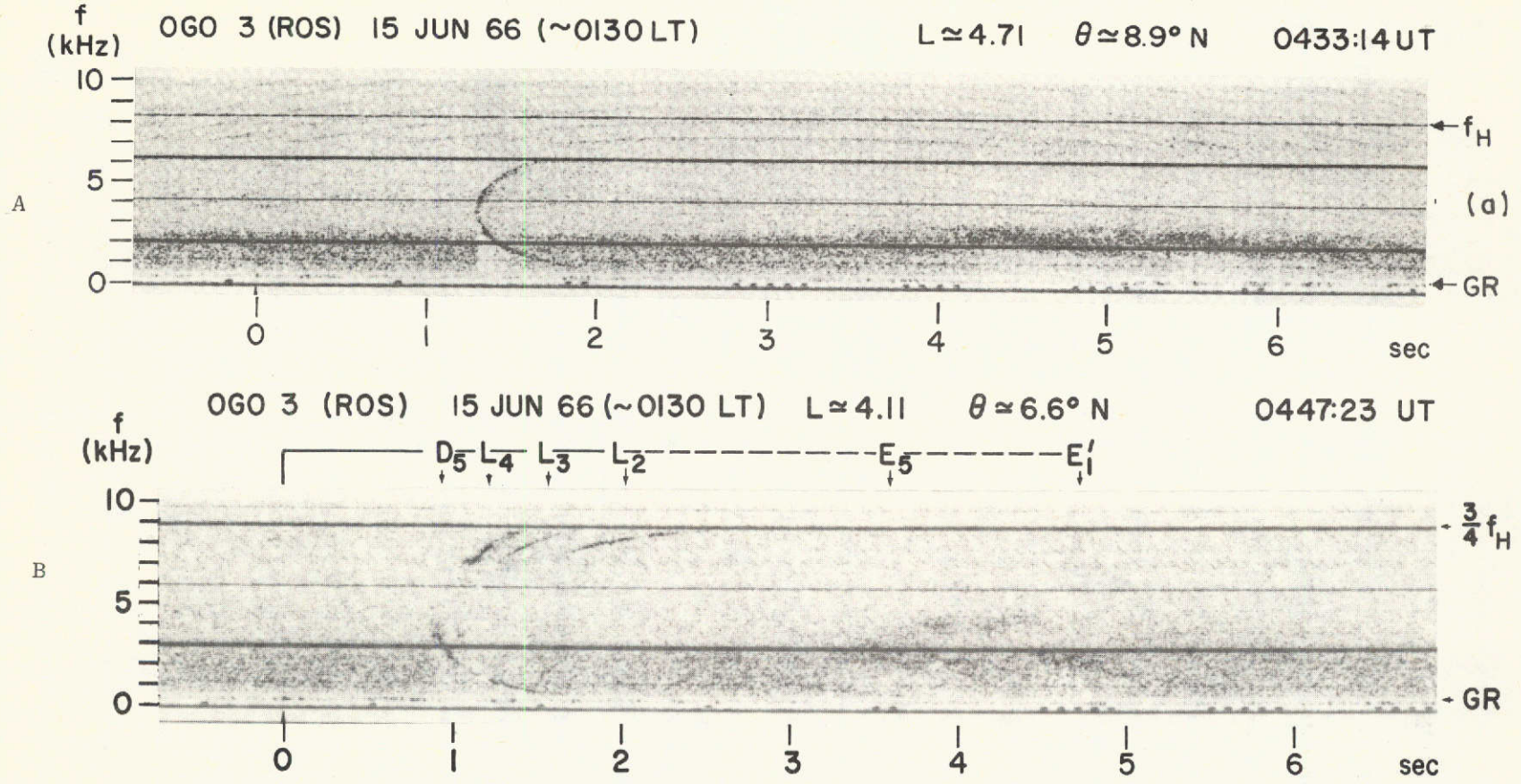

FIGURE 4.1. TIME FREQUENCY SPECTROGRAMS OF WHISTLERS RECEIVED ON OGO 3. Detailed explanation of the records is found in Angerami [1970]. (a) shows a whistler propagating in a duct up to 3/4 of the local gyrofrequency (see Figure 4.2). (b) high-frequency leakages from whistler ducts (see Angerami [1970] and Figure 4.3).

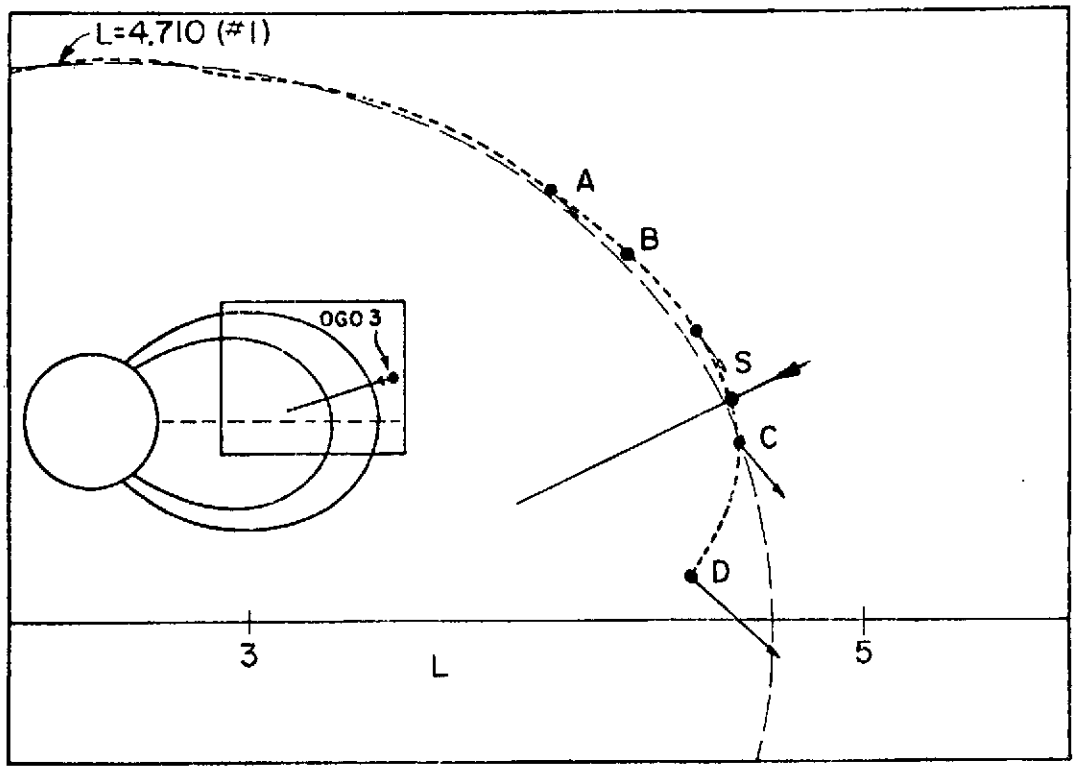

FIGURE 4.2. RAY TRACING TO EXPLAIN WHISTLER UPPER CUTOFF FREQUENCY OF FIGURE 4.1a. The values of the ray tracing parameters at different points along the path are the following:

A:	L = 4.7407	λ = 19.48	θ = 6.00	Λ = 0.500	W_{RO} = 404	W_{R1} = 404
B:	4.7467	15.42	5.21	0.601	281	124
S:	4.7406	9.32	-7.45	0.731	158	21.5
C:	4.7102	7.43	-15.60	0.748	132	15.8
D:	4.4696	2.20	-41.33	0.884	78.5	16.7

L and Λ are the geomagnetic dipole coordinates. The angle θ (in degrees) is measured clockwise from the local magnetic field. Λ is the wave frequency normalized to the local magnetic field. W_{RO} and W_{R1} (in eV) are the minimum energies of resonance of Landau and fundamental cyclotron resonances respectively.

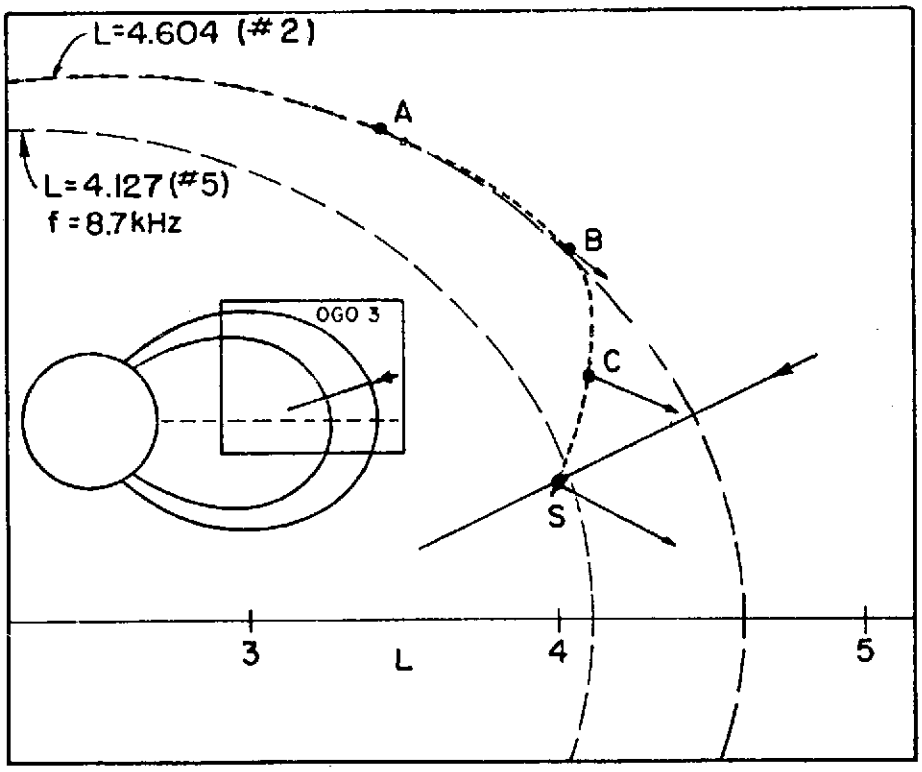

FIGURE 4.3. RAY TRACING TO EXPLAIN UPPER CUTOFF FREQUENCY OF LEAKAGE FROM DUCT 2, AS OBSERVED ON FIGURE 4.1b (L_2 component).

	L	λ	θ	Λ	W_{RO}	W_{R1}
A:	4.6110	24.66	3.50	0.492	712	759
B:	4.6011	16.36	-8.54	0.751	246	26.9
C:	4.3428	10.98	-33.83	0.766	104	9.7
S:	4.0747	6.45	-43.19	0.703	57.8	10.3

TABLE 4.2. GAIN FOR SEPARABLE DISTRIBUTIONS. The gain is expressed in decibels. Cases I and II refer respectively to Figures 4.1a,b. The frequencies shown are the following: Case I: f = 6.1 kHz is the highest observed frequency, and f = 4.17 kHz is the frequency which value normalized to the local magnetic field is 0.5 at the satellite location; Case II: f = 8.7 kHz and f = 7.7 kHz are respectively the highest and lowest observed frequency. The values of the parameters used in ray tracing of 6.1, 8.7 and 7.7 kHz components are taken from Angerami [1970]. The variables ν and q are the energy and pitch angle parameters. The functions GT and GL are respectively the total and the Landau gains expressed in db, integrated between A and S (see Figures 4.2 and 4.3). For the unducted paths the values of the parallel approximation gain GP is also given. The normalization of the distribution function for the computations is $\delta_{El} = 4 \times 10^{-3}$, to which corresponds $n(W > 100 \text{ eV}) \sim 1 \text{cm}^{-3}$. W_H is chosen lower than the lowest resonance energy along the paths.

Case	f(kHz)	ν=	4	4	4	4	6	6	6
		q=	0	2	4	6	0	2	4
I	6.1	GT=	-394	-117	-3.23	+50.3	-1429	-341	-45.5
		GL=	-3.2	-1.5	-2.34	-1.0	-4.2	-1.25	-0.7
	4.17	GT=	-117	+15.4	+65.2	+86.6	-58.6	2.7	+21.1
		GL=	-0.75	-0.37	-0.5	-0.6	-1.2	-1.8	-1.2
II	8.7	GT=	-1830	-754	-296	-67.4	-18000	-5170	-1450
		GL=	-525	-296	-188	-127	-2110	-851	-432
		GP=	-2210	-891	-287	+40.6	-11000	-3070	-814
	7.7	GT=	-871	-300	-70.8	+32.8	-3190	-800	-141
		GL=	-316	-172	-106	-63.6	-821	-323	-160
		GP=	-1100	-348	-817	+171	-2260	-497	-19.5

components. (On the average, a difference of 20 db between two frequencies would be readily observable on the records.)

Therefore we rule out separable distributions such as Liemohn's [1967]

as a possibility. It should be pointed out that for the unducted paths, computations with the precise values of θ had to be done, in contrast to ducted propagation for which the parallel propagation approximation is valid. We have written a program which includes 7 harmonics (see Appendix A), however a reasonable approximation could be made by keeping only the $m = 0$ (Landau) and $m = 1$ (fundamental cyclotron) harmonics and neglecting all other cyclotron harmonics.

We have repeated the duct leakage calculations using a nonseparable distribution of the class developed in the last chapter, and present the results in Table 4.3. From the ducted path of Figure 4.2, we have determined, for two fixed values of ν and ν_q, what value of the anisotropy parameter q which would yield small gain between points A and S and small differences in gains between any two frequencies. (As an example, we have chosen 6.1 kHz and 4.1 kHz which correspond respectively to the highest frequency observed in Figure 4.1a and the frequency to which corresponds $\Lambda = 0.5$ at the satellite.) A value of q between 4.8 and 5.0 seems adequate. Note though the high sensitivity on the value of q. (There is a big difference in gain values with as little a change as q varying from 4.5 to 5.) The reason for the choice of parameter values is the following: ν is chosen to match the measured energy spectrum and we have seen (Chapter 3) that $\nu \sim 5$ is a reasonable value. The parameter q is chosen so that the highest observed frequency is not damped. From Section 4B, the parallel propagation approximation can be considered as approximately correct. From Figure 3.8, we see that the highest unstable frequency is less than the marginal stability frequency Λ_{st} of the distribution having the same values of ν and q but a value of $\nu_q = 0$. In the case of $\nu = 4$ and $\nu_q = 0$, Λ_{st} can be obtained analytically:

TABLE 4.3. GAIN FOR NONSEPARABLE DISTRIBUTIONS. A table similar to 4.2 but for nonseparable distributions. ν_q is the coefficient of coupling between energy and pitch angle. GC is the fundamental cyclotron part of the gain. $\delta_{El} = 4 \times 10^{-3}$, and $W_H = 20$ eV.

Case	f(kHz)	ν=	5	5	5
		q=	4.5	4.8	5
		ν_q=	0.4	0.4	0.4
I	6.1	GT=	-18.9	-1.87	+8.0
		GL=	-1.97	-1.80	-1.7
	4.17	GT=	+4.1	+4.5	+4.8
		GL=	-0.34	-0.31	-0.29
II	8.7	GC=	+12.3	+116	+181
	7.7	GC=	+71.9	+96.6	+123

$$\Lambda_{st} = 1 - \frac{1-e^{-q/b}}{q/b} \tag{4.2}$$

For high values of q/b:

$$\Lambda_{st} \sim 1 - b/q \tag{4.3}$$

We therefore expect a value

$$q > \frac{b_S}{1-\Lambda_u} \tag{4.4}$$

where $\Lambda_u = 0.73$ corresponds to the highest frequency observed on Figure 4.1a, and b_S is the ratio B_S/B_E at the satellite position. Close to the equator:

$$b \sim 1 + \frac{9}{2} \lambda^2(\text{rd}) \ . \tag{4.5}$$

At the satellite, $\lambda_S \sim 9^o$ and $b_S \sim 1.11$, and we deduce from Eq. (4.4)

that $q > 4.1$.

The quantity ν_q is chosen so that there is small difference in gain between different frequencies. From Figure 3.8, such a difference diminishes when ν_q increases, and we can set up a lower bound on ν_q, which depends only weakly upon q.

As it can be seen by looking at the values of k_{ig} from point to point along the ducted ray path, the instability characteristic of a nonseparable distribution is more complex than for a separable function. For a fixed wave frequency, a nonseparable distribution function can be unstable at equator and be stable off equator, along the same field line, in contrast to a separable distribution. Physically, this comes about due to the fact that the resonant energy is increasing going from equator poleward and for a nonseparable distribution, the anisotropy of the function at resonance is decreasing towards isotropy and correspondingly the distribution becomes less unstable.

For the unducted path of Figure 4.3, only the fundamental cyclotron part of the gain could be determined because we developed a program only for small values of parameter $d_m = |(\Lambda-m)\tan\theta|$ (see Appendix A). Note the high sensitivity of parameter q on the cyclotron contribution. As pointed out earlier, the instability behavior of a nonseparable distribution may be complex. Also, for the distributions we chose, there is both damping and growth along the path. Finally, because of unducting, the relative range of resonant energy is large and gain rates change markedly towards the resonance cone.

The Landau contribution for the unducted path can be estimated to be of the same order for the class of separable and nonseparable distributions we have chosen. Both derivative terms with respect to energy

and pitch angle add up to contribute Landau damping (see Eq. (2.70)), in contrast to cyclotron interaction where they compete with each other. The essential difference between separable and nonseparable distributions was precisely that these derivative terms almost cancel each other for a large frequency band in the case of nonseparable distributions and do not in the other case. Therefore we expect from Tables 4.2 and 4.3 that the Landau interaction will dominate for our model. The nonseparable model we proposed is certainly not adequate for the unducted path for several reasons:

1. We looked at wave-plasma equilibrium only with respect to cyclotron interaction. In the unducted case, a distribution at equilibrium with both Landau and cyclotron interactions should be looked for (this becomes especially important close to the resonance cone where the Landau interaction eventually dominates), for separable and nonseparable distributions.

2. There is complete lack of information about particle distributions in the energy range below 100 eV and the whistler of Figure 4.1b interacts with electrons well below this energy. If used below 100 eV our model eventually violates the condition $\delta_{EH} \ll 1$, which is necessary for the validity of the gain expressions.

We may suggest a type of distribution which is at equilibrium with respect to Landau interaction. Looking back at Figure 2.4, we see that $N_{\parallel}$ is fairly constant over a wide range of frequencies and angles θ (but a few degrees from θ_R) and so is the minimum energy of resonance of Landau interaction from Eq. (2.12).

A peak in the distribution function or at least a flattening in the vicinity of the average Landau energy of resonance would reduce Landau damping. To a minimum Landau resonance energy $W_{RO} = 150$ eV, there corresponds an average energy of interaction

$$< W > = W_{RO}[1 + < \tan^2 \alpha >] \ . \qquad (4.6)$$

For $\nu = 5$, $\nu_q = 0.4$ and $q = 5$, $< W > = 750$ eV. We see indeed such a flattening around 750 eV on experimental spectra (see Figures 3.4a,b). The flattening of the spectrum being repeatable in two events separable by 20 days, it seems more than fortuitous and may well be related to Landau interaction.

Several important results have been established in this section:

1. Separable distributions such as Liemohn's [1967] cannot account for Angerami's [1970] observations.

2. The class of nonseparable distributions we proposed in Chapter 3 is compatible with the high frequency cutoff at $\Lambda_u \sim 0.75$ of Figure 4.1a. In turn the value of this cutoff determines a lower bound for one parameter (q). A lower bound on the coupling parameter ν_q is determined by the condition that the difference in gain should be small for different frequencies.

3. Our model is probably not adequate for very low energy electrons (a few tens of eV) because if it is accurate the unducted whistler components of Figure 4.1b should have been absorbed. This suggests that the observed flattening of the distribution in the 500 eV range reduces Landau damping.

The nonseparable distribution we propose incorporates the idea of equilibrium between plasma and waves in the magnetosphere. This equilibrium was investigated by Kennel and Petscheck [1966] and Lyons et al [1972] for high energy particles. We suggest here that waves may control efficiently the distribution of low energy electrons as well. Of course the picture of the mechanism should be completed by taking into account also sources and sinks of particles.

Considerable attention has been focused recently on plasma injection experiments [Brice, 1970; Cornwall, 1972]. By injecting cold plasma in the magnetosphere the resonance energy decreases and it is expected that wave-particle interactions become stronger as more particles will be available at resonance. The fact that, in certain (quiet) times, the

hot particle distribution is quite stable to electromagnetic waves casts a doubt on the efficiency of such an experiment.

We have also demonstrated here that our method to study wave amplitude variations caused by wave-particle interaction provides valuable information concerning distribution functions. Provided we know the flux of particles (which fixes the number of hot particles and one parameter, namely, the energy parameter ν), our method determines very sensitively the anisotropy of the distribution function. As of now, the number of available data is scarce, but a controlled experiment looks very promising with the advent of ground based vlf transmitters such as the transmitter of the Stanford VLF group, located at Siple, Antarctica (75.55°S, 83.55°W). Waves of frequency comparable to the minimum electron gyrofrequency of the Siple field line should be transmitted. The observation of the amplitude characteristics of these waves onboard a satellite orbiting close to the equatorial plane would provide particle distribution information along the way described in this section.

D. WHISTLERS OBSERVED AT FREQUENCIES NEAR THE LOCAL ELECTRON GYROFREQUENCY

Dunckel and Helliwell [1973] observed signals at frequencies close to the local electron gyrofrequency, e.g., as close as $\Lambda \sim 0.9$ onboard OGO-1 satellite. They successfully interpreted with ray tracing how the wave could propagate. Since Λ is high, these signals must interact with very low energy electrons. The cyclotron resonance energy tends toward zero when $\Lambda \to 1$ and secondly for $\Lambda > 0.5$, the wave becomes eventually unducted and propagates close to the resonance cone. This lowers the energy of resonance again.

Choosing the same values of ray tracing parameters they used, we investigated whether the distribution used in the preceding section is compatible with these observations or if we should have a different model.

The caption of Figure 4.4 explains the data and shows the value of parameters and Table 4.4 shows the corresponding values of integrated gain from 1000 km altitude up to satellite location.

TABLE 4.4. GAIN BETWEEN 1000 KM ALTITUDE AND SATELLITE. The gain is expressed in decibels. f = 80 kHz: The ray starts at 55° latitude, vertical incidence. In the ray tracing, the plasmapause is located at L = 3.9 (see Dunckel and Helliwell [1973]). The parameters of the ray tracing are:

	L	$\lambda^{(o)}$	$\theta^{(o)}$	Λ	$W_{RO(keV)}$	$W_{R1(eV)}$
S:	3.6766	36.67	-13.66	0.883	4.46	78.1
B:	3.2894	32.27	-18.42	0.916	1.65	13.7

$\delta_{El} = 4 \times 10^{-3}$ and $n(W > 100 \text{ eV}) \sim 1 \text{ cm}^{-3}$; $W_H = 20$ eV.

PATH	ν=	5	5	5	5	5	5
	q=	4.5	4.8	5	0	2	4
	ν_q=	0.4	0.4	0.4			
AS	GT=	-7.61	-6.12	-5.28	-128	-11.3	-1.17
	GL=	-0.43	-0.36	-0.32	-1.34	-0.13	-0.015
	GP=	-6.27	-5.02	-4.33	-124	-10.9	-1.14
AB	GT=	-72.6	-59.4	-51.9	-1100	-140	-21.6
	GL=	-4.62	-3.93	-3.52	-14.3	-1.95	-0.32
	GP=	-44.4	-36.0	-31.3	-916	-126	-17.7

It is seen in Table 4.4 that the gain with a nonseparable distribution or a separable distribution with an anisotropy of q = 2 would

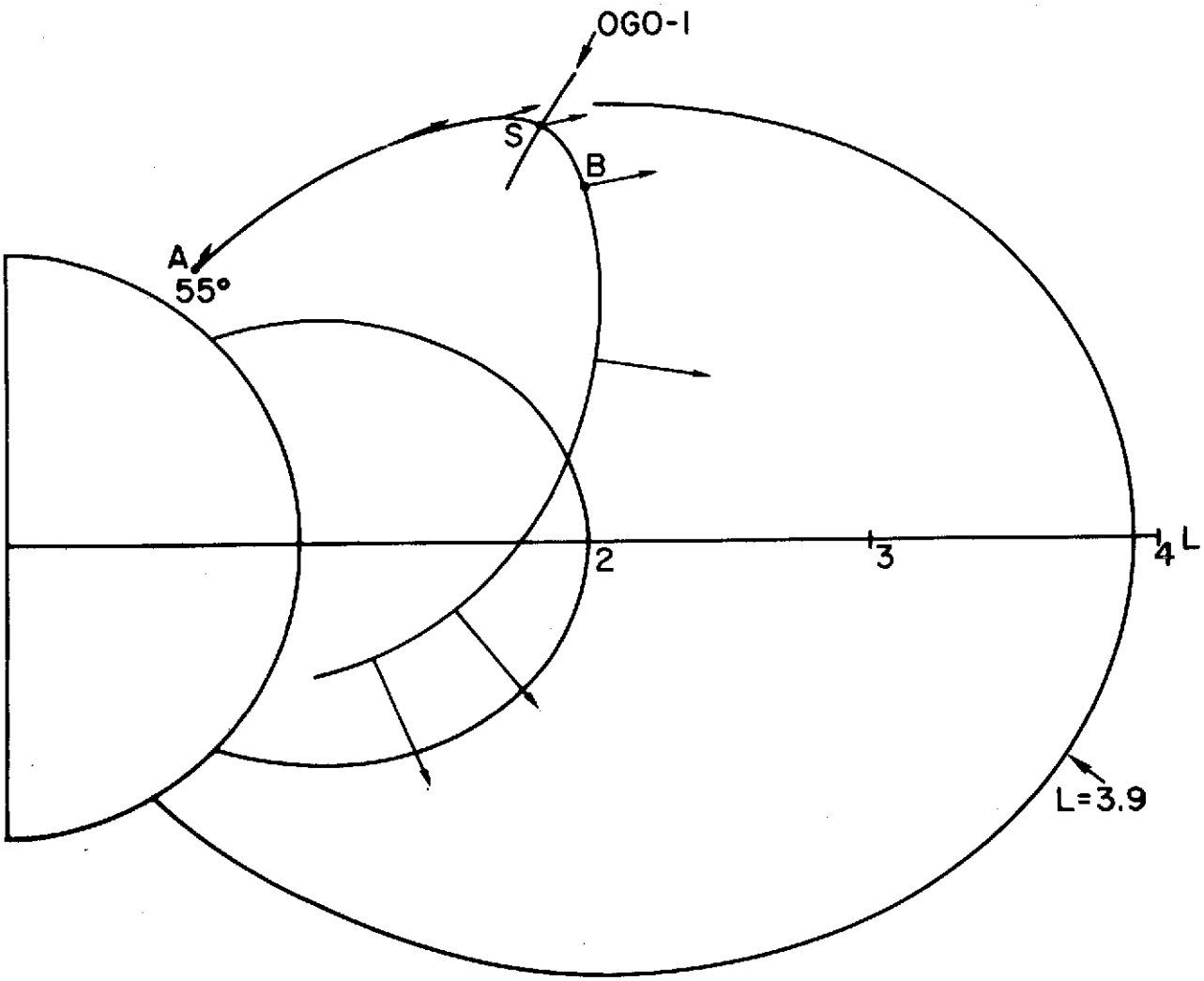

FIGURE 4.4. RAY TRACING AT 80 KHZ TO SIMULATE OBSERVATION OF LF SIGNAL ON OGO 1. Ray commences at 1000 km altitude, vertical incidence, and 55° magnetic latitude.

S:	L = 3.6766	λ = 36.67°	θ = -13.66°	Λ = 0.883	W_{RO} = 4.46 keV	W_{R1} = 77.5 eV
B:	3.2894	32.27	-18.42	0.916	1.62	13.5

Point B corresponds to the highest normalized frequency along the path. For further details see Dunckel and Helliwell [1973].

yield small attenuation at the satellite location. The reason is because the satellite is far from the equator ($\lambda_s \approx 37^o$) and there are few resonant particles available at the satellite location because of two reasons: 1) Many particles have mirrored before the satellite location; and 2) the refractive index decreases with latitude which causes increasing energy of resonance and hence fewer particles at resonance.

It is interesting though to notice that if the satellite had crossed the ray path a few degrees lower in latitude at $\lambda \sim 32^o$, to which corresponds the highest value of $\Lambda(\sim 0.92)$ along the path, the damping would have been important for the nonseparable distribution. Such a satellite path would have been most interesting to test the validity of our model.

For all distributions the Landau interaction is negligible, and the wave is interacting mostly with very low energy electrons in some portions of the path.

This LF wave, though of much higher frequency than the waves considered in the last section, has some identical characteristics. Namely, the wave propagates in the ducted mode up to a high normalized frequency and then rotates inward and propagates in the unducted mode. Both because the normalized frequency is high on the unducted part and because on the unducted part they eventually propagate very close to the resonance cone, these waves interact with very low energy electrons (i.e., less than 100 eV). Because there is a complete lack of data in that energy range and because satellite measurements become more difficult at low energy (spacecraft potential effect, etc.), whistlers may very well prove to be a unique tool for measuring very low energy particles. An experiment similar to the experiment described in the last section may be envisioned

for that purpose.

E. MR WHISTLERS

Magnetospherically reflected (MR) whistlers were observed for the first time by Smith and Angerami [1968] and studied rather extensively by Edgar [1972]. An example of an MR whistler spectrogram is given in Figure 4.5. The explanation of such whistlers in terms of accessibility (see above references and Figure 4.6) is the following: These waves are generated at low L values and their frequency, normalized to the equatorial gyrofrequency of the field line of generation, is small and stays below the LHR during an important portion of their path. In the absence of ducts, the wave propagates with a large wave normal angle which generally increases with distance. Since the wave frequency is below the LHR, the refractive index surface is closed (see Chapter 2), there is no limit for the wave propagation angle and reflections can occur. According to the input latitude, the satellite can record different components which have been reflected a different number of times, labelled as MR 0+, 1-, 1+, etc., as sketched in Figure 4.6.

Edgar [1972] explained the characteristics of the spectrogram of Figure 4.5 (and similar other spectrograms) through arguments invoking accessibility. We see several important features of MR whistlers in this spectrogram, namely, both upper and lower frequency cutoffs, and emission-like structures at the upper cutoffs. This last feature suggests that wave-particle interactions may play a role in MR whistlers and may account for both upper and lower frequency cutoffs.

Thorne [1968] postulated that all but the Landau interaction can be neglected both because $\Lambda \ll 1$ and θ is large along the major portion

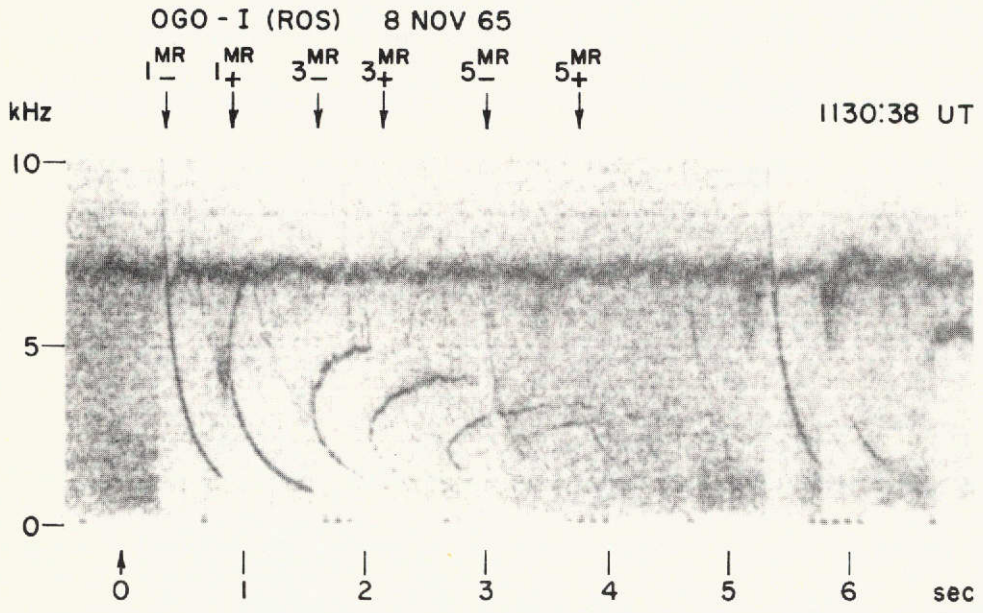

FIGURE 4.5. FREQUENCY-TIME SPECTROGRAM OF A TYPICAL MR WHISTLER OBSERVED NEAR THE MAGNETIC EQUATOR.

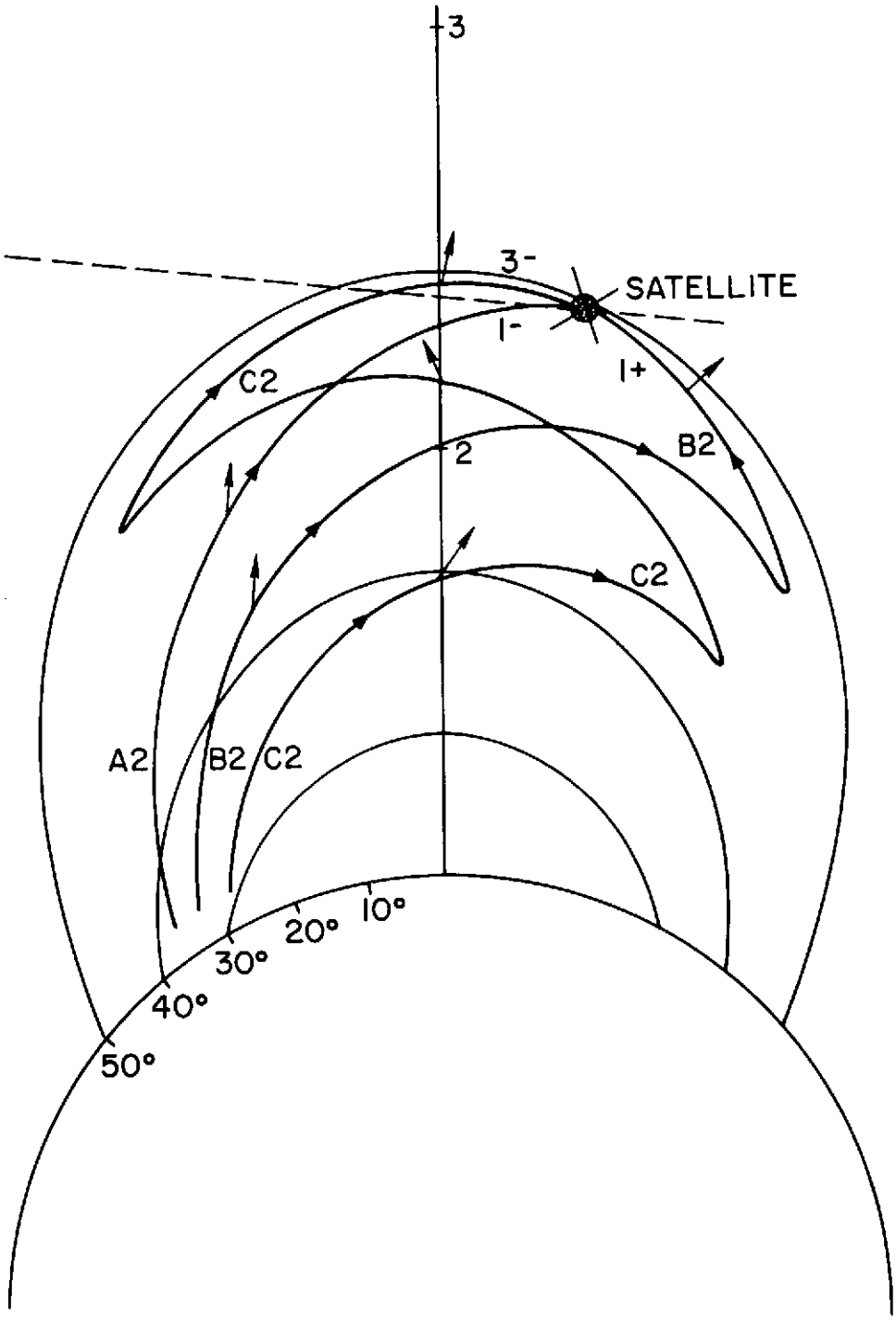

FIGURE 4.6. SKETCHES OF RAY TRACINGS TO EXPLAIN THE FIRST THREE COMPONENTS OF WHISTLER SHOWN IN FIGURE 4.5. The ray tracing parameters are given in Table 4.5.

of the path, and computed total amplitude gain over a few typical MR ray paths. He first used isotropic distribution $\propto \frac{1}{v^{\nu}}$. He concluded that such distributions give too much damping and he resorted to distribution with a secondary peak around 10 keV. The peak causes Landau growth along part of the path, therefore reducing the damping.

Edgar explained the upper frequency cutoff as well as "emissions" structures at the high frequencies purely on accessibility grounds. The high frequency distortions are caused by the presence of ducts, and density irregularities can account for the upper cutoffs. Edgar [1972] could not explain the low frequency cutoff but we can suggest a very simple explanation [R. A. Helliwell, private communication]: namely, the earth-ionosphere waveguide acts as a high frequency filter with cutoff frequency at $\sim$ 1.5 kHz during nighttime [Helliwell, 1965]. (Note that the spectrogram of Figure 4.5 was recorded in the early morning.)

Therefore it seems of interest to re-examine Thorne's [1968] computations.

We integrated the wave amplitude gains for separable distributions along ray paths whose parameters are defined in Edgar [1972] (see Table 4.5). We had to resort to separable distributions because of large values of θ and we have developed a program for arbitrary θ only for separable distributions. The choice though is not unreasonable. For cyclotron harmonics, the energy of resonance is very high and we have seen (Chapter 3) that for high energy, the assumption of separability is reasonable. The Landau interaction is much less sensitive to nonseparability than the cyclotron interaction.

We present in Figure 4.7 the results of our computations for the first

TABLE 4.5. RAY TRACING PARAMETERS TO EXPLAIN THE MR WHISTLER OF FIGURE 4.5. The parameters were chosen after Edgar [1972]. The rays begin at 500 km altitude, vertical incidence, and latitudes between 20^{o} and 40^{o} to intercept the satellite located at $L \sim 2.4$, $\lambda \sim 52^{o}S$. The diffusive equilibrium model is used with 50% H^{+}, 50% O^{+} at 1000 km, $T = 1600\ ^{o}K$, and $n(1000\ km) = 1.15 \times 10^{4}$, with an irregularity of the form $n(r,L) = n_{DE}(r) \cdot n_{c}(L)$. n_{DE} is the DE model expression and $n_{c} = 1 - 0.9 \exp\left[-\frac{(L-4)^{2}}{1.6}\right]$. The sign of θ is defined as positive measured clockwise from $\underline{B}_{0}$.

f(kHz)	MR	Λ	$\theta^{(o)}$	W_{R0}(keV)	W_{R1}(keV)
1.5	1-	0.023	-70.1	0.314	556
	1+		-102.3	0.448	821
	3-		-84.1	1.01	1710
3	1-	0.046	-69.5	0.519	217
	1+		-101.9	0.827	328
	3-		-83.5	1.60	750
5	1-	0.076	-68.7	0.752	119
	1+		-102.3	1.36	209
	3-		-83.7	1.48	233
7	1-	0.105	-67.5	1.11	80.1
	1+		-101.3	1.63	122
10	1-	0.150	-66.6	1.40	45.0

three MR components. In this case, the parameters influence in a complex way the values of the gain and no simple discussion of the influence of each parameter individually is possible. We see already from Table 4.5 that the ray path is fairly complicated. The ray path though is similar for different frequencies but the same MR component. The wave propagation angle is moving towards 90^{o} as the number of the component is increasing.

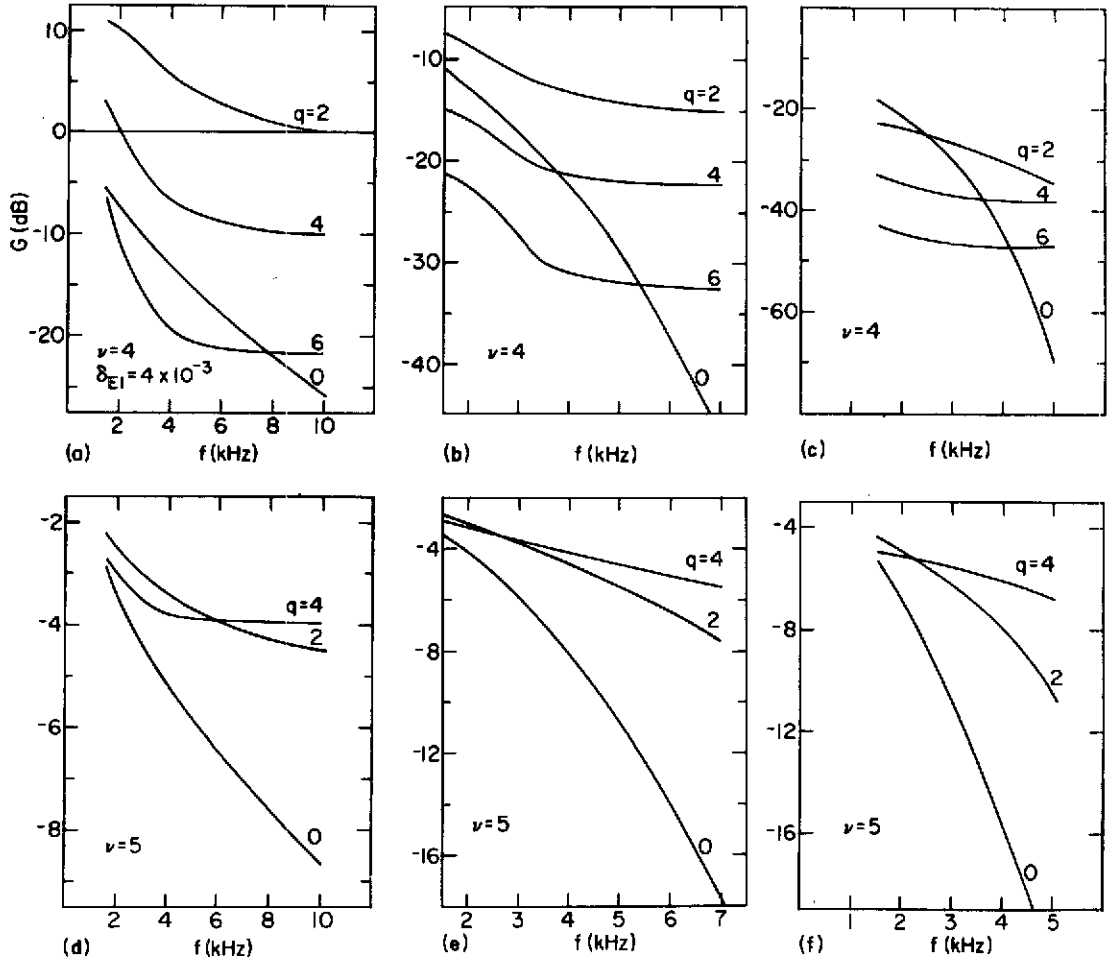

FIGURE 4.7. INTEGRATED GAIN RATES OVER RAY PATHS SKETCHED IN FIGURE 4.6. Several combinations of energy (ν) and pitch angle (q) parameters have been chosen. $\delta_{E1} = n(W \geq 100\ eV)/n(W \geq 0)$ in the equatorial plane.

When θ is close to the Gendrin angle θ_G and ω is fairly close to the LHR, a few degrees difference in θ may yield a big difference in resonance energy as illustrated by the difference in resonance energies for the 1+ and 3- components of the 3 kHz frequency. It is important to compare the value of θ at the satellite (which is close to the equator where the interaction is most important) with θ_G. When θ increases (as it does for increasing component number), two opposite situations develop depending upon whether θ is below or above θ_G. Referring to Figure 2.4, when ω is slightly above the LHR, $N_{||}$ decreases significantly when θ increases while below θ_G, and increases very rapidly when θ increases while above θ_G. Correspondingly, as the minimum energy of Landau resonance is inversely proportional to $N_{||}$, the strength of the interaction decreases (increases) when θ is below (above) θ_G. This may be in favor of Landau damping for higher frequency and higher component number, assuming the ray path behavior is the same for different frequencies and the same component number. For instance, denoting by θ_S the value of θ at the satellite location, $\theta_S \sim \theta_G$ for $f = 5$ kHz and the 3- component, and therefore θ_S would be beyond θ_G for $f = 7$ kHz and the 3- component.

The Landau interaction is almost always dominating, though neglecting the cyclotron interaction, as Thorne [1968] did, is invalid in some cases. For example, for the case $\nu = 4$, $q = 2$ and the first MR component, cyclotron growth overtakes Landau damping for all frequencies. Apart from this case, the Landau damping dominates, but it would still be incorrect to neglect the cyclotron interaction, at least for $\nu = 4$. As pointed out in Section 3E, though the cyclotron resonance energies are much higher than the Landau resonance energy for $\Lambda \ll 1$, the parallel component of the electric field, which excites the Landau resonance, is small. For increasing ν, the

Landau interaction becomes more important relative to the cyclotron interaction. For $\nu = 5$, the ratio of cyclotron gain to Landau gain is of the order of 10 to 20% and becomes negligible for $\nu = 6$ (of the order of 1 to 2%).

The question arises of what is the importance of the gain around the turnaround point. In this case the approximation Eq. (2.71) is no longer valid because the ions were neglected, and we have to take the correct limit of Eq. (2.69). When $\theta \to 90^o$ and $\omega < \omega_{LHR}$, $\cos\alpha_g \to 1$, $\cos\theta \to 0$ and there is an apparent divergence of the order $1/\cos\theta$. But $p_{Rm} \to \infty$, with the order $(\cos\theta)^{\nu-3}$. At the same time $d_m = |(\Lambda-m)\tan\theta| \to \infty$ like $1/\cos\theta$ and the integral in Eq. (2.68) $\to 0$ like $\frac{1}{d_m} \sim \cos\theta$ (see Appendix A). It can be shown that H and F defined in Eqs. (2.68) and (2.69) remain finite. Therefore

$$k_{ig} \sim (\cos\theta)^{\nu-3}, \quad \theta \to 90^o \tag{4.7}$$

For $\nu \geq 4$, there is no interaction around the turnaround point. This result just expresses that when $\theta \to 90^o$, the resonant energy tends toward infinity, and as the number of particles must remain finite, the number of particles at infinite energy is null. (Boundedness of the number of particles means $\nu > 3$ and therefore from Eq. (4.7), $k_{ig} \to 0$ as $\theta \to 90^o$.)

The damping is larger for $\nu = 4$ than $\nu = 5$ because of choice of normalization. The minimum energy of interaction is always bigger than 100 eV and we keep the number of particles above 100 eV to be the same for every distribution. As already mentioned in Chapter 3, this means more resonant particles and hence stronger interaction for harder spectra.

The influence of the anisotropy factor is more complex because of opposing effects (see Section 3C). Higher anisotropy means stronger

interaction because of increasing slope of the distribution with respect to pitch angle. It means also weaker interaction because of a decreasing number of particles at resonance (the average resonance energy increases and particles mirror closer to the equator). Finally, the cyclotron interaction acts differently for isotropic and anisotropic distributions.

The most important fact to notice is that for an anisotropy $q = 2$, the damping is never important enough to cause a sharp cutoff, in contrast to an isotropic distribution which could explain the higher frequency cutoff. Therefore, a distribution with a secondary peak in energy is not at all necessary to explain the observation of high frequency portions of MR whistler components as suggested by Thorne [1968]. The anisotropy of the distribution is sufficient for this purpose. Anisotropy must be present because of the loss cone (the more important, the lower the L shell) and isotropic distribution may not be likely in general, according to Sections 4B and 4D.

In fact, for $\nu = 5$, even an isotropic distribution would yield reasonable attenuation. Moreover, let us be more explicit about the normalization we chose and express it in terms of differential flux at 90^{o} pitch angle. At the satellite the total particle density we used for ray tracing is $\sim 2500\ cm^{-3}$. With our normalization ($\delta_{E1} = 4 \times 10^{-3}$), there corresponds a differential flux at 10 keV (see Figure 3.5):

$$d\Phi(10\ keV) \sim 4 \times 10^{4}\ cm^{-2} \cdot sec^{-1} \cdot sr^{-1} \cdot eV^{-1}, \quad \nu=4,\ q=2;$$
$$d\Phi(10\ keV) \sim 6 \times 10^{3}\ cm^{-2} \cdot sec^{-1} \cdot sr^{-1} \cdot eV\ , \quad \nu=5,\ q=2. \quad (4.8)$$

Therefore, even for a value of $\nu = 4$, if we take a more reasonable value of the flux of the order of $10^{4}\ cm^{-2} \cdot sec^{-1} \cdot sr^{-1} \cdot eV^{-1}$ like Thorne [1968], we do not obtain much attenuation.

We deduce that the analysis of MR whistlers for monitoring the hot electrons in the magnetosphere is, at the present time, limited. Knowledge of the particle flux is a prerequisite to drawing any conclusions. It may be interesting though in the future to test whether the high MR whistler frequencies may suffer high Landau damping relative to lower frequencies because high frequencies propagate sooner beyond the Gendrin angle. An experiment to test this effect should be done on satellites above ionosphere irregularities to eliminate the accessibility problem. An interesting experiment has been proposed by Edgar [1972]. He showed that it would be possible for a wave excited close to the Gendrin angle to propagate in the MR mode along field lines, reflect and come back to the satellite (the "boomerang mode"). On the return path to the satellite, the wave would propagate beyond the Gendrin angle, favoring heavy Landau damping.

F. CONCLUSION

We have demonstrated that separable distributions proposed by Liemohm [1967] are incompatible with Angerami's [1970] observations provided:

1. The theory presented in Chapter 2 is adequate
2. Particle fluxes at the time of Angerami's [1970] observations are comparable to fluxes observed by Schield and Frank [1970].

We have shown that the model of nonseparable distribution we have proposed in Chapter 3 is consistent with both these observations and particle observations. We summarize in this section the implications of this new model, and the application of our analysis to a diagnostic tool for monitoring the energetic electrons in the magnetosphere.

Our model of distribution involves a certain equilibrium between low energetic particles and electromagnetic waves in the magnetosphere

(neglecting sources and sinks of particles). The fact that the hot particle distribution may be quite stable to electromagnetic waves casts a doubt upon the efficiency of plasma injection experiments.

With our analysis, we have obtained valuable information concerning the hot plasma in the magnetosphere. Knowing the energy parameter ν from Schield and Frank's [1970] data, we assessed a lower bound on the anisotropy factor q of our model from the value of the upper cutoff frequency of the whistler shown in Figure 4.1a. From the condition that the difference in gain should be small between this upper frequency and any lower frequency, we assessed a lower bound on the coupling factor ν_q of our model. This method could be used in a systematic way in a controlled experiment which would involve a ground based transmitter and a satellite orbiting near the equatorial plane. Data similar to Angerami's [1970] or Dunckel and Helliwell [1973] should be obtained with such an experiment. An experiment using MR whistlers and a satellite seems also desirable to obtain information about hot electrons. The boomerang mode looks most suitable for that purpose.

V. GENERAL CONCLUSION AND SUGGESTIONS FOR FURTHER WORK

The purpose of the present work was the consideration of two problems. The first problem involves the study of wave amplitude variations for arbitrary wave frequency below the electron gyrofrequency and arbitrary direction of propagation. The second problem involves the determination of a realistic model of energetic electrons of the magnetosphere.

The instability characteristics of a few whistler observations, whose accessibility characteristics were already thoroughly established, have been investigated, and limits of distribution function models have been set up.

The theory we used to compute the wave amplitude variations caused by wave-particle interaction (i.e., whistler-electron interaction) was based upon several assumptions. In Section A, we briefly discuss where some of these assumptions break down. Section B will present a summary of our study. Finally, in Section C we give some suggestions for future work.

A. LIMITS OF THE THEORY

The theory we developed was based on the assumptions that:

A) The expression of the imaginary part $\underline{k}_i$ of the wave vector $\underline{k}$ is obtained from the coupled set of Maxwell equations and Vlasov equation after linearization.

B) $$|\underline{k}_i| \ll |\underline{k}| \ . \qquad (5.1)$$

Our purpose here is to discuss succinctly when these assumptions may break down. From Chapter 2, Assumption A is no longer valid if particle trapping by the wave becomes important. This occurs if wave signal

duration is of the order of trapping time, or more. We look briefly at this question in Appendix B, where we take into consideration:

1. Natural whistlers. In this case, though the duration of the signal is shorter than a trapping time, the question arises whether the electron can be trapped because of wave dispersion and space inhomogeneity.

2. Ducted whistlers. For unducted whistlers, the wave moves across field lines and interacts during a shorter time with electrons which are compelled to drift along magnetic field lines than for ducted whistlers.

3. The region around the equator, because the important part of the interaction takes place there (Chapter 3).

We used the criterion developed by Sudan and Ott [1971] and Dysthe [1971] and conclude that in those conditions, trapping can only take place for waves much more intense than average intensity waves [Burtis, 1969].

Assumption B insures that:

1. The real part of wave refractive index need not include hot plasma corrections.

2. The ray propagates along the ray path predicted by cold plasma theory and the group velocity keeps its full meaning. A "signal velocity" concept [Brillouin, 1960] need not be introduced.

In Appendix C, we look at question (1) for parallel propagating waves. We conclude that nose whistler dispersion cannot be used to test (1), and that hot plasma corrections should be included at the resonance cone.

B. SUMMARY OF RESULTS

Based upon the above mentioned theory, a general expression has been derived for the wave-amplitude variations of an electromagnetic wave in a magnetoplasma. This expression is algebraically simpler than previously derived expressions [Kennel, 1966; Brinca, 1972] and, as such enables easier computations and allows some conclusions by inspection:

1. The instability character of each harmonic of the interaction is straightforward.

2. The validity of the low-frequency approximation of Kennel [1966] is tested. It is valid for $\theta < \theta_G$ but not for $\theta \to \theta_R$; Kennel's [1966] approximation is incorrect for the Landau interaction because it neglects an important term, even for $\theta < \theta_G$. However this does not invalidate his conclusion that at $\theta \neq 0$, there is growth for a cone of angle $\theta < \theta_S$, though his value of θ_S is incorrect.

3. Significantly more anisotropic distributions are required for growth when $\theta \to \theta_R$ than when $\theta \to 0$.

A new model of distribution function has been proposed. This new class of distribution is nonseparable in particle energy and pitch angle, or in other terms, particles of different energy have different pitch-angle distributions.

Our model is expressed mathematically by

$$f(v,\alpha) \propto \frac{\exp[q(v_1/v)^{\nu_q}\sin^2\alpha]}{v^{\nu}} \tag{5.2}$$

where v_1 is a normalization parameter. The parameters ν, q, and ν_q have a simple physical meaning: ν and q express the energy and pitch-angle dependence respectively, and ν_q expresses the coupling between energy and pitch angle.

This function can be almost marginally stable over a large frequency band for parallel and almost parallel wave propagation, in contrast to previous separable distributions such as Liemohn's [1967]. This model is more realistic than separable models. It predicts an increasing slope in spectrum with decreasing energy, in agreement with Schield and Frank's

[1970] data. It predicts near isotropy at high energy, in agreement with Bogott and Mozer's [1971] data. There is indirect confirmation of our model, in the high energy range, by Kennel and Petschek's [1966] mechanism extended to arbitrary angle of propagation by Lyons et al [1972].

Fortran programs have been developed to compute total wave amplitude variations caused by whistler-electron interaction, integrated over a ray path. The following conclusions were reached:

1. For a whistler trapped in a duct, the parallel propagation approximation is valid for all frequencies (that is, below the frequency of untrapping $\Lambda \sim 0.5$) and is valid for nonseparable distributions for all frequencies except frequencies close to $\Lambda \sim 0.5$.

2. From almost simultaneous measurements of electrons [Schield and Frank, 1970] and whistler observations [Angerami, 1970] we conclude that separable distributions previously proposed by Liemohn [1967] are incompatible with observation. For the class of nonseparable distributions we have proposed, bounds on the values of the three parameters, ν, q, and ν_q are assessed. $\nu \sim 5$ is determined by the experimental spectrum [Schield and Frank, 1970]. $q \sim 5$ is determined by the highest observed frequency, and $\nu_q \sim 0.5$ is determined by the condition that the difference in gain between two frequencies is small. The sensitivity of the parameter q is important. There is a strong suggestion that the flattening of the distribution around 750 eV in Schield and Frank [1970] is caused by Landau interaction, because a flattening in the distribution reduces the Landau interaction which eventually dominates for moderately anisotropic distributions when $\theta \rightarrow \theta_R$. There is a suggestion also that a peak in energy should exist around a few tens of

eV, otherwise the gain rates would be too large.

3. It is possible to observe whistler waves in the magnetosphere at a frequency close to the local gyrofrequency, provided the observer location in latitude is far from the equator, simply because there are few resonant particles at high latitude. If the distribution is anisotropic, many particles mirror before reaching high latitude. Furthermore inside the plasmasphere, the refractive index increases with latitude, leading to an increase in the energy of resonance, and fewer particles resonate with the wave.

4. Computations of total wave amplitude gain have been done over some MR whistler ray paths, similar to Thorne's [1968] computations. However in Thorne's paper the cyclotron interactions were neglected on the grounds that the cyclotron resonance energies are much higher than the Landau resonance energy, for $\Lambda \ll 1$. This assumption is incorrect if the spectrum is hard enough, because, though there are many more Landau particles than cyclotron particles, the Landau interaction is weighted by a factor which decreases with frequency. However the Landau interaction always dominates after the first reflection. Anisotropic distributions greatly reduce the damping so that it is possible to explain MR whistler attenuation only by anisotropy without resorting to peaked energy distributions as Thorne [1968] did.

Our model has some implications:

1. This model involves a certain equilibrium between plasma and the electromagnetic waves that propagate in the magnetosphere. This situation was predicted by Kennel and Petschek [1966], and Lyons et al [1972] for high energy particle fluxes. Our analysis suggests that waves efficiently control the low energy particles also.

2. Plasma injection experiments rely on the fact that increasing the

cold plasma density lowers the particle resonance energy and therefore increases the number of resonant particles. Wave-particle interaction effects should then become more important, and noticeable effects may ensue. However, at times when the distribution is quasi-stable (to electromagnetic waves) the efficiency of the experiment is doubtful.

Extension of our analysis to a diagnostic method for monitoring the distribution of energetic electrons in the magnetosphere may be envisioned. However a selection in the type of whistler data is necessary:

1. Ground recorded whistlers are of some value for the purpose of hot plasma diagnostics. They may be useful to confirm a known change in distribution or to show that the distribution is not isotropic. However they cannot be used to obtain the precise shape of the distribution.

2. MR whistlers recorded on satellites and generated close to the earth are of limited value. The particle fluxes necessary to yield noticeable effects seem high, and a precise knowledge of the actual flux is prerequisite to any further conclusions. High MR whistler frequencies propagate sooner beyond the Gendrin angle than low frequencies as the number of reflections increases. As a result, the Landau damping increases with frequency and it will be interesting to test whether the high frequency components suffer heavy Landau absorption after the first or second reflections. To eliminate the problem of accessibility a satellite-to-satellite experiment is most desirable. The "boomerang mode" [Edgar, 1972] has the merit of requiring only one satellite, transmission and reception being done on the same satellite. It has the other advantage of using propagation at the Gendrin angle and beyond, therefore increasing Landau attenuation, and also, optimizing the transmitting power [Wang, 1970]. A strong recommendation is made for a detailed study of this experiment.

3. A controlled experiment using a ground-based transmitter and a

satellite would be most valuable for the purpose of hot plasma diagnostics, provided that the frequency of the transmitted wave is comparable to, or higher than, the minimum electron gyrofrequency of the field line of propagation and provided that the satellite orbits close to the equatorial plane. In these conditions the energies of interaction can be very low, for two reasons. The wave propagates a certain time in the ducted mode with a high value of Λ (low energy of cyclotron resonance) after which it propagates in the unducted mode and approachs the resonance cone angle (where both Landau and cyclotron interactions become important). Because the lower the particle energy, the more difficult the satellite particle measurements, this method may very well prove to be unique in measuring very low energy particles (of the order of a few tens of eV).

4. Because of the scarcity of available relevant data, we could not make a systematic test of how best to conduct the process of measurement for the purpose of diagnostics. Two orders of sophistication in the process are foreseen. The first method would eliminate an accessibility study and would require only the measurements of upper and lower cutoff frequencies. From the measurement of the higher frequency a lower bound on the parameter q is determined and from the condition that the difference in gain for different observed frequencies should be minimized, a lower bound on the parameter ν_q is estimated (along the way described in Section 4C). For ducted propagation, the knowledge of the particle flux seems a prerequisite (determination of parameter ν). On the contrary, for unducted propagation, knowledge of ν may not be necessary, as the conditions from one ray path to another may be quite different and from the observed differences, ν itself might be determined (or, it might be deduced that a different energy law variation is needed to represent

the energy spectrum). The second method would require the measurement of $dG/d\omega$. This method is more sophisticated than the previous one because it would first require a study of $dG/d\omega$ due to accessibility (a problem only recently approached [Dantas, 1972]), to clearly assess the relative importance of accessibility and instability effects.

C. SUGGESTIONS FOR FUTURE WORK

Besides the experiments we have mentioned, several suggestions for future work can be made:

1. Similar computations should be done outside the plasmapause. Going from inside to outside the plasmapause, the cold plasma density drops abruptly. There is a change also in hot plasma distribution, but apparently it is not the same change and probably the instability characteristics are different inside and outside the plasmapause.

2. A program should be developed to include a general distribution function for arbitrary direction of wave propagation. In particular, this will allow a study of very low energy electrons, when a wave becomes unducted and eventually propagates very close to the resonance cone angle. At the same time, hot plasma corrections to the real part of the refractive index should be looked for.

3. The stochastic analysis of Kennel and Petschek [1966], and Lyons et al [1972], which takes into account possible sources and sinks of particles, should be extended to higher frequency waves and low energy particles.

APPENDIX A. PROGRAM TO COMPUTE NONPARALLEL GAINS

Separable distributions:

Inserting g_0 given by Eq. (3.6) into Eq. (2.71) yields:

$$k_{ig} = k_{iL} + k_{ic} = -\zeta \frac{\pi}{8} \delta_{El} A_{\nu q} b^{-q/2} p_1^{\nu-3} \frac{\cos\alpha_g}{\cos^3\theta} \frac{M\omega_p^2}{\omega N^2} \left[\underline{k}_{iL} + \underline{k}_{ic}\right] ,$$

$$\underline{k}_{iL} = -\int_0^\infty 4(\nu+q) (\sin\alpha)^{q+2} \Big|_{R0}$$

$$\times \left[\left(\frac{N_\perp}{C_0}\right)^2 \left(\frac{p_0}{p_\perp}\right)^2 J_0^2(N_\perp \Lambda p_\perp/p_0) - 2 \frac{DHN_\perp}{C_0^2} \frac{p_0}{p_\perp} J_0 J_1 + \left(\frac{DH}{C_0}\right)^2 J_1^2\right] p_\perp dp_\perp$$

$$\underline{k}_{ic} = \sum_{m\neq 0} \int_0^\infty \left[\frac{mq}{\Lambda} - (\nu+q)(\sin\alpha)^{q+2}\right] \Big|_{Rm}$$

$$\times \left[\left(\frac{C_{m1}}{C_0}\right)^2 J_{m-1}^2(N_\perp \Lambda p_\perp/p_0) + \frac{2C_{m1}C_{m0}}{C_0^2} J_{m-1} J_{m+1} + \left(\frac{C_{m2}}{C_0}\right)^2 J_{m+1}^2\right] p_\perp dp_\perp \qquad (A.1)$$

k_{iL} and k_{ic} represent the contribution of the Landau and the cyclotron interactions respectively to the overall whistler mode wave interaction.

In the last expression we have to compute integrals of the form:

$$\int_0^\infty \frac{\sin^q\alpha}{p^\nu} J_r J_s(N_\perp \Lambda p_\perp/p_0) p_\perp dp_\perp \Big|_{Rm} = \left|p_{Rm}\right|^{2-\nu} B_{\nu q}^{rs}(d_m) ,$$

$$B_{\nu q}^{rs}(d_m) = \int_0^{\pi/2} (\sin\alpha)^{q+1} (\cos\alpha)^{\nu-3} J_r J_s(d_m \tan\alpha) d\alpha = d_m^{\nu-2} \int_0^\infty \frac{a^{q+1} J_r J_s(a) da}{[d_m^2 + a^2]^{\frac{q+\nu}{2}}}$$

$$d_m = |\Lambda - m| \tan\theta; \qquad r,s = \begin{cases} m-1, & m-1 \\ m-1, & m+1 \\ m+1, & m+1 \end{cases} . \qquad (A.2)$$

Inserting the coefficients $B^{r,s}_{\nu,q}$ given by Eqs. (A.2) into (A.1) yields:

$$\frac{k_{ig}}{k} = -\zeta \frac{\pi}{8} \delta_{El} A_{\nu,q} b^{-q/2} \frac{\cos\alpha_g}{\cos^2\theta} \left[\left(\frac{k_{iL}}{k}\right) + \left(\frac{k_{ic}}{k}\right) \right],$$

$$\frac{k_{iL}}{k} = -\left|\frac{p_1}{p_{R0}}\right|^{\nu-3} \frac{\cos\theta-\Lambda}{\Lambda} 4(\nu+q) \left\{ \left(\frac{N_{\parallel} N_{\perp}}{C_0}\right)^2 B^{00}_{\nu+2,q}(d_0) \right.$$

$$\left. - \frac{N_{\parallel} N_{\perp} DH}{\Lambda C_0^2} \tan^{-1}\theta \left[(q+2) B^{00}_{\nu+2,q} - (\nu+q+2) B^{00}_{\nu+2,q+2}\right] + \left(\frac{DH}{C_0}\right)^2 B^{11}_{\nu,q+2} \right\},$$

$$\left(\frac{k_{ic}}{k}\right) = \sum_{m\neq 0} \left|\frac{p_1}{p_{Rm}}\right|^{\nu-3} \left|\frac{\cos\theta-\Lambda}{m-\Lambda}\right| \left\{ \left(\frac{C_{m1}}{C_0}\right)^2 \left[\frac{mq}{\Lambda} B^{m-1,m-1}_{\nu,q}(d_m) - (\nu+q) B^{m-1,m-1}_{\nu,q+2}\right] \right.$$

$$+ \frac{2C_{m1}C_{m2}}{C_0^2} \left[\frac{mq}{\Lambda} B^{m-1,m+1}_{\nu,q} - (\nu+q) B^{m-1,m+1}_{\nu,q+2}\right]$$

$$\left. + \left(\frac{C_{m2}}{C_0}\right)^2 \left[\frac{mq}{\Lambda} B^{m+1,m+1}_{\nu,q} - (\nu+q) B^{m+1,m+1}_{\nu,q+2}\right] \right\}. \qquad (A.3)$$

From Eq. (A.2), there is an identity between distributions of different order in ν and q:

$$B_{\nu,q+2} = B_{\nu,q} - B_{\nu+2,q} \qquad (A.4)$$

Similarly, there exists a couple of recurrence relationships between sucessive resonance harmonics. Using the identity

$$J^2_{m-1}(x) + J^2_{m+1} = \frac{2m}{x} \frac{d}{dx} \left|J^2_m\right| ,$$

$$B^{m+1,m+1}_{\nu,q}(d_m) = B^{m-1,m-1}_{\nu,q} + \left[q B^{mm}_{\nu+2,q-2} - (q+\nu) B^{mm}_{\nu+2,q}\right] \qquad (A.5)$$

and using the identity

$$J_{m-1}(x)\ J_{m+1} = -\frac{1}{2}\ (J^2_{m-1} + J^2_{m+1}) + \frac{2m^2}{x^2}\ J^2_m\ ,$$

$$B^{m-1,m+1}_{\nu,q}(d_m) = -\frac{1}{2}\ [B^{m-1,m-1}_{\nu,q} + B^{m+1,m+1}_{\nu,q}] + \frac{2m^2}{d_m^2}\ B^{mm}_{\nu+2,q-2}\ . \qquad (A.6)$$

These last two relations permit us to deduce all the coefficients $B^{mn}_{\nu,q}$, $mn \neq 00,11$, from the values of $B^{00}_{\nu,q}$ and $B^{11}_{\nu,q}$.

When ν is an integer, the coefficients B_ν can be integrated analytically by means of relations involving different kinds of Bessel functions derived in Watson [1958], for example:

$$\int_0^\infty \frac{ada}{a^2 + d^2}\ J^2_m(a) = I_m(d)\ K_m(d) = B^{mm}_{20}\ (d) \qquad (A.7)$$

where I_0 and K_0 are the modified Bessel functions of first and second kind respectively.

By derivation with respect to d, we can obtain the values of the coefficients $B^{mm}_{\nu 0}$, $m = 0.1$, and ν even:

$$B^{mm}_{40} = -\frac{d}{2}\frac{\partial}{\partial d}\ [B^{mm}_{20}]\ , \text{ etc.} \qquad (A.8)$$

From the asymptotic expressions of $I_n(x)$ and $K_n(x)$ for $|x| \gg n,\ 1$ (see Watson [1958] for example), we deduce:

$$I_0(d)\ K_0(d) \sim \frac{1}{2d} + \frac{1}{16d^3} + \frac{27}{256d^5} + \ldots$$

$$I_1(d)\ K_1(d) \sim \frac{1}{2d} - \frac{3}{16d^3} - \frac{45}{256d^5} - \ , \ |d| \gg 1\ . \qquad (A.9)$$

Keeping the first term in Eq. (A.9), we see that

$$B^{mm}_{40} \propto \sim \frac{1}{d}\ , \quad |d| \gg 1\ . \qquad (A.10)$$

For higher values of ν, the coefficient $B^{mm}_{\nu 0}$ tends also asymptotically towards a $1/d$ variation, and from Eqs. (A.4), (A.5), and

(A.6) all the coefficients have this asymptotic behavior.

For odd integer values of ν, we can also obtain the coefficients $B^{mm}_{\nu q}$ in closed form [T. F. Bell, private communication], though not by straightforward derivation. Even for even integer values of ν but for high values of ν and q, a closed form for $B^{mm}_{\nu q}$ requires calculations of high order derivatives. This may be tedious and it is easier to integrate numerically the coefficients $B^{mm}_{\nu q}$ for $0 < d < d_a$, and use the asymptotic form Eq. (A.10) for $d > d_a$.

A listing of the program is given in Table A.1, and an example of the computer output is given in Table A.2.

Nonseparable distributions:

A program is developed for small values of θ, for a distribution function given by Eq. (3.22). From Eq. (3.25), k_{ig} is given by:

$$\frac{k_{ig}}{k} = \zeta \frac{\pi}{8} A_1 \frac{\cos\alpha_g}{\cos^2\theta} \left[\left(\frac{k_{iL}}{k}\right) + \left(\frac{k_{ic1}}{k}\right) + \left(\frac{k_{ic2}}{k}\right) \right] ,$$

$$\left(\frac{k_{iL}}{k}\right) \approx \sum_{n=0}^{\infty} b^{-n} \frac{q^n}{n!} (\nu+n\nu_q+2) \frac{p_1}{p_{R0}} (\nu+n\nu_q+2) \left|\frac{p_1}{p_{R0}}\right|^{\nu+n\nu_q-3} \left(\frac{\cos\theta}{\Lambda} - 1\right)$$

$$\times \left[\left(\frac{\Lambda\sin\theta}{\cos-\Lambda}\right)^2 B_{\nu+n+2,2} - \cos\theta \frac{\Lambda\sin\theta}{\cos\theta-\Lambda} d_0 B_{\nu+n\nu_q,2n+2} + \frac{\cos^2\theta d_0^2}{4} B_{\nu+n_q-2,2n+4} \right],$$

$$\left(\frac{k_{ic1}}{k}\right) \approx \sum_{n=0}^{\infty} b^{-n} \frac{q^n}{n!} \left|\frac{p_1}{p_{R1}}\right|^{\nu+n\nu_q} \left(\frac{\cos\theta-1}{1-\Lambda}\right)$$

$$\times \left[1 + \cos\theta + \frac{\Lambda^2\sin^2\theta}{(\cos\theta-\Lambda)}\right]^2 \left\{ (\nu+n\nu_q+2n) B_{\nu+n\nu_q,2+2n} - \frac{2n}{\Lambda} B_{\nu-2+n\nu_q,2n} \right.$$

$$\left. - \frac{d_1^2}{2} \left[(\nu+2n+n\nu_q) B_{\nu-2+n\nu_q,4+2n} - \frac{2n}{\Lambda} B_{\nu-2+n\nu_q,2+2n} \right] \right\},$$

$$\left(\frac{k}{\pm ic2}\right) \sim \sum_{n=0}^{\infty} b^{-n} \frac{q^n}{n!} \left|\frac{p_1}{p_{R2}}\right|^{\nu+n\nu_q-3} \left(\frac{\cos\theta-\Lambda}{2-\Lambda}\right) d_2^2$$

$$\times \left[(\nu+n\nu_q+2n)\ B_{\nu-2+n\nu_q,4+2n} - \frac{4n}{\Lambda}\ B_{\nu-2+n\nu_q,2+2n}\right]. \qquad (A.11)$$

A listing of the program is given in Table A.3, and an example of the computer output is given in Table A.4.

TABLE A.1. LISTING OF THE PROGRAM TO COMPUTE THE GAIN INTEGRATED ALONG A RAY PATH FOR SEPARABLE DISTRIBUTIONS.

```
      $WATFIV
      C THIS PROGRAM COMPUTES THE WHISTLER MODE WAVE AMPLITUDE GAINS (IN DB.),
      C INTEGRATED OVER A RAY PATH WHOSE PARAMETERS ARE GIVEN BY THE STANFORD
      C VLF GROUP RAY TRACING PROGRAM. POSITIVE (NEGATIVE) GAIN MEANS WAVE
      C GROWTH(DAMPING). THE ENERGETIC ELECTRON DISTRIBUTION IS PROPORTIONAL TO
      C SIN(ALPHA)**Q/P**NU, WHERE ALPHA AND P ARE RESPECTIVELY THE ELECTRON
      C PITCH-ANGLE AND MOMENTUM, NU CAN TAKE INTEGER VALUES FROM 4 TO 10,
      C AND Q CAN TAKE EVEN INTEGER VALUES FROM 0 TO 10-2*INT(NU/2). M IS THE
      C ORDER OF CYCLOTRON HARMONICS. THIS PROGRAM INCLUDES VALUES FROM M=0 TO
      C ABS(M)=3 (M=0 FOR LANDAU HARMONIC, M=1 FOR FUNDAMENTAL CYCLOTRON
      C HARMONIC)
      C
      C INPUT:
      C         FREQUENCY OF THE WAVE(KHZ), INITIAL AND FINAL GROUP TIMES
      C         (LINES 46 AND 47).
      C         L VALUE, LATITUDE(DEG.), NORMALIZED FREQUENCY, WAVE PROPAGATION
      C         ANGLE(DEG.), DENSITY(CM-3),GROUP TIME(SEC) (LINES 57 AND 58).
      C
      C OUTPUT
      C         FREQUENCY OF THE WAVE(KHZ), INITIAL AND FINAL GROUP TIMES
      C         L VALUE,LATITUDE(DEG.), NORMALIZED FREQUENCY, WAVE PROPAGATION
      C         ANGLE(DEG.), DENSITY(CM-3), PLASMA FREQUENCY NORMALIZED TO
      C         GYROFREQUENCY, PARALLEL COMPONENT OF REFRACTIVE INDEX, MINIMUM
      C         RESONANCE ENERGY FOR LANDAU AND FUNDAMENTAL CYCLOTRON INTER-
      C         ACTIONS (KEV).
      C         GAINS INTEGRATED FROM INITIAL TIME, INCLUDING RESPECTIVELY:
      C         ALL HARMONICS(M<4), LANDAU HARMONIC,FUNDAMENTAL HARMONIC,HIGHER
      C         HARMONICS, PARALLEL PROPAGATION APPROXIMATION, NU, AND Q.
      C
      C LIMITS
      C         HIGH PLASMA FREQUENCY APPROXIMATION FOR REFRACTIVE INDEX, BUT
      C         INCLUDE IONS. RELATIVITY NOT INCLUDED.TO PRINT DIFFERENT VALUES
      C         OF NU AND Q (BUT IN THE PREVIOUSLY DEFINED RANGE), CHANGE
      C         ACCORDINGLY LINES 126 TO 146, 191 TO 211, AND 254 TO 274.
      C         TO INCLUDE DESIRED NUMBER OF HARMONICS, CHOSE APPROPRIATE VALUE
      C         OF M IN LINE 244.THE INTERVAL OF INTEGRATION IS DTAIG=0.02 SEC
      C         OR MORE AND CAN BE CHANGED APPROPRIATELY IN LINES 63 AND 64.
      C         THE DISTRIBUTION FUNCTION IS NORMALIZED TO DF=0.004, WHERE
      C         DE=RATIO HOT PLASMA DENSITY FOR ENERGY>100EV TO COLD PLASMA
      C         DENSITY; CHOSE APPROPRIATE VALUE OF DE IN LINE 248.
      C
      C FUNCTION FACTORIAL
    1         FUNCTION FFF(N)
    2         IF (N.EQ.0) GO TO 2
    3         FFF=1
    4         DO 1 I=1,N
    5       1 FFF=FFF*I
    6         GO TO 3
    7       2 FFF=1
    8       3 RETURN
    9         END


   10         FUNCTION ANQ(NU,NQ)
   11         ANQ=1
   12         JQM=NQ/2+1
   13         DO 11 JQ=1,JQM
   14      11 ANQ=(FLOAT(JQ)-0.5)*ANQ
   15         ANQ=ANQ*2*(NU-3)/FFF(NQ/2)
   16         RETURN
   17         END



   18         FUNCTION BNQ(NU,NQ)
   19         BNQ=1
   20         JQM=NQ/2+1
   21         DO 10 JQ=1,JQM
   22      10 BNQ=BNQ/(NU/2.-2.+FLOAT(JQ))
   23         BNQ=FFF(NQ/2)*BNQ/2
   24         RETURN
   25         END
```

```
      DIMENSION S(20),SC(20),SL(20),SCI(20)
      DIMENSION GWSI(20),GWSC(20),GWSL(20),GWSS(20)
      DIMENSION PGWS(20)
      DIMENSION BJ(11,2,5I)
C BJ=INTEGRAL FROM 0 TO PI/2 OF SINX*COSX**(NU-3)*JD,I((D*TANX)**2.
C D VARIES FROM 1 TO 5 BY STEP 0.1.
C BJ(*,*,1)= B(D=0) , BJ(*,*,2) = B(D=.1) ,ETC...
C I1=NUVARIATION, I2=M VARIATION, I3=D VARIATION
      DIMENSION BN(11,6,2)
C I1 FOR NU VAR.V NU-3 I2 FOR Q VAR. = Q/2+1 I3= M VARIATION
C BN(1,6,1I=B(4,0,2,2), BN(10,6,1)=B(5,0,2,2),ETC...
C BN(11,5,2)=B(4,2,0,2),BN(10,5,2I=B(5,2,0,2),ETC...
      INTEGER NU,NQ
C NU=NU;NQ=Q.
      REAL KIK,KIKLAN,KIKCYL
      REAL LA,KIG
      REAL INVL
      REAL LAT
      LOGICAL TRUC
      DO 200 L=1,2
      DO 200 NU=1,11
      READ (5,24) BJ(NU,L,1)
   24 FORMAT (F9.6)
      DO 200 K=1,10
      READ(5,23) (BJ(NU,L,J+(K-1)*5),J=2,6)
   23 FORMAT(5E14.7)
  200 CONTINUE
C READ INPUT DATA FROM COL ) PLASMA RAY TRACING
10001 READ (5,460) FKC,TGNEW,TGLAST
  460 FORMAT(F10.4,F10.6,F13.6)
      WRITE(6,4550) FKC ,TGNEW,TGLAST
 4550 FORMAT('1FKC=', F13.4, '   TGO=',F10.6,'   TGLAST=',F10.6)
C FKC IS FREQUENCY SIGNAL IN KHZ
      TRUC = .FALSE.
      DO 118 I=1,20
      PGWS(I) = 0.
      GWSI(I)=0.
      GWSL(I) = 0.
      GWSC(I) = 0.
      GWSS(I) = 0.
  118 CONTINUE
10000 READ(5,490,END=900)
     %              INVL,LAT,LA,THETA,IDENS,TG
  490 FORMAT(F10.5,F10.2,F10.4,F10.2,I10  ,F1).6)
      TRUC = .NOT.TRUC
      IF (TRUC) TGOLD=TG
      IF (.NOT.TRUC) TGNEW=TG
      DTATG = ABS(TGNEW-TGOLD)
      IF (DTATG.LT.0.32) TRUC = .NOT. TRUC
      IF (DTATG.LT.0.02) GO TO 10000
      DEGRAD = 3.141592/180
      IF (THETA.EQ.90.) THETA=89.99
      THETAR = THETA*DEGRAD
      BETA = LA*8.984*SQRT(FLOAT(IDENS))/FKC
      OCI = (1-LA)*TAN(THETAR)
      OLAN = LA*TAN(THETAR)
C IDENS IS DENSITY IN PARTICLES/CUBIC CENTIMETERS
C BETA=PLASMA FREQUENCY/GYROFREQUENCY
C LA=WAVE FREQUENCY/GYROFREQUENCY
C THETA=ANGLE OF PROPAGATION WITH RESPECT TO THE MAGNETIC FIELD
```

```
      COSTA = ABS(COS(THETAR))
      SINTA = ABS(SIN(THETAR))
      DELTA =1-1/(43*LA)**2
      COSTAD  = COSTA-LA*DELTA
      TALPHA=SINTA/(2*(COSTAD  ))
C THETA HERE IS EXPRESSED IN DEGREES
      CALPHA=1/SQRT(1+TALPHA**2)
      RIND = BETA/SQRT((COSTA-LA*DELTA)*LA)
C RIND=REFRACTIVE INDEX
      P10=.02
      PRIND=BETA/SQRT((1-LA)*LA)
C PRIND=PARALLEL REFRACTIVE INDEX
      RPAR= RIND*COSTA
      RPER=RIND*SINTA
      H = COSTA*(1/LA-LA)
      SD = BETA**2 / (LA*(1-LA**2))
      SP=-(BETA/LA)**2
C SP = STIX P PARAMETER
      PR1=ABS((LA-1)/(PRIND*LA))
C SD= STIX D PARAMETER
      CO=2*ABS(SP)
      PRIWAT = (1-LA)/(RPAR*LA)
C PRIWAT IS THE FUND. MOMENTUM OF RESONANCE
C PR1=MOMENTUM ERR PARALLEL PROPAGATION
      WO = 512.
      WC1 = WO*(PRIWAT)**2/2
      PROWAT = 1/RPAR
      WLAN = WO*(PROWAT)**2/2
C PROWAT IS THE RESONANCE MOMENTUM FOR LANDAU INTERACTION
      RWC1WL = WC1/WLAN
C WO=MO*C**2
C WC1 AND WLAN ARE RESPECTIVELY THE MINIMUM ENERGIES OF RESONEANCE FOR
C FUNDAMENTAL AND LANDAU RESONANCES (IN KEV)
      WRITE(6,480)
  480 FORMAT('0','       L          LAT        LAMBDA     THETA       BETA
     $ DENS     TG          MUCOS      WLAN       WC1')
      WRITE(6,470) INVL,LAT,LA,THETA,BETA,IDENS,TG,RPAR,WLAN,WC1
  470 FORMAT(F10.5,F13.2,F10.4,F13.2,F10.2,I10,F10.4,F10.2, 2E11.3)
      WRITE(6,440)
  440 FORMAT('        GMT       GWL          GWC          GWS          PGW
     $      NU   Q')
      M=0
      IF (M.EQ.0) GO TO 43
  157 CONTINUE
      CM1 =((BETA/LA)**2*(1+COSTA) + RPER**2*LA/M)/CO
      CM2 =((BETA/LA)**2*(1-COSTA) + RPER**2*LA/M)/CO
C CM1=COEFFICIENT OF BESSELF FUNCTION OF ORDER (M-1) IN KIG AND
C CM2=COEFF. OF BESSEL FUNCTION OF ORDER (M+1)
   43 PRM =    ABS(LA-M)/RPAR*LA)
C PRM = NORMALIZED MOMENTUM OF RESONNANCE (TO PO=MO*C)
      D =ABS((LA-M)*SIN(A/COSTA)
      IF (D.EQ.0) GO TO 159
C STATEMENT 159 FOR PARALLELE PROPAGATION
C BEGIN DEFINITION OF JO**2 AND J1**2 TERMS
C INTERPOLATION FOR B(Q=0)
   55 RJ=10*D
      J=INT(RJ)
      DO 95 L=1,2
      DO 95 NU=1,11
      IF (D.LT.0.1) SN(NU,1,L) = B0(NU,L,1) + D**2*100*(B0(NU,L,2)
```

```
          $ -BO(NU,L,1))
112         IF ( (D.GE.0.0) .AND. (D.LT.5.) )
          $BN(NU,L,1) = (RJ-J) * (BO(NU,L,J+2) - BO(NU,L,J+1)) + BO(NU,L,J+1)
      C ASYMPTOTIC EXPRESSION WHEN D>5
113         IF(D.GE.5.) BN(NU,L,L)=BO(NU,L,51)
114       95 CONTINUE
      C END INTERPOLATION
      C COMPUTE B(Q-=0) AND (00,L1) FOR M
115         DO 12 L=1,2
116         MTRUE=L-1
117         DO 12 JQ=1,5
118         JNM=11 -2*JQ
119         NQTRUE=2*JQ
120         DO 10 JNU = 1,JNM
121         BN(JNU,JQ+1,L) = BN(JNU,JQ,L) - BN(JNU+2,JQ,L)
122       10 CONTINUE
123       12 CONTINUE
      C END OF DEFINITION OF J0**2 AND J1**2 TERMS
124         IF (M.NE.0) GO TO 163
      C BEGIN LANDAU TERM
125         DO 5100 I=1,10
126         IF (I.EQ.1) AU=4
127         IF (I.EQ.2) AU=4
128         IF (I.EQ.3) AU=4
129         IF (I.EQ.4) AU=4
130         IF (I.EQ.5) AU=5
131         IF (I.EQ.6) AU=5
132         IF (I.EQ.7) AU=5
133         IF (I.EQ.8) AU=6
134         IF (I.EQ.9) AU=6
135         IF (I.EQ.10) AU=6
136         IF (I.EQ.1 ) AQ=0
137         IF (I.EQ.2 ) AQ=2
138         IF (I.EQ.3 ) AQ=4
139         IF (I.EQ.4 ) AQ=6
140         IF (I.EQ.5 ) AQ=0
141         IF (I.EQ.6 ) AQ=2
142         IF (I.EQ.7 ) AQ=4
143         IF (I.EQ.8 ) AQ=0
144         IF (I.EQ.9 ) AQ=2
145         IF (I.EQ.10) AQ=4
146         NU=AU
147         NQ=AQ
148         JNU=NU-3
149         JQ=NQ/2+1
150         T1 = (RPAR*RPER)**2*BN(JNU+2,JQ,1)/C0**2
151         IF (D.LT.0.2) T2=      D*BNQ(NU,NQ+2)*RPAR*RPER*SD*H/C0**2
152         IF (D.GE.0.2)
          $T2 = ((NQ+2)*BN(JNU+2,JQ,1)-(NU+NQ+2)*BN(JNU+2,JQ+1,1))
          * *RPAR*RPER*SD*H/(D*C0**2)
153         T3 =(SD*H)**2*BN(JNU,JQ+1,2)/C0**2
154         SUMLAN =-(NU+NQ)*(T1-T2+T3)*4
155         SUMLAN=SUMLAN*(P10/P**)**(NU-3)*(COSTA-LAI/L
156         IF (D.GE.5.) SUMLAN = SUMLAN*S/D
157         SUM=SUMLAN
158         S(I) = SUM
159         SL(I) = SUMLAN
160       5100 CONTINUE
      C END LANDAU TERM
```

```
162         M=1
163         GO TO 157
164       163 CONTINUE
      C END COMPUTING THE COEFFICIENT B(NU,Q,M,M)(D)
      C BEGIN TERMS IN J2**2 AND JQ*J2 AND SUPERIOR ORDERS
      C COMPUTE B(NU,0,2,2)
165       14 NUM=9
166         MTRUE=M+1
167         MM=MTRUE-2
168         IF (NUM.LT.0) GO TO 1001
169         DO 28 NU=1,NUM
170         BN(12-NU,6,1) = BN(NU,1,1) - 2*(NU+3)*BN(NU+2,1,2)/D**2
171         BN(12-NU,6,2)=1
172       28 CONTINUE
173         NUM=NUM-2
174         IF (NUM.LT.0) GO TO 999
175         DO 29 NU=1,NUM
176         BN(12-NU,5,1) = BN(12-NU,6,1) - BN(10-NU,5,1)
177         BN(12-NU,5,2) = -(BN(NU,2,1)+BN(12-NU,5,1))/2+BN(NU+2,1,2)*2
           $ *(1/D)**2
178       29 CONTINUE
179      999 CONTINUE
      C COMPUTE B(NU,Q>=0 AND 2,2,2) AND B(NU,Q>=0 AND 2,0,2)
180         DO 15 L=1,2
181         DO 13 JQ=1,3
182         NQTRUE=2*JQ+2
183         JNM=NUM-2*JQ
184         IF (JNM.LT.0) GO TO 998
185         DO 11 JNU=1,JNM
186         BN(12-JNU,6-JQ,L) = BN(12-JNU,6-JQ,L) - BN(10-JNU,6-JQ,L)
187       11 CONTINUE
188       13 CONTINUE
189      998 CONTINUE
190       15 CONTINUE
      C END TERMS J2**2 AND JQ*J2
      C BEGIN FIRST CYCLOTRON TERM
191         DO 9101 I=1,10
192         IF (I.EQ.1) AU=4
193         IF (I.EQ.2) AU=4
194         IF (I.EQ.3) AU=4
195         IF (I.EQ.4) AU=4
196         IF (I.EQ.5) AU=5
197         IF (I.EQ.6) AU=5
198         IF (I.EQ.7) AU=5
199         IF (I.EQ.8) AU=6
200         IF (I.EQ.9) AU=6
201         IF (I.EQ.10) AU=6
202         IF (I.EQ.1 ) AQ=0
203         IF (I.EQ.2 ) AQ=2
204         IF (I.EQ.3 ) AQ=4
205         IF (I.EQ.4 ) AQ=6
206         IF (I.EQ.5 ) AQ=0
207         IF (I.EQ.6 ) AQ=2
208         IF (I.EQ.7 ) AQ=4
209         IF (I.EQ.8 ) AQ=0
210         IF (I.EQ.9 ) AQ=2
211         IF (I.EQ.10) AQ=4
212         NU=AU
213         NQ=AQ
214         JQ=NQ/2+1
```

```
215         JN=NU-3
216         T2 = 2*CM1*CM2 * ( BN(12-JN,7-JQ,2)*M*NQ/LA - (NQ+NU) *
           $ BN(12-JN,6-JQ,2) )
217           IF (D.LT.0.2) T2=0
218           IF (IABS(M).GT.1) T2=0
219           IF (M) 1,1,2
220         1 CONTINUE
221           IF (I.GT.1) GO TO 2
222           CM12=CM1
223           CM1=CM2
224           CM2=CM12
225         2 T1 = CM1**2 * ( BN(JN,JQ,1)*M*NQ/LA - (NQ+NU)*BN(JN,JQ+1,1))
226           IF (M.LT.-1) T1=0
227           IF (M.EQ.2)
           $T1 = CM1**2 * ( BN(JN,JQ,2)*M*NQ/LA - (NQ+NU)*BN(JN,JQ+1,2))
228           T3 = CM2**2 * ( BN(12-JN,7-JQ,1)*M*NQ/LA - (NQ+NU) *
           $ BN(12-JN,6-JQ,1) )
229           IF (M.EQ.3)
           $T1 = CM1**2 * ( BN(12-JN,7-JQ,1)*M*NQ/LA - (NQ+NU) *
           $ BN(12-JN,6-JQ,1) )
230           IF ((D.LT.0.2).AND.(M.EQ.3)) T1=0
231           IF (D.LT.0.2) T3=0
232           IF (IABS(M).GT.1) T3=0
233           SUMCYC = T1+T2+T3
234           SUMCYC=SUMCYC*(P10/PRM)**(NU-3)*ABS((COSTA-LA)/(M-LA))
235           IF (D.GE.5.) SUMCYC = SUMCYC*5/D
236           SC(I) = SUMCYC
237           S(I) = S(I) + SC(I)
238           IF (M.EQ.1) SC1(I)=SUMCYC
239      5101 CONTINUE
     C END FIRST CYCLOTRON TERM
     C RETURN TO HIGHER ORDER HARMONIC
240           IF (M) 156,156,158
241        158 M=-M
242           GO TO 157
243        156 M = IABS(M)+1
244           IF (IABS(M).GT.3) GO TO 1001
245           GO TO 157
     C END RETURN TO HIGHER ORDER HARMONIC
246      1001 CONTINUE
247       159 CONTINUE
     C SUBPROGRAM FOR PARALLEL GAIN
248           DE=.004
249           PLAT = LAT*0.0174533
250           X = SIN(PLAT)
     C INVL=INVARIANT LATITUDE
     C DF=RATIO HOT PLASMA DENSITY FOR ENERGY>100EV TO COLD PLASMA DENSITY
     C LAT=LATITUDE
     C BF=NORMALIZED MAGNETIC FIELD TO EQUATORIAL VALUE
251           BT=SQRT(1+3*X**2)/(1-X**2)**3
252           P1R=P10/PR1
253           DO 5102 I=1,10
254           IF (I.EQ.1) AU=4
255           IF (I.EQ.2) AU=4
256           IF (I.EQ.3) AU=4
257           IF (I.EQ.4) AU=4
258           IF (I.EQ.5) AU=5
259           IF (I.EQ.6) AU=5
260           IF (I.EQ.7) AU=5
261           IF (I.EQ.8) AU=6
```

```
      IF (I.EQ.9) AU=6
      IF (I.EQ.10) AU=6
      IF (I.EQ.1 ) AQ=0
      IF (I.EQ.2 ) AQ=2
      IF (I.EQ.3 ) AQ=4
      IF (I.EQ.4 ) AQ=6
      IF (I.EQ.5 ) AQ=0
      IF (I.EQ.6 ) AQ=0
      IF (I.EQ.6 ) AQ=2
      IF (I.EQ.7 ) AQ=4
      IF (I.EQ.8 ) AQ=0
      IF (I.EQ.9 ) AQ=2
      IF (I.EQ.10) AQ=4
      NU=AU
      NQ=AQ
      COEFKC=-AM(NU,NQ)*(3.141592/8)*DE**(1/BT)**(NQ/2)
      PSUM=BNQ(NU,NQ)*(2+(1-1/LA)*NQ)
     $ *P1K**(NU-3)
      PKIK = -COEFKC*PSUM
      APVGC=SQRT(LA)* SQRT(1-LA)**3*2/BETA
      PWIW=-PKIK*APVGC*RIND
C AVGC AND APGC = MODULUS OF GROUP VELOCITIES(GENERAL AND PARALLELCASES)
C NORMALIZED TO C
C WIW'S ARE IM(OMEGA)/RE(OMEGA)
C PKIK=KIK FOR PARALLEL PROPAGATION
      PGDEFG=-160000*BT*LA*RIND/INVL**3
      PG1000=PGDEFG*PKIK
C END SUBPROGRAM FOR PARALLEL GAIN
      COEFKI= COEFKC
     $*CALPHA/(   COSTA)**2
      KIKLAN=COEFKI*SL(I)
      KIK=COEFKI*S(I)
      KIKCYL=COEFKI*SC1(I)
      AVGC=SQRT(LA*(COSTAD  )*(4*(COSTAD  )**2+SINTA**2))/
     $ (BETA*COSTA+2*LA*(1-DELTA))
      COEWIW=AVGC*RIND
      WIWLAN=-KIKLAN*COEWIW
      WIWCYL=-KIKCYL*COEWIW
      WIW=-KIK*COEWIW
      COEFG=-160000*LA**BT*RIND/INVL**3
      G1000=COEFG*KIK
      G1000L=COEFG*KIKLAN
      G1000C=COEFG*KIKCYL
      G1000S = G1000-G1000L-G1000C
      IF (ABS(PG1000).GT.1.E-30 ) RATIOG = G1000/PG1000
      IF (ABS(PG1000).LT.1.E-30 ) RATIOG = 123456
      IF (ID.EQ.0) RATIOG=1
      COEFGW = 8686*FKC*6.283184
      PGW = COEFGW*DTATG*PWIW
      GW  = COEFGW*DTATG*WIW
      GWL = COEFGW*DTATG*WIWLAN
      GWC = COEFGW*DTATG*WIWCYL
      PGWS(I) = PGWS(I) + PGW
      GWS (I) = GWS (I) + GW
      GWSL(I) = GWSL(I) + GWL
      GWSC(I) = GWSC(I) + GWC
      GWSS(I) = GWS(I)-GWSL(I)-GWSC(I)
      WRITE(6,430)         GWS(I),GWSL(I),GWSC(I),GWSS(I),PGWS(I),AU,AQ
  430 FORMAT(5E12.3,2I4)
 5102 CONTINUE


      IF (TG.EQ.TGLAST) GO TO 10001
      GO TO 10000
  909 STOP
      END
```

TABLE A.2. AN EXAMPLE OF THE COMPUTER OUTPUT OF THE PROGRAM LISTED IN TABLE A.1.

FKC= 0.7000 TGO= 0.000000 TGLAST= 2.011502

L	LAT	LAMBDA	THETA	BETA	DENS	TG	MUCOS	WLAN	WC1
4.61105	24.11	0.5091	3.27	9.76	345	0.0204	19.51	0.672E 00	0.525E 00

GWT	GWL	GWC	GWS	PGW	NU	Q
-0.606E 01	-0.190E-01	-0.603E 01	-0.898E-02	-0.606E 01	4	0
-0.757E-01	-0.882E-02	-0.707E-01	0.376E-02	-0.767E-01	4	2
0.784E 00	-0.507E-02	0.782E 00	0.709E-02	0.784E 00	4	4
0.660E 00	-0.304E-02	0.657E 00	0.623E-02	0.660E 00	4	6
-0.328E 01	-0.124E-01	-0.326E 01	-0.707E-03	-0.327E 01	5	0
-0.349E-01	-0.321E-02	-0.319E-01	0.204E-03	-0.332E-01	5	2
0.289E 00	-0.115E-02	0.290E 00	0.391E-03	0.290E 00	5	4
-0.149E 01	-0.730E-02	-0.149E 01	-0.601E-04	-0.149E 01	6	0
-0.137E-01	-0.145E-02	-0.123E-01	0.138E-04	-0.126E-01	6	2
0.958E-01	-0.379E-03	0.962E-01	0.245E-04	0.965E-01	6	4

L	LAT	LAMBDA	THETA	BETA	DENS	TG	MUCOS	WLAN	WC1
4.61125	23.51	0.5274	2.94	10.07	342	0.0439	20.15	0.630E 00	0.506E 00

GWT	GWL	GWC	GWS	PGW	NU	Q
-0.135E 02	-0.375E-01	-0.135E 02	-0.173E-01	-0.135E 02	4	0
-0.359E 00	-0.175E-01	-0.349E 00	0.695E-02	-0.361E 00	4	2
0.167E 01	-0.102E-01	0.167E 01	0.137E-01	0.167E 01	4	4
0.147E 01	-0.616E-02	0.146E 01	0.123E-01	0.147E 01	4	6
-0.776E 01	-0.252E-01	-0.773E 01	-0.141E-02	-0.776E 01	5	0
-0.173E 00	-0.661E-02	-0.167E 00	0.388E-03	-0.170E 00	5	2
0.652E 00	-0.239E-02	0.653E 00	0.781E-03	0.654E 00	5	4
-0.376E 01	-0.151E-01	-0.375E 01	-0.127E-03	-0.376E 01	6	0
-0.725E-01	-0.305E-02	-0.695E-01	0.271E-04	-0.703E-01	6	2
0.229E 00	-0.812E-03	0.230E 00	0.511E-04	0.231E 00	6	4

L	LAT	LAMBDA	THETA	BETA	DENS	TG	MUCOS	WLAN	WC1
4.61165	22.82	0.5490	2.62	10.44	339	0.0733	20.96	0.583E 00	0.393E 00

GWT	GWL	GWC	GWS	PGW	NU	Q
-0.236E 02	-0.557E-01	-0.236E 02	-0.248E-01	-0.236E 02	4	0
-0.105E 01	-0.261E-01	-0.103E 01	0.952E-02	-0.105E 01	4	2
0.272E 01	-0.152E-01	0.272E 01	0.196E-01	0.272E 01	4	4
0.254E 01	-0.936E-02	0.253E 01	0.180E-01	0.253E 01	4	6
-0.146E 02	-0.385E-01	-0.146E 02	-0.212E-02	-0.146E 02	5	0
-0.550E 00	-0.103E-01	-0.540E 00	0.546E-03	-0.545E 00	5	2
0.114E 01	-0.374E-02	0.114E 01	0.117E-02	0.115E 01	5	4
-0.772E 01	-0.236E-01	-0.769E 01	-0.196E-03	-0.772E 01	6	0
-0.253E 00	-0.486E-02	-0.248E 00	0.397E-04	-0.250E 00	6	2
0.435E 00	-0.132E-02	0.436E 00	0.800E-04	0.437E 00	6	4

L	LAT	LAMBDA	THETA	BETA	DENS	TG	MUCOS	WLAN	WC1
4.61198	22.38	0.5631	2.24	10.66	336	0.0937	21.47	0.555E 00	0.334E 00

GWT	GWL	GWC	GWS	PGW	NU	Q
-0.310E 02	-0.661E-01	-0.309E 02	-0.288E-01	-0.310E 02	4	0
-0.169E 01	-0.310E-01	-0.167E 01	0.106E-01	-0.170E 01	4	2
0.342E 01	-0.182E-01	0.341E 01	0.228E-01	0.341E 01	4	4
0.330E 01	-0.112E-01	0.329E 01	0.212E-01	0.329E 01	4	6
-0.201E 02	-0.463E-01	-0.200E 02	-0.252E-02	-0.201E 02	5	0
-0.932E 00	-0.124E-01	-0.923E 00	0.627E-03	-0.926E 00	5	2
0.149E 01	-0.456E-02	0.149E 01	0.139E-02	0.150E 01	5	4
-0.111E 02	-0.287E-01	-0.111E 02	-0.237E-03	-0.111E 02	6	0
-0.452E 00	-0.600E-02	-0.446E 00	0.464E-04	-0.448E 00	6	2
0.593E 00	-0.165E-02	0.595E 00	0.975E-04	0.596E 00	6	4

L	LAT	LAMBDA	THETA	BETA	DENS	TG	MUCOS	WLAN	WC1
4.61234	21.94	0.5770	1.97	10.89	334	0.1148	22.02	0.528E 00	0.284E 00

```
      $WATFIV
      C THIS PROGRAM COMPUTES THE WHISTLER MODE WAVE AMPLITUDE GAINS (IN DB.),
      C INTEGRATED OVER A RAY PATH WHOSE PARAMETERS ARE GIVEN BY THE STANFORD
      C VLF GROUP RAY TRACING PROGRAM. POSITIVE (NEGATIVE) GAIN MEANS WAVE
      C GROWTH(DAMPING). THE ENERGETIC ELECTRON DISTIBUTION IS EQUAL TO DE*
      C (A1/4*PI)*H(P-PH)*EXP(Q*(P1/P)**NUQ*SIN(ALPHA)**2/BT)/P**NU,WHERE
      C ALPHA AND P ARE RESPECTIVELY THE ELECTRON PITCH-ANGLE AND MOMENTUM,
      C H IS THE STEP FUNCTION, A1 AND P1(=100EV) ARE NORMALIZATION CONSTANTS,
      C BT IS THE MAGNETIC FIELD NORMALIZED TO THE EQUATORIAL VALUE, NU CAN
      C TAKE ANY VALUE >4, Q AND NUQ CAN TAKE ARBITRARY VALUES.
      C
      C INPUT:
      C         NU,Q,NUQ (LINES 46 AND 47)
      C         FREQUENCY OF THE WAVE(KHZ), INITIAL AND FINAL GROUP TIMES
      C         (LINES 58 AND 59)
      C         L VALUE, LATITUDE(DEG.), NORMALIZED FREQUENCY, WAVE PROPAGATION
      C         ANGLE(DEG.), DENSITY(CM-3),GROUP TIME(SEC) (LINES 69 AND 70).
      C
      C OUTPUT:
      C         FREQUENCY OF THE WAVE(KHZ), INITIAL AND FINAL GROUP TIMES
      C         L VALUE,LATITUDE(DEG.), NORMALIZED FREQUENCY, WAVE PROPAGATION
      C         ANGLE(DEG.), DENSITY(CM-3), PLASMA FREQUENCY NORMALIZED TO
      C         ANGLE(DEG.), DENSITY(CM-3),GROUP TIME(SEC) (LINES 69 AND 73).
      C         GYROFREQUENCY, PARALLEL COMPONENT OF REFRACTIVE INDEX, MINIMUM
      C         RESONANCE ENERGY FOR LANDAU AND FUNDAMENTAL CYCLOTRON INTER-
      C         ACTIONS (KEV), C0, D1, AND D2.
      C         GAINS INTEGRATED FROM INITIAL TIME, INCLUDING RESPECTIVELY:
      C         HARMONICS M=0,1,2; LANDAU HARMONIC(M=0); FUNDAMENTAL CYCLOTRON
      C         HARMONIC(M=1) ; 2ND CYCLOTRON HARMONIC(M=2); PARALLEL PROPAGA-
      C         TION APPROXIMATION.
      C
      C LIMITS:
      C         HIGH PASMA FREQUENCY APPROXIMATION FOR REFRACTIVE INDEX, BUT
      C         INCLUDE IONS. RELATIVITY NOT INCLUDED.
      C                          THE INTERVAL OF INTEGRATION IS DTATG=0.02 SEC
      C         OR MORE AND CAN BE CHANGED APPROPRIATELY IN LINES 75 AND 76.
      C         THE DISTRIBUTION FUNCTION IS NORMALIZED TO DE=0.004, WHERE
      C         DE=RATIO HOT PLASMA DENSITY FOR ENERGY>100EV TO COLD PLASMA
      C         DENSITY; CHOSE APPROPRIATE VALUE OF DE IN LINE 98.
      C         THIS PROGRAM IS APPROXIMATE AND ONLY VALID FOR NEAR
      C         PARALLEL PROPAGATION. HARMONIC OF ORDER M CAN BE CONSIDERED
      C         AS APPROXIMATELY CORRECT WHEN DM<0.3 WHERE DM=D0,D1,D2 IF
      C         M=0,1,2.
      C         CHOSE APPROPRIATE VALUE OF PH IN LINE 187.
      C
      C FUNCTION FACTORIAL
    1       FUNCTION FFF(N)
    2       IF (N.EQ.0) GO TO 2
    3       FFF=1
    4       DO 1 I=1,N
    5     1 FFF=FFF*I
    6       GO TO 3
    7     2 FFF=1
    8     3 RETURN
    9       END


   10       FUNCTION ANQ(NU,NQ)
   11       ANQ=1
   12       JQM=NQ/2+1
   13       DO 11 JQ=1,JQM
   14    11 ANQ=(FLOAT(JQ)-0.5)*ANQ
   15       ANQ=ANQ*2*(NU-3)/FFF(NQ/2)
   16       RETURN
   17       END


   18       FUNCTION BNQ(UN,NQ)
   19       BNQ=1
   20       JQM=NQ/2+1
   21       DO 10 JQ=1,JQM
   22    10 BNQ=BNQ/(UN/2.-2.+FLOAT(JQ))
   23       BNQ=FFF(NQ/2)*BNQ/2
   24       RETURN
   25       END
```

TABLE A.3. LISTING OF THE PROGRAM TO COMPUTE THE GAIN INTEGRATED ALONG A RAY PATH FOR NONSEPARABLE DISTRIBUTIONS AND SMALL WAVE NORMAL ANGLE.

```
      FUNCTION BNOT(UN,NQ,P)
      BNOT = P**(UN-2)/(UN-2)
      IF (NQ.EQ.0) GO TO 8
      NQM = NQ/2
      DO 9 M=1,NQM
   11 BNOT = BNOT +(-1)**M*(FFF(NQ/2))/(FFF(M)*FFF(NQ/2-M))
     $ * P**(UN-2+2*M)/(UN-2+2*M)
    9 CONTINUE
    8 CONTINUE
      RETURN
      END



      REAL KIKS
      REAL NQ
      REAL KIKLU
      REAL KIK,KIKLAN,KIKCYL
      REAL LA,KIG
      REAL INVL
      REAL LAT
      REAL KIKL,KIKC,KIKCU
      REAL NU
      LOGICAL TRUC
      READ(5,199) NU,NQ,QN
  199 FORMAT(3F10.6)
      WRITE(6,198) NU,NQ,QN
  198 FORMAT( 'NU=',F10.3,'Q=',F10.3,'NUQ=',F10.3)
      PIPI=3.141592
      A=1./(NU-3)
      N=0
 2000 N=N+1
      ANEW =       NQ **N*2.**(2*N) *FFF(N) /(FFF(2*N+1)*(NU-3+N*QN))
      A = A + ANEW
      IF (ABS(ANEW)/ABS(A).GT..001) GO TO 2000
 2001 A = 1./A
C READ INPUT DATA FROM COLD PLASMA RAY TRACING
10001 READ (5,460,END=999) FKC,TGNEW,TGLAST
  460 FORMAT(F10.4,F10.6,F10.6)
      WRITE(6,4550) FKC ,TGNEW,TGLAST
 4550 FORMAT('1FKC=', F10.4, '   TGO=',F10.6,'   TGLAST=',F10.6)
C FKC IS FREQUENCY SIGNAL IN KHZ
      TRUC = .FALSE.
      PGWSUM = 0.
      GWTSUM=0.
      GWLSUM=0.
      GWCSUM=0.
      GWLUSM=0.
      GWSSUM = 0.
      GWCUSM=0.
10000 READ(5,490) INVL,LAT,LS,THETA,IDENS,TG
  490 FORMAT(F10.5,F10.2,F10.4,F10.2,I10  ,F10.6)
      TRUC = .NOT.TRUC
      IF (TRUC) TGOLD=TG
      IF (.NOT.TRUC) TGNEW=TG
      DTATG = ABS (TGNEW-TGOLD)
      IF (DTATG.LT.0.02) TRUC = .NOT. TRUC
      IF (DTATG.LT.0.02) GO TO 10000
      DEGRAD = 3.141592/180
      THETAR = THETA*DEGRAD
      BETA = LA*8.984*SQRT(FLOAT(IDENS))/FKC
      CC1 = (1-LA)*TAN(THETAR)
      CLAN = LA*TAN(THETAR)
C IDENS IS DENSITY IN PARTICLES/CUBIC CENTIMETERS
C BETA=PLASMA FREQUENCY/GYROFREQUENCY
C LA=WAVE FREQUENCY/GYROFREQUENCY
C THETA=ANGLE OF PROPAGATION WITH RESPECT TITHE MAGNETIC FIELD
C END OF COLD PLASMA PARAMETER DECLARATION
      COSTA = ABS(COS(THETAR))
      SINTA = ABS(SIN(THETAR))
      DELTA =1-1/(43*LA)**2
      COSTAD  = COSTA-LA*DELTA
      TALPHA=SINTA/(2*(COSTA)  ))
C THETA HERE IS EXPRESSED IN DEGREES
```

```
      CALPHA=1/SQRT(1+TALPHA**2)
      RIND = BETA/SQRT((COSTA-LA*DELTA)*LA)
C RIND=REFRACTIVE INDEX
      P10=.02
      PRIND=BETA/SQRT((1-LA)*LA)
C PRIND=PARALLEL REFRACTIVE INDEX
      RPAR= RIND*COSTA
      RPER=RIND*SINTA
      H = COSTA*(1/LA-LA)
      SG = BETA**2 / (LA*(1-LA**2))
      SP=-(BETA/LA)**2
C SP = STIX P PARAMETER
      PRIWAT = (1-LA)/(RPAR*LA)
C PRIWAT IS THE FUND. MOMENTUM OF RESONANCE
C SUBPROGRAM FOR PARALLEL GAIN
      DE=.004
      RLAT = LAT*DEGRAD
      X = SIN(RLAT)
C INVL=INVARIANT LATITUDE
C DE=RATIO HOT PLASMA DENSITY FOR ENERGY>100EV TO COLD PLASMA DENSITY
C LAT=LATITUDE
C BT=NORMALIZED MAGNETIC FIEL TO EQUATORIAL VALUE
      BT=SQRT(1+3*X**2)/(1-X**2)**3
      PRP=ABS(LA-1)/(PRIND*LA)
      PPR = P10/PRP
      COEFKC = -A*(PIPI/8)*DE
      PKIK = PPR**(NU-3)            *(PIPI/4)*DE*BNQ( NU,0)
      N=0
 1000 N=N+1
      PKIKNW = (1/BT)**N*(1+N          ) * PPR**(NU-3+N*QN)*
     $ (PIPI/4)*DE*(NQ**N/FFF(N)) * BNQ(NU+N*QN,2*N)
      PKIK = PKIK + PKIKNW
      IF   (ABS(PKIKNW)/ABS(PKIK) .GT..001)
     $ GO TO 1000
      N=1
      AKIK   = (1/BT)**N*(-N/LA        ) * PPR**(NU-3+N*QN)*
     $ (PIPI/4)*DE*(NQ**N/FFF(N)) * BNQ(NU+N*QN,2*N)
 1001 N=N+1
      AKIKNW = (1/BT)**N*(-N/LA        ) * PPR**(NU-3+N*QN)*
     $ (PIPI/4)*DE*(NQ**N/FFF(N)) * BNQ(NU+N*QN,2*N)
      AKIK = AKIK + AKIKNW
      IF   (ABS(AKIKNW)/ABS(AKIK) .GT..001)
     $ GO TO 1001
      PKIK = A * (PKIK+AKIK)
      APVGC=SQRT(LA)* SQRT(1-LA)**3*2/BETA
      AVGC=SQRT(LA*(COSTAD  )*14*(COSTAD  )**2+SINTA**2))/
     $ (BETA*COSTA+2*LA*(1-DELTA))
      PWIW=-PKIK*APVGC*RIND
C AVGC AND APGGC = MODULUS OF GROUP VELOCITIES(GENERAL AND PARALLELCASES)
C NORMALIZED TO C
C WIW'S ARE IN(OMEGA)/RE(OMEGA)
C PKIK=KIK FOR PARALLEL PROPAGATION
      PCOEFG=-160000*BT*LA*PRIND  /INVL**3
      PG1000=PCOEFG*PKIK
      PRIWAT = (1-LA)/(RPAR*LA)
C PRIWAT IS THE FUND. MOMENTUM OF RESONANCE
C PR1=MOMENTUM FOR PARALLEL PROPAGATION
      WO = 512.
      WC1 = WO*(PRIWAT)**2/2
      PROWAT = 1/RPAR
```

```
      WLAN = WO*(PROWAT)**2/2
C PROWAT IS THE RESONANCE MOMENTUM FOR LANDAU INTERACTION
      RWC1WL = WC1/WLAN
C WO=MO*C**2
C WC1 AND WLAN ARE RESPECTIVELY THE MINIMUM ENERGIES OF RESONEANCE FOR
C FUNDAMENTAL AND LANDAU RESONANCES (IN KEV)
      DO = LA*SINTA/COSTA
      D1 = (1-LA)*SINTA/COSTA
      D2 = (2-LA)*SINTA/COSTA
      DO=ABS(DO)
      D1=ABS(D1)
      D2=ABS(D2)
      WRITE(6,25)
   25 FORMAT('0    L          LAT        LA         THETA      BETA       DE
     $NS      TG         MUCOS    WLAN       WC1          DO    D1    D2')
      WRITE(6,26)INVL,LAT,LA,THETA,BETA,IONS,TG,RPAR,WLAN,WC1,DO,D1,D2
   26 FORMAT(5F10.4,I10,F10.4,F10.2,2E11.3,3F5.2)
      CO = 2*ABS(SP)
      C1L = (RPAR*RPER/CO)**2
      C2L = RPAR*RPER*H*SO/CO**2
      C3L = (SO*H/CO)**2
      C11 = ((BETA/LA)**2*(1+COSTA)+RPER**2*LA/1)/CO
      C21 = ((BETA/LA)**2*(1+COSTA)+RPER**2*LA/2)/CO
      PRO=1/RPAR
      PR1=(1-LA)/(LA*RPAR)
      POR = P10/PRO
      P1R = P10/PR1
      PR2 = (2-LA)/(LA*RPAR)
      P2R = P10/PR2
C BEGIN LANDAU TERM
      SL = -NU*(COSTA/LA-1)*(POR)**(NU-3)*4
     $*(C1L*BNC(NU+2,0)-C2L*BNC(NU,2)*DO+ BNQ(NU-2,4)*DO**2*C3L/4)
      N=0
 3000 N=N+1
      SLNW = -(1/BT)**N*(NO**N/FFF(N))* (NU+2*N+N*QN)*(POR)*(NU-3+N*QN)
     $ *4*(COSTA/LA-1)  * ( C1L*BNQ(NU+N*QN+2,2*N) - C2L*BNQ(NU+N*QN ,
     $2*N+2)*DO+ C3L*BNQ(NU+N*QN-2,4+2*N)*DO**2/4)
      SL = SL+SLNW
      IF (ABS(SLNW)/ABS( SL) .GT..001) GO TO 3000
C END LANDAU TERM
      SLU= -NU*(COSTA/LA-1)*(POR)**(NU-3)*4  *(C1L*BNC(NU+2,0))
      N=0
 2999 N=N+1
      SLUNW= -(1/BT)**N*(NO**N/FFF(N))* (NU+2*N+N*QN)*(POR)*(NU-3+N*QN)
     $ *4*(COSTA/LA-1)  * ( C1L*BNQ(NU+N*QN+2,2*N) )
      SLU = SLU+SLUNW
      IF (ABS(SLUNW)/ABS(SLU).GT..001) GO TO 2999
C BEGIN 1ST CYCLOTRON HARMONIC
      SC = -P1R**(NU-3) * ((COSTA-LA)/(1-LA)) * C11**2
     $ *(NU*BNQ(NU,2) -.50*D1**2*NU*BNQ(NU-2,4) )
      N=0
 3001 N=N+1
      SCNW = -P1R**(NU+N*QN-3)*((COSTA-LA)/(1-LA))*C11**2*(1/BT)**N
     $ *(NO**N/FFF(N))*
     $ ( (NU+2*N+N*QN)*BNQ(NU+N*QN,2+2*N)-.50*D1**2*(NU+2*N+N*QN)
     $ * BNQ(NU-2+N*QN,4+2*N) )
      SC = SC+SCNW
      IF (ABS(SCNW)/ABS( SC) .GT..001) GO TO 3001
      N=1
      ASC =  P1R**(NU+N*QN-3)*((COSTA-LA)/(1-LA))*C11**2*(1/BT)**N
```

```
     $ *(NQ**N/FFF(N))* ( 2*N*BNQ(NU+N*QN,2*N)/LA-0.50*D1**2
     $ *(2*N*BNQ(NU+N*QN-2,2*N+2)/LA) )
171   3002 N=N+1
172        ASCNW= P1R**(NU+N*QN-3)*((COSTA-LA)/(1-LA))*C11**2*(1/BT)**N
     $ *(NQ**N/FFF(N))* ( 2*N*BNQ(NU+N*QN,2*N)/LA-0.50*D1**2
     $ *(2*A*BNQ(NU+N*QN-2,2*N+2)/LA) )
173        ASC = ASC+ASCNW
174        IF (ABS(ASCNW)/ABS(ASC) .GT..001) GO TO 3002
     C END 1ST CYCLOTRON HARMONIC
     C BEGIN 2ND CYCLOTRON HARMONIC
175        SC2= -P2R**(NU-3) * ((COSTA-LA)/(2-LA)) * C21**2
     $ * NU*BNQ(NU-2,4)*D2**2/4
176        N=0
177   3004 N=N+1
178        SC2NW= -P2R**(NU+N*QN-3)*((COSTA-LA)/(2-LA))*C21**2*(1/BT)**N
     $ *(NQ**N/FFF(N))*
     $ D2**2*(NU+2*N+N*QN)*BNQ(NU-2+N*QN,4+2*N)/4
179        SC2 = SC2 + SC2NW
180        IF (ABS(SC2NW)/ABS(SC2) .GT..001 ) GO TO 3004
181        N=1
182        ASC2=  P2R**(NU+N*QN-3)*((COSTA-LA)/(2-LA))*C21**2*(1/BT)**N
     $ *(NQ**N/FFF(N))* (D2**2/4)*
     $ 4*N*BNQ(NU+N*QN-2,2*N+2)/LA
183   3005 N=N+1
184        ASC2NW=P2R**(NU+N*QN-3)*((COSTA-LA)/(2-LA))*C21**2*(1/BT)**N
     $ *(NQ**N/FFF(N))* (D2**2/4)*
     $ 4*N*BNQ(NU+N*QN-2,2*N+2)/LA
185        ASC2 = ASC2 + ASC2NW
186        IF (ABS(ASC2NW)/ABS(ASC2) .GT. .001) GO TO 3005
     C END 2ND CYCLOTRON HARMONIC
187        COEFKI = COEFKC*CALPHA/COSTA**2
188        KIKL = COEFKI*SL
189        KIKC = COEFKI*(SC+ASC)
190        P1PMIN=2.24
191        P1PMIN=P1PMIN/P1R
192        IF (P1PMIN.GT.1.) GO TO 293
193        CN = BNQT(NU,0,P1PMIN)
194        M=0
195   2005 M=M+1
196        CNNW = NQ**M*P1PMIN**(M*QN)*BNQT(NU+M*QN,2*M,P1PMIN)/FFF(M)
197        CN = CN+CNNW
198        IF(ABS(CNNW)/ABS(CN).GT.0.001) GO TO 2005
199        P1PMIN=1.
200        CD = BNQT(NU,0,P1PMIN)
201        M=0
202   2006 M=M+1
203        CDNW = NQ**M*P1PMIN**(M*QN)*BNQT(NU+M*QN,2*M,P1PMIN)/FFF(M)
204        CD = CD+CDNW
205        IF(ABS(CDNW)/ABS(CD).GT.0.001) GO TO 2006
206        COEF = CN/CD
207        KIKC = KIKC*COEF
208    293 CONTINUE
209        KIK=KIKL+KIKC
210        COEFG = -160000*LA*BT*RIND/INVL**3
211        G1000 = COEFG * KIK
212        KIKS = COEFKI*(SC2+ASC2)
213        G1000L= COEFG * KIKL
214        G1000C= COEFG * KIKC
215        G1000S = COEFG*KIKS
216        KIKLU = COEFKI*SLU
```

```
217         GLU = COEFG*KIKLU
218         GCU = PG1000*((COSTA-LA)/(1-LA))*(CALPHA/COSTA**2)*(RIND/PRIND)
           $ *C11**2*(PPR/P1P)**(NU-3)
219         KIKCU = GCU / COEFG
220         APVGC=SQRT(LA)* SQRT(1-LA)**3*Z/BETA
221         PWIW=-PKIK*APVGC*PRIND
222         WIWT = -KIK *AVGC*RIND
223         WIWL =- KIKL*AVGC*RIND
224         WIWC = -KIKC*AVGC*RIND
225         WIWLU = -KIKLU*AVGC*RIND
226         WIWCU = -KIKCU*AVGC*RIND
227         WIWS = -KIKS*AVGC*RIND
      C AVGC AND APCGC = MODULUS OF GROUP VELOCITIES(GENERAL AND PARALLELCASES)
      C NORMALIZED TO C
      C WIW'S ARE IN(OMEGA)/RE(OMEGA)
      C PKIK=KIK FOR PARALLEL PROPAGATION
228         PCOEFG=-160000*BT*LA*PRIND  /INVL**3
229         PG1000=PCOEFG*PKIK
230         COEFGW = 8686*FKC*6.283184
231         PGW = COEFGW*DTATG*PWIW
232         CCC = COEFGW*DTATG
233         GWT     = CCC*WIWT
234         GWL     = CCC*WIWL
235         GWC     = CCC*WIWC
236         GWLU    = CCC*WIWLU
237         GWCU    = CCC*WIWCU
238         GWS = CCC*WIWS
239         PGWSUM = PGWSUM + PGW
240         GWSSUM = GWSSUM + GWS
241         GWTSUM = GWTSUM + GWT
242         GWLSUM = GWLSUM + GWL
243         GWCSUM = GWCSUM + GWC
244         GWLUSM = GWLUSM + GWLU
245         GWCUSM = GWCUSM + GWCU
246         PRINT 703
247       703 FORMAT('    GWT         GWL         GWC1        GWC2        PGW')
248         WRITE(6,430) GWTSUM,GWLSUM,GWCSUM,GWSSUM,PGWSUM
249       430 FORMAT(5E11.3)
250         IF (TG.EQ.TGLAST) GO TO 10001
251         GO TO 10000
252       999 STOP
253         END
```

TABLE A.4. AN EXAMPLE OF THE COMPUTER OUTPUT OF THE PROGRAM LISTED IN TABLE A.3.

```
FKC=   80.0000   TGO=  0.000000   TGLAST=  0.524752

    L         LAT         LA         THETA      BETA       DENS      TG        MUCOS    WLAN       WC1        D0   D1   D2
  3.9623    47.9800    0.9297    -13.3700    1.0544       811     0.0215      2.22   0.517E 02  0.214E 03 0.08 0.16 0.40
   GWT         GWL         GWC1        GWC2        PGW
-0.703E-02 -0.351E-02 -0.352E-02 -0.373E-04 -0.385E-02

    L         LAT         LA         THETA      BETA       DENS      TG        MUCOS    WLAN       WC1        D0   D1   D2
  3.9620    43.1400    0.9815     -4.6200    1.5754       582     0.0429      3.19   0.251E 02  0.130E 02 0.05 0.03 0.11
   GWT         GWL         GWC1        GWC2        PGW
-0.486E-01 -0.528E-02 -0.433E-01 -0.503E-04 -0.439E-01

    L         LAT         LA         THETA      BETA       DENS      TG        MUCOS    WLAN       WC1        D0   D1   D2
  3.9150    40.4900    0.9404     -6.6800    1.8979       521     0.0652      4.35   0.135E 02  0.166E 01 0.09 0.03 0.15
   GWT         GWL         GWC1        GWC2        PGW
-0.273E 00 -0.152E-01 -0.257E 00 -0.880E-04 -0.258E 00

    L         LAT         LA         THETA      BETA       DENS      TG        MUCOS    WLAN       WC1        D0   D1   D2
  3.8114    38.4200    0.8364    -10.9300    2.0898       495     0.0938      5.87   0.743E 01  0.284E 00 0.16 0.03 0.22
   GWT         GWL         GWC1        GWC2        PGW
-0.143E 01 -0.880E-01 -0.134E 01 -0.211E-03 -0.129E 01

    L         LAT         LA         THETA      BETA       DENS      TG        MUCOS    WLAN       WC1        D0   D1   D2
  3.6766    36.6700    0.8832    -13.6600    2.1865       486     0.1270      7.57   0.446E 01  0.781E-01 0.21 0.03 0.27
   GWT         GWL         GWC1        GWC2        PGW
-0.528E 01 -0.324E 00 -0.496E 01 -0.408E-03 -0.433E 01

    L         LAT         LA         THETA      BETA       DENS      TG        MUCOS    WLAN       WC1        D0   D1   D2
  3.5797    35.6500    0.9000    -15.0700    2.2258       485     0.1529      8.80   0.330E 01  0.408E-01 0.24 0.03 0.30
   GWT         GWL         GWC1        GWC2        PGW
-0.106E 02 -0.633E 00 -0.992E 01 -0.585E-03 -0.799E 01

    L         LAT         LA         THETA      BETA       DENS      TG        MUCOS    WLAN       WC1        D0   D1   D2
  3.4549    34.1500    0.9116    -16.6000    2.2568       486     0.1907     10.41   0.236E 01  0.222E-01 0.27 0.03 0.32
   GWT         GWL         GWC1        GWC2        PGW
-0.244E 02 -0.142E 01 -0.230E 02 -0.892E-03 -0.158E 02

    L         LAT         LA         THETA      BETA       DENS      TG        MUCOS    WLAN       WC1        D0   D1   D2
  3.3784    33.2900    0.9150    -17.4600    2.2699       488     0.2172     11.39   0.197E 01  0.170E-01 0.29 0.03 0.34
   GWT         GWL         GWC1        GWC2        PGW
-0.357E 02 -0.217E 01 -0.336E 02 -0.114E-02 -0.221E 02

    L         LAT         LA         THETA      BETA       DENS      TG        MUCOS    WLAN       WC1        D0   D1   D2
  3.2894    32.2700    0.9164    -18.4200    2.2804       491     0.2522     12.45   0.165E 01  0.137E-01 0.31 0.03 0.36
   GWT         GWL         GWC1        GWC2        PGW
-0.519E 02 -0.352E 01 -0.484E 02 -0.151E-02 -0.313E 02

    L         LAT         LA         THETA      BETA       DENS      TG        MUCOS    WLAN       WC1        D0   D1   D2
  3.1840    31.0200    0.9154    -19.5400    2.2871       495     0.3004     13.56   0.139E 01  0.119E-01 0.32 0.03 0.38
   GWT         GWL         GWC1        GWC2        PGW
-0.762E 02 -0.614E 01 -0.701E 02 -0.216E-02 -0.444E 02

    L         LAT         LA         THETA      BETA       DENS      TG        MUCOS    WLAN       WC1        D0   D1   D2
  3.1245    30.2900    0.9138    -20.1700    2.2901       498     0.3315     14.09   0.129E 01  0.115E-01 0.34 0.03 0.40
   GWT         GWL         GWC1        GWC2        PGW
-0.929E 02 -0.816E 01 -0.847E 02 -0.263E-02 -0.527E 02

    L         LAT         LA         THETA      BETA       DENS      TG        MUCOS    WLAN       WC1        D0   D1   D2
  3.0579    29.4500    0.9112    -20.9000    2.2927       502     0.3704     14.61   0.120E 01  0.114E-01 0.35 0.03 0.42
   GWT         GWL         GWC1        GWC2        PGW
```

APPENDIX B. POSSIBLE TRAPPING BY A NATURAL WHISTLER

When a whistler is emitted by a lightning discharge of duration much shorter than the trapping time, the question arises whether the wave can change the trajectory of the particle enough to trap it. We make an analysis here on the assumption that the medium is one dimensional (axis $\underline{Oz}$ along $\underline{B}_0$). The interaction is only important around the equator, and the propagation is parallel (for nonparallel propagation the wave propagates across L shells and interacts during a shorter time with particles compelled to drift along magnetic field lines than for parallel propagation).

Cyclotron trapping:

In this case we assume parallel propagation. Let us suppose that at some point

$$v_{\parallel} = v_R \tag{B.1}$$

where

$$v_R = \frac{\omega_c - \omega}{k} \tag{B.2}$$

$v_{\parallel}$ = parallel velocity of an electron.

Along the lines of Dysthe [1971] and Sudan and Ott [1971], we will consider the particle as trapped (see Section 2B) if the condition

$$\frac{d}{dt}(v_{\parallel} - v_R) = 0 \tag{B.3}$$

can be realized during a trapping time $T_c = 2\pi(\omega_{c1} k v_{\perp})^{-1/2}$ or correspondingly along a length $L = v_{\parallel} T_c$ as the particle moves.

We can write Eq. (B.3) as:

$$\Delta v_{\parallel} = \Delta v_R \tag{B.4}$$

where $\Delta v_{\parallel}$ and Δv_R represent the variations of $v_{\parallel,R}$ as the particle travels Δz.

$\Delta v_{\parallel}$ is the sum of two terms depending upon:

1. the interaction of the wave on the particle (depends on the angle ψ between $v_{\perp}$ and B_1);
2. the variation of the static magnetic field, i.e., particle mirroring.

$$\Delta v_{\parallel} = \left(\frac{v_{\perp}}{v_{\parallel}} \omega_{c1} \sin\psi - \frac{v_{\perp}^2}{v_{\parallel}} \frac{1}{2\omega_c} \frac{d\omega_c}{dz} \right) \Delta z \ . \qquad \text{(B.5)}$$

dv_R is the sum of two terms depending upon:

1. the variation of electron gyrofrequency with distance (because of the medium inhomogeneity);
2. the variation of wave frequency with distance (because of wave dispersion)

$$\Delta v_R = \left[\left(\frac{3}{2} \frac{1}{\omega_c - \omega} - \frac{1}{\omega_p} \frac{d\omega_p}{d\omega_c} \right) \frac{d\omega_c}{dz} - \left(\frac{1}{kv_g} + \frac{1}{\omega_c - \omega} \right) \frac{d\omega}{dz} \right] v_R \Delta z \qquad \text{(B.6)}$$

$$\frac{d\omega}{dz} = \frac{-1}{v_{\parallel}} \frac{\partial\omega}{\partial t} + \frac{\partial\omega}{\partial z} \qquad \text{(B.7)}$$

(electron and wave are counterstreaming).

The whistler time delay is given by

$$\tau(z,\omega) = \int_{z_0}^{z} \frac{dz}{v_g} \qquad \text{(B.8)}$$

so that:

$$\frac{\partial\omega}{\partial z} = \frac{-1/v_g}{\partial\tau/\partial\omega} \ ,$$

$$\frac{\partial\omega}{\partial\tau} = \frac{1}{\partial\tau/\partial\omega} \qquad \text{(B.9)}$$

We see from Eqs. (B.5) and (B.6) that Eq. (B.4) is fulfilled if,

$$kv_{\perp}\omega_{c1} \geq v_R \left| \left(\frac{3}{2} + \frac{\omega_c - \omega}{2\omega_c} \tan^2\alpha - \frac{\omega_c - \omega}{\omega_p} \frac{d\omega_p}{d\omega_c} \right) \frac{d\omega_c}{dz} + \left(\frac{v_R}{v_g} + 1 \right)^2 \frac{1}{v_R \partial\tau/\partial\omega} \right| . \qquad \text{(B.10)}$$

Around the equator:

$$\omega_c \sim \omega_{cE} \left[1 + \frac{9}{2} \left(\frac{z}{R_E} \right)^2 \right] . \qquad \text{(B.11)}$$

and we assume $\omega_p \sim$ constant.

According to Eq. (B.11), the variation of ω_c is a second order quantity in (z/R_E) around the equator. The variation of ω is a first-order quantity but for $\omega \to 0$; therefore, we can neglect the first term in the RHS of Eq. (B.10) and express $\partial\tau/\partial\omega$ at the equator ($\omega \neq \sim 0$). We use the hyperbola approximation for the whistler dispersion [Bernard, 1973]:

$$\tau \sim \tau_E \sim \frac{D_{0m}}{2} \frac{\omega_{cE} - A\omega}{\sqrt{\omega}(\omega_{cE} - \omega)} ,$$

$$D_{0m} = \frac{R_E \omega_{pE}}{c\sqrt{\omega_{cE}}} d_0 , \qquad \text{(B.12)}$$

and for the D.E. model the values of the dimensionless parameters A and d_0 are [Bernard, 1973]:

$$A \sim .25 ,$$

$$d_0 \sim .7 . \qquad \text{(B.13)}$$

Using Eq. (B.13) we get:

$$\frac{\partial \tau_E}{\partial \omega} = \frac{D_{0m}}{4} \frac{\omega_{cE}(3\omega - \omega_{cE}) - A\omega(\omega + \omega_{cE})}{\omega^{3/2}(\omega_{cE} - \omega)^2} \qquad \text{(B.14)}$$

which can be inserted into Eq. (B.10) (neglecting $d\omega_c/dz$) to yield:

$$k \tan\alpha \, \omega_{c1} \geq \left(1 + \frac{\omega_{cE}}{2\omega} \right)^2 \frac{4\omega^2 (\omega_{cE} - \omega)^{1/2} \omega_{cE}^{1/2}}{R_E d_0 [\omega_{cE}(3\omega - \omega_{cE}) - A\omega(\omega + \omega_{cE})]} \qquad \text{(B.15)}$$

Whistlers trigger emissions primarily at $\omega \sim \omega_{cE}/2$ and also at lower frequencies at the bottom of whistler traces.

As an example, we choose $\omega = \omega_{cE}/2$, $\alpha = 30^{o}$, $L = 3$, and $\lambda_w = 2\pi/k = 2$ km. Then Eq. (B.15) reads

$$\frac{\omega_{c1}}{\omega_{cE}} \cong \sim 3.5\times10^{-4} \tag{B.16}$$

for

$$B_{0E} \sim 1.2\times10^{-5}\text{Wb/m}^2, \quad B_1 \cong 4\times10^{-10}\text{Wb/m}^2 \ . \tag{B.17}$$

The minimum field required to have trapping is excessively high compared to typical values ($B_1 \sim 10^{-12}$-10^{-11}Wb/m^2). For a frequency where $\partial\tau/\partial\omega$ is comparable to, or higher than, its value at $\omega_{cE}/2$, trapping would need the same order of magnitude for B_1.

Low frequencies are not more favorable either because here $k \sim \frac{\omega_p}{c\sqrt{\omega_c}}\sqrt{\omega}$ decreases with frequency and v_R increases. This makes it more difficult for inequality (B.10) to be fulfilled.

The RHS of Eq. (B.10) may vanish at a point off the equator. In this case approximations (B.11) to (B.12) are no longer valid, and a more refined analysis should be made.

Landau trapping:

The Gendrin mode is the most favorable for trapping because the group velocity and resonant velocity are equal and ray direction and particle drift directions are the same. As we are concerned here with ducted whistlers, we will suppose $\cos\theta \sim 1$.

Computations similar to those above yield:

$$v_R = \frac{\omega}{k} \tag{B.18}$$

$$\Delta v_{\parallel} = \left[\frac{eE_1}{M} \frac{1}{v_{\parallel}} \sin(kz-\omega t) - \frac{v_{\perp}^2}{v_{\parallel}} \frac{1}{2\omega_c} \frac{d\omega_c}{dz} \right] \Delta z \ , \tag{B.19}$$

$$\Delta v_R = \left[\left(\frac{1}{2} \frac{1}{\omega_c - \omega} - \frac{1}{\omega_p} \frac{d\omega_p}{d\omega_c} \right) \frac{d\omega_c}{dz} - \left(\frac{1}{kv_g} - \frac{1}{\omega} \right) \frac{d\omega}{dz} \right] v_R \Delta z \ . \qquad (B.20)$$

A condition similar to Eq. (B.10) is found for the minimum field amplitude required for trapping.

$$\frac{eE_1 k}{M} \geq v_R \left| \left(\tan^2\alpha \ \frac{\omega}{2\omega_c} - \frac{\omega}{\omega_p} \frac{d\omega_p}{d\omega_c} \right) \frac{d\omega_c}{dz} - \left(\frac{v_R}{v_g} - 1 \right) \frac{1}{v_R \partial\tau / \partial\omega} \right| . \qquad (B.21)$$

This time, $v_R \sim v_g$ and the wave dispersion can be neglected, and the space inhomogeneity is more effective in preventing trapping. Neglecting the wave dispersion, Eq. (B.21) can be fulfilled up to a certain distance z from the equator given by:

$$\frac{z}{R_E} \leq (\omega_{cE} v_R)^{-1} \left| \tan^2\alpha \ \frac{\omega}{2\omega_c} - \frac{\omega}{\omega_p} \frac{d\omega_p}{d\omega_c} \right|^{-1} \cdot \frac{2\pi e E_1}{9\lambda_w M R_E} \qquad (B.22)$$

Let us take the same example as previously $\lambda_w = 2\text{km}$, $\omega = \omega_{cE}/2$, $\alpha = 45^o$, and $L = 3$.

$$E_1 = E_z \sim v_p B_1 \sin\theta \qquad (B.23)$$

Eq. (B.22) reads

$$\frac{z}{R_E} \leq 1.6 \times 10^{10} B_1 \sin\theta \qquad (B.24)$$

There will be trapping if this value is bigger than a trapping length. For a ducted whistler, $\theta \leq 30^o$ and trapping would require a minimum field of

$$B_1 \sim 4 \times 10^{-11} \text{Wb/m}^2 \qquad (B.25)$$

This field is still high compared to typical values.

APPENDIX C. HOT PLASMA CORRECTION TO THE REAL PART OF THE REFRACTIVE INDEX

The refractive index is given by the expression:

$$N^2 = 1 - \pi \frac{\omega_p^2}{\omega^2} \int_0^{\infty} \int_{-\infty}^{-\infty} \left[\frac{k^2 v_\perp^2}{(kv_\parallel - \omega + \omega_c)^2} - \frac{2(\omega - kv)}{kv_\parallel - \omega + \omega_c} \right] g_0 v_\perp dv_\perp dv_\parallel \quad (C.1)$$

For small $v_\parallel$ we treat $\frac{kv_\parallel}{\omega_c - \omega}$ as a first order quantity and we arrive at:

$$N^2 = 1 + \frac{\omega_p^2}{\omega(\omega_c - \omega)} + \frac{\omega_p^2 \omega_c}{(\omega - \omega)^3 \omega^2} k^2 < v_\parallel^2 > - \frac{\omega_p^2}{(\omega_c - \omega)^2 \omega^2} k^2 < \frac{v_\perp^2}{2} > , \quad (C.2)$$

where:

$$< v_{\parallel,\perp}^2 > = \int_0^{\infty} v_{\parallel,\perp}^2 \, g_0 d^3 v$$

We rewrite Eq. (C.2) as:

$$N^2 \sim N_c^2 \, (1 + \epsilon_H) \, , \quad (C.3)$$

where:

$$\epsilon_H = 1 + \frac{\beta^2}{(1-\Lambda)^3} \left(< \frac{v_\parallel}{c} >^2 - \frac{1-\Lambda}{2} < \frac{v_\perp}{c} >^2 \right)$$

and where N_c^2 is the cold plasma refractive index expression.

For isotropic distributions, $< v_\parallel >^2 = \frac{1}{2} < v_\perp >^2$ and ϵ_H reduces to

$$\epsilon_H = 1 + \frac{\beta^2 \Lambda}{2(1-\Lambda)^3} < \frac{v_\parallel}{c} >^2 . \quad (C.4)$$

This result was already derived by Guthart [1964] where he chose for g_0 a Maxwellian distribution for which $< v_\parallel >^2 = 2KT/M$.

Equation (C.4) is also given by the full adiabatic macroscopic theory [Quemada, 1968].

We choose now Eq. (3.6) for g_0. Then

$$\epsilon_H = \frac{\beta^2}{(1-\Lambda)^3} \frac{B_{3q} A_{\nu q}}{(\nu-5)(q+3)} b^{-q/2} \left[1 - \frac{(1-\Lambda)(q+2)}{2} \right] \delta_{EH} \left(\frac{v_H}{c} \right)^2 \qquad (C.5)$$

As an example, we chose $\nu = 6$ and $q = 6$ (the distribution is thought to be quite anisotropic towards low energies) and evaluate roughly the corrective term ϵ_{HE} at the equator where the contribution to whistler dispersion is most important:

$$\epsilon_{HE} \approx \frac{-\beta^2}{(1-\Lambda)^3} \delta_{EH} \left(\frac{v_H}{c} \right)^2 . \qquad (C.6)$$

With $W_H = 10$ eV, at $L \sim 4$, $\beta \sim 10$, $\delta_{EH} \sim 10^{-1}$ (for $\nu = 6$) and

$$\epsilon_{HE} \ (\Lambda \ll 1) \sim - 4 \times 10^{-4},$$

$$\epsilon_{HE} \ (\Lambda \sim 0.5) \sim - 4 \times 10^{-3}. \qquad (C.7)$$

Such a difference in the dispersion would be unnoticeable.

Unfortunately, a similar computation for $\theta \neq 0$ becomes fairly complex as a cubic equation has to be solved. This was done by Wang [1970] for the scalar pressure theory [Denisse and Delacroix, 1963]. He found corrections became important close to the resonance cone, as expected. A solution for $\theta \neq 0$ will contain terms such as Eq. (C.6) but where $1-\Lambda$ is replaced by $\cos\theta-\Lambda$ and ϵ_H increases very rapidly for $\theta \Rightarrow \theta_R$. Wang's [1970] computations could be improved using the full adiabatic theory [Quemada, 1968].

REFERENCES

Akhiezer, A. I., I. A. Akhiezer, R. V. Polovin, A. G. Sitenko and K. N. Stepanov, Collective Oscillations in a Plasma, M.I.T. Press, Cambridge, Mass., 1967.

Allis, W. P., S. J. Buchsbaum and A. Bers, Waves in Anisotropic Plasmas, M.I.T. Press, Cambridge, Mass., 1963.

Angerami, J. J., A whistler study of the distribution of thermal electrons in the magnetosphere, Ph.D. Thesis, Stanford University, Stanford, Calif., May 1966.

Angerami, J. J., Whistler duct properties deduced from vlf observations made with the OGO-3 satellite near the magnetic equator, J. Geophys. Res., 75, 6115, 1970.

Angerami, J. J. and D. L. Carpenter, Whistler studies of the plasmapause in the magnetosphere, 2, electron density and total tube electron content near the knee in magnetospheric ionization, J. Geophys. Res., 71, 711, 1966.

Bekefi, G., Radiation Processes in Plasmas, Wiley, New York, 1966.

Bell, T. F., Wave particle gyroresonance interactions in the earth's outer ionosphere, Ph.D. Thesis, Stanford University, Stanford, Calif., May 1964.

Bell, T. F., Nonlinear Alfven waves in a Vlasov plasma, Phys. of Fluids, 8, 1829, 1965.

Benoit-Cattin, P., and L. C. Bernard, Anomalies of the energy of positive ions extracted from high frequency ion sources, a theoretical study, J. Appl. Phys., 39, 5723, 1968.

Bernard, L. C., Interpretation de la distribution des energies des ions positifs produits par une source d'ions a excitation electrique de haute frequence, These de Doctorat de specialite, Toulouse, France, 1967.

Bernard,L. C., A new nose extension method for whistlers, J. Atmos. Terr. Phys., 35, 871, 1973.

Bogott, F. H. and F. S. Mozer, Magnetopause electric field inferred from energetic particle measurements on ATS 5, J. Geophys. Res., 76, 892, 1971.

Brice, N. M., Discrete vlf emissions from the upper atmosphere, Ph.D. Thesis, Stanford Univ., Stanford, Calif., August 1964.

Brice, N. M., Artificial enhancement of energetic particle precipitation through cold plasma injection: a technique for seeding substorms? J. Geophys. Res., 75, 4890, 1970.

Briggs, R. J., Electron-stream Interaction with Plasmas, M.I.T. Press, Cambridge, Mass., 1964.

Brillouin, L., Wave Propagation and Group Velocity, Academic Press, New York, 1960.

Brinca, A. L., On the stability of obliquely propagating whistlers, J. Geophys. Res., 77, 3495, 1972.

Burtis, W. J., Magnetic radiation observed by the OGO-1 and OGO-3 broad-band vlf receivers, Tech. Rept. 3438-1, Radioscience Lab., Stanford Electronics Labs., Stanford Univ., Stanford, Calif., August 1969.

Carpenter, D. L., The magnetosphere during magnetic storms; a whistler analysis, Ph.D. Thesis, Stanford Univ., Stanford, Calif., June 1962.

Carpenter, D. L., Whistler evidence of a 'knee' in the magnetospheric ionization density profile, J. Geophys. Res., 68, 1675, 1963.

Carpenter, D. L., Whistler studies of the plasmapause in the magnetosphere -1; temporal variations in the position of the knee and some evidence on plasma motions near the knee, J. Geophys. Res., 71, 693, 1966.

Carpenter, D. L., Ducted whistler-mode propagation in the magnetosphere; a half-gyrofrequency upper intensity cutoff and some associated wave growth phenomena, J. Geophys. Res., 73, 2919, 1968.

Carpenter, D. L., Whistler evidence of the dynamic behavior of the duskside bulge in the plasmasphere, J. Geophys. Res., 75, 3837, 1970.

Carpenter, D. L. and R. L. Smith, Whistler measurements of electron density in the magnetosphere, Rev. Geophys., 2, 415, 1964.

Carpenter, D. L., K. Stone, J. C. Siren and T. L. Crystal, Magnetospheric electric fields deduced from drifting whistler paths, J. Geophys. Res., 77, 2819, 1972.

Cornwall, J. M., Precipitation of auroral and ring current particles by artificial plasma injection, Rev. Geophys., 10, 993, 1972.

Dantas, N., OGO-4 satellite observations of whistler-mode propagation effects associated with caustics in the magnetosphere, Ph.D. Thesis, Stanford Univ., Stanford, Calif., October 1972.

Denisse, J. and J. L. Delcroix, Plasma Waves, Interscience Publishers, New York, 1963.

Derfler, H., Growing wave and instability criteria for hot plasmas, Phys. Letts., 24A, 763, 1967.

Derfler, H., Frequency cusp, a means for discriminating between convective and nonconvective instability, Phys. Rev. A, 1, 1467, 1970.

Dunckel, N. and R. A. Helliwell, Whistler-mode emissions on OGO-1 satellite, J. Geophys. Res., 74, 6371, 1969.

Dunckel, N. and R. A. Helliwell, Whistler-mode signals observed near the local electron gyrofrequency, (in preparation), 1973.

Dungey, J. W., Plasma Waves in Space and in the Laboratory, (eds.) J. O. Thomas and B. J. Landmark, Edinburgh University Press, Edinburgh, 1969.

Dysthe, K. B., Some studies of triggered whistler emissions, J. Geophys. Res., 76, 6915, 1971.

Edgar, B. C., The structure of the magnetosphere as deduced from magnetospherically reflected whistlers, Ph.D. Thesis, Stanford University, Stanford, Calif., March 1972.

Feynman, R. P., The Electromagnetic Field, Vol. 2, Addison-Wesley, Reading, Mass., 1964.

Gendrin, R., Pitch angle diffusion of low energy protons due to gyroresonant interaction with hydromagnetic waves, J. Atmos. Terr. Phys., 30, 1313, 1968.

Guthart, H., Whistlers in a thermal magnetosphere, Stanford Research Institute, Menlo Park, Calif., 1964.

Guthart, H., An anisotropic electron velocity distribution for the cyclotron absorption of whistlers and vlf emissions, Radio Science, 63D, 1403, 1965.

Helliwell, R. A., Whistlers and Related Ionospheric Phenomena, Stanford University Press, Stanford, Calif., 1965.

Helliwell, R. A., A theory of discrete vlf emissions from the magnetosphere, J. Geophys. Res., 72, 4773, 1967.

Helliwell, R. A. and T. L. Crystal, A feedback model of cyclotron interaction between whistler-mode waves and energetic electrons in the magnetosphere, (submitted to J. Geophys. Res., 1973).

Hess, W. N., The Radiation Belt and Magnetosphere, Blaisdell, Waltham, Mass., 1968.

Ho, D. and L. C. Bernard, A fast method to determine the nose frequency and minimum group delay of a whistler when the causative spheric is unknown, J. Atmos. Terr. Phys., 35, 881, 1973.

Kennel, C. F., Low-frequency whistler mode, Phys. Fluids, 9, 2190, 1966.

Kennel, C. F. and F. Engelmann, Velocity space diffusion from weak plasma turbulence in a magnetic field, Phys. Fluids, 9, 2377, 1966.

Kennel, C. F. and H. E. Petschek, Limit on stably trapped particle fluxes, J. Geophys. Res., 71, 1, 1966.

Kennel, C. F. and R. M. Thorne, Unstable growth of unducted whistlers propagating at an angle to the geomagnetic field, J. Geophys. Res., 72, 871, 1967.

Laird, M. J., On gyroresonance, J. Plasma Phys., 2, Part 1, 59, 1968.

Laird, M. J. and F. B. Knox, Exact solution for charged particle trajectories in an electromagnetic field, Phys. Fluids, 8, 755, 1965.

Landau, L. D., On the vibrations of the electronic plasma, JETP, 16, 574, 1946.

Lee, J. C., Whistler propagation and instability characteristics, Ph.D. Thesis, Stanford University, Stanford, Calif., May 1969.

Lee, J. C. and F. W. Crawford, Stability analysis of whistler amplification, J. Geophys. Res., 75, 85, 1970.

Liemohn, H. B., Cyclotron-resonance amplification of vlf and ulf whistlers, J. Geophys. Res., 72, 39, 1967.

Liemohn, H. B., Plasma Waves in Space and in the Laboratory, (eds.) J. O. Thomas and B. J. Landmark, Edinburgh University Press, Edinburgh, 1969.

Liemohn, H. B. and F. L. Scarf, Exospheric electron temperatures from nose whistler attenuation, J. Geophys. Res., 67, 1785, 1962a.

Liemohn, H. B. and F. L. Scarf, Whistler attenuation by electrons with an $E^{-2.5}$ distribution, J. Geophys. Res., 67, 4163, 1962b.

Liemohn, H. B. and F. L. Scarf, Whistler determination of electron energy and density distributions in the magnetosphere, J. Geophys. Res., 69, 883, 1964.

Lutomirski, R. F. and R. N. Sudan, Exact nonlinear electromagnetic whistler modes, Phys. Rev., 147, 156, 1966.

Lyons, L. R., R. M. Thorne and C. F. Kennel, Pitch-angle diffusion of radiation belt electrons within the plasmasphere, J. Geophys. Res., 77, 3455, 1972.

Montgomery, D. C. and D. A. Tidman, Plasma Kinetic Theory, McGraw-Hill, New York, 1964.

Palmadesso, P. J., Resonance, particle trapping and Landau damping in finite amplitude obliquely propagating waves, GSFC Rept., Greenbelt, Maryland, Marcy 1972.

Palmadesso, P. J. and G. Schmidt, Collisionless damping of a large amplitude whistler wave, Phys. Fluids, 14, 1411, 1971.

Park, C. G., Whistler observations of the interchange of ionization between the ionosphere and the protonosphere, J. Geophys. Res., 75, 4249, 1970.

Park, C. G., Methods of determining electron concentrations in the magnetosphere from nose whistlers, SEL Rept. 3454-1, Stanford Univ., Jan. 1972.

Park, C. G. and D. L. Carpenter, Whistler evidence of large-scale electron-density irregularities in the plasmasphere, J. Geophys. Res., 75, 3825, 1970.

Quemada, D., Ondes Dans Les Plasmas, Hermann, Paris, 1968.

Roberts, C. S. and S. J. Bucksbaum, Motion of a charged particle in a constant magnetic field and a transverse electromagnetic wave propagating along the field, Phys. Rev., 135, A361, 1964.

Roux, A and J. Solomon, Mecanismes non lineaires associes aux interactions ondes-particles dans la magnetosphere, Ann. Geophys., 26, 279, 1970.

Russell, C. T. and R. M. Thorne, On the structure of the inner magnetosphere, Rept. No. 809, Institute of Geophysics & Planetary Physics, UCLA, Los Angeles, Calif., September 1969.

Scarf, F. L., Landau damping and the attenuation of whistlers, Phys. Fluids, 5, 6, 1962.

Schield, M. A. and L. A. Frank, Electron observations between the inner edge of the plasma sheet and the plasmasphere, J. Geophys. Res., 75, 5401, 1970.

Smith, R. L., The use of nose whistlers in the study of the outer ionosphere, Ph.D. Thesis, Stanford University, Stanford, Calif., July 1960.

Smith, R. L., Propagation characteristics of whistlers trapped in field-aligned columns of enhanced ionization, J. Geophys. Res., 66, 3699, 1961.

Smith, R. L. and J. J. Angerami, Magnetospheric properties deduced from OGO-1 observations of ducted and nonducted whistlers, J. Geophys. Res., 73, 1, 1968.

Stix, T. H., Theory of Waves in Plasmas, McGraw-Hill, New York, 1962.

Storey, L.R.O., An investigation of whistling atmospherics, Phil. Trans. Roy. Soc. A., 246, 113, 1953.

Sturrock, P. A., Kinematics of growing waves, Phys. Rev., 112, 1488, 1958.

Sudan, R. N. and E. Ott, Theory of triggered vlf emissions, J. Geophys. Res., 76, 4463, 1971.

Thorne, R. M., Unducted whistler evidence for a secondary peak in the electron energy spectrum near 10 kev, J. Geophys. Res., 73, 4895, 1968.

Tidman, D. A. and R. K. Jaggi, Landau damping of transverse waves in the exosphere by fast-particle fluxes, J. Geophys. Res., 67, 2215, 1962.

Vasyliunas, V. M., Low energy particle fluxes in the geomagnetic tail, CSR-P-69-17 Rept., Dept. of Physics & Center for Space Research, M.I.T., Cambridge, Mass., June 1969.

Walter, F., Nonducted vlf propagation in the magnetosphere, Ph.D. Thesis, Stanford University, Stanford, Calif., 1969.

Wang, T.N.C., VLF input impedance characteristics of an electric antenna in a magnetoplasma, Ph.D. Thesis, Stanford University, Stanford, Calif., May 1970.

Watson, G. N., Theory of Bessel Functions,(3rd ed.), Cambridge University Press, Cambridge, 1958.